



UNIVERSIDADE DE  
COIMBRA

Simaura Grilo Henriques

**DEVELOPMENT OF A NOVEL POLYMERIC  
NANOCARRIER TO MEDIATE GENE THERAPY  
FOR HEPATOCELLULAR CARCINOMA**

**Dissertação no âmbito do Mestrado em Bioquímica orientada pelo  
Professor Doutor Henrique Manuel dos Santos Faneca e pela  
Professora Doutora Paula Cristina Veríssimo Pires e apresentada  
ao Departamento de Ciências da Vida da Universidade de Coimbra**

Outubro de 2021





UNIVERSIDADE D  
COIMBRA

Simaura Grilo Henriques

**DEVELOPMENT OF A NOVEL POLYMERIC  
NANOCARRIER TO MEDIATE GENE THERAPY  
FOR HEPATOCELLULAR CARCINOMA**

Dissertação no âmbito do Mestrado em Bioquímica orientada pelo  
Professor Doutor Henrique Manuel dos Santos Faneca e pela  
Professora Doutora Paula Cristina Veríssimo Pires e apresentada  
ao Departamento de Ciências da Vida da Universidade de Coimbra

Outubro de 2021



# Agradecimentos

Início esta dissertação em tom de agradecimento, com algumas palavras de apreço a todos aqueles me incentivaram a colocar todo o meu empenho neste trabalho e que me apoiaram nos momentos de desânimo e frustração ao longo deste último ano. Apesar de ter sido realizada por mim, esta dissertação não seria possível sem estas pessoas.

Em primeiro lugar, ao Doutor Henrique Faneca por me ter acolhido como orientanda e deixado trabalhar num tema tão interessante. Por ter confiado sempre no meu trabalho e por toda a motivação, disponibilidade e paciência. Fico muito grata por ter contribuído para o meu crescimento como estudante e para a minha aproximação à investigação científica.

À Professora Doutora Paula Veríssimo, não só por ter aceitado ser minha orientadora interna, mas também por todo o rigor que impõe no seu trabalho realizado em prol dos alunos de Bioquímica.

À Daniela por toda a ajuda e disponibilidade. Por todas as explicações pacientes, todas as palavras de apoio, todos os conhecimentos partilhados, todas as chamadas de atenção, sejam por momentos de distração no laboratório ou por lanches pouco saudáveis. O prazer foi todo meu.

À Rose por toda a disponibilidade que demonstrou para me ajudar, pelo rigor e profissionalismo, que me inspiraram a fazer sempre mais e melhor. Ao Daniel pelas maiores gargalhadas no laboratório e à Dina por todas as dúvidas esclarecidas.

Aos meus pais pelos valores e educação que me transmitiram. Pelo apoio incondicional, pela motivação, pelo amor, pelo esforço e dedicação. Por me terem ensinado a seguir, não o caminho mais fácil, mas aquele que me fizer mais feliz. À Inês pelas gargalhadas mais genuínas, as discussões menos fundamentadas e por ser a melhor irmã que alguém pode ter. À avó Maria ao avô Manel, à avó Tita e ao avô Nito por todo o carinho e pela dedicação.

À Luana e à Sofia, que terão sempre um lugar muito especial no meu coração, por terem partilhado comigo os momentos mais enriquecedores da minha vida académica, pela paciência e pela preocupação, por estarem sempre disponíveis para me ouvir e terem sempre uma palavra amiga de volta. Ao Machop e ao Bernardo pelo companheirismo e por nunca terem desistido da minha amizade.

Por último, um agradecimento muito especial ao meu grupo de amigos de Monte Redondo e arredores, que me faz sentir uma pessoa extremamente sortuda. Ao Juliano, ao João Pedro e ao Rodrigo por terem partilhado Coimbra comigo. Ao Pedro e ao João Vítor por serem dos melhores ouvintes, ao Francisco por partilhar comigo o bom gosto por séries, ao Pacheco por me ter dado a pior alcunha, ao Rogério, ao Leandro, ao Rafa. À Joana e à Ana por me ajudarem a suportar os restantes. Estou muito grata pela vossa amizade, por estarem sempre disponíveis, por me apoiarem em todas as circunstâncias, pelas melhores e mais altas gargalhadas, pelos cafés que não acabam sem um baralho de cartas em cima da mesa, pelas saídas mais divertidas. Também à Bruna por mantermos uma amizade de longa data e que, apesar dos poucos momentos juntas, permanece inabalável.

Um sincero obrigado!

# Resumo

Ao longo das últimas décadas, o cancro tornou-se um dos maiores problemas de saúde a nível mundial. Entre os tipos de cancro mais comuns encontra-se o cancro do fígado, que inclui o Carcinoma Hepatocelular. Este carcinoma é a quarta causa de morte por cancro e a sua incidência tem vindo a aumentar. As opções de tratamento atualmente disponíveis são pouco eficazes, além de serem bastantes restritas em casos de doença avançada. Nestes casos, geralmente, é aplicada a quimioterapia. No entanto, este tipo de terapia é sempre acompanhada por efeitos secundários indesejados e está associada a uma taxa elevada de recorrência de cancro. Deste modo, tornou-se necessário desenvolver novas estratégias, capazes de ultrapassar estas limitações.

A terapia génica tem sido intensivamente estudada e tem demonstrado resultados promissores no tratamento de diversas doenças, incluindo o cancro. Esta consiste na entrega de material genético a células alvo, com o intuito de induzir um efeito de supressão tumoral. Apesar dos sistemas de transporte virais serem mais comumente aplicados na clínica, os sistemas de transporte não-virais têm-se destacado por serem mais seguros. De entre os vários sistemas de transporte não-virais, as nanopartículas poliméricas destacam-se devido à sua biocompatibilidade e versatilidade. Para além disso, as técnicas usadas para produzir estes sistemas permitem controlar as características finais das nanopartículas e modificar a sua superfície de acordo com a finalidade ou células alvo. As nanopartículas poliméricas incluem, entre outros, micelas poliméricas e poliplexos, que podem ser desenvolvidos a partir de glicopolímeros. Estes são polímeros sintéticos que contêm grupos carboidrato na sua composição, capazes de promover o direcionamento. Assim, glicopolímeros que contêm o monómero LAMA (2-lactobionamidoetil metacrilato), que possui um resíduo de galactose na sua estrutura, foram usados para produzir micelas poliméricas e poliplexos. Este monómero apresenta a capacidade de se ligar ao recetor das asialoglicoproteínas, que se encontra sobreexpresso na superfície das células de HCC. Assim, o principal objetivo desta dissertação consistiu no desenvolvimento de um nanossistema de base polimérica capaz de entregar eficaz e especificamente material genético às células de HCC.

Tendo isto em conta, inicialmente, foram produzidas micelas poliméricas usando glicopolímeros anfifílicos, PAMA<sub>103-*co*</sub>-PLAMA<sub>19-*b*</sub>-PDEAEMA<sub>63</sub> e PAMA<sub>50-*co*</sub>-PLAMA<sub>10-*b*</sub>-PDEAEMA<sub>16</sub>. Estes nanossistemas foram extensivamente caracterizados, apresentando um tamanho de aproximadamente 70 nm, e capacidade para condensar e proteger o material

genético. Contudo, os resultados obtidos após transfeção de células HepG2 mostraram níveis elevados de toxicidade e baixos níveis de atividade biológica. Adicionalmente, foi avaliado o potencial destas micelas poliméricas para entrega de fármacos. Micelas produzidas com o polímero PAMA<sub>50-co</sub>-PLAMA<sub>10-b</sub>-PDEAEMA<sub>16</sub> foram carregadas com sorafenib, um fármaco de primeira linha aprovado para o tratamento de HCC. Os valores obtidos para a eficiência de encapsulação e capacidade de carga foram de 15 e 4 %, respetivamente, encontrando-se acima do que está reportado na literatura para este tipo de nanossistemas. No entanto, estas micelas resultaram em níveis elevados de toxicidade nas células HepG2 e, como tal, foi avaliada outra abordagem.

Essa nova abordagem consistiu na produção de políplexos usando o polímero PAMA<sub>73-co</sub>-PLAMA<sub>21</sub>. Este nanossistemas apresentam um tamanho de cerca de 150 nm e, de um modo geral, apresentam capacidade para condensar e proteger o material genético, mantendo a sua estabilidade ao longo do tempo. Os políplexos foram produzidos em diferentes rácios de carga N/P e resultaram em níveis notáveis de expressão do transgene nas várias linhas celulares de carcinoma hepatocelular utilizadas. A eficiência de transfeção destes políplexos, preparados no rácio de carga (+/-) 40/1, foi avaliada por citometria de fluxo, demonstrando uma percentagem elevada de células transfetadas quando comparado com o controlo comercial, PEI, o que foi confirmado através de microscopia de fluorescência. Para além disso, a especificidade destes nanossistemas para com o recetor das asiologlicoproteínas foi comprovada através de um ensaio de competição, usando o ligando natural deste recetor, a asialofetuína. Os resultados obtidos foram confirmados por citometria de fluxo e microscopia de fluorescência. A internalização celular e distribuição intracelular dos políplexos foram avaliadas por microscopia confocal, demonstrando que alguns dos políplexos se encontravam nos endossomas. Como tal, com o intuito de promover o escape endossomal, foi usado um fármaco estabilizador de microtúbulos, o docetaxel, que resultou num aumento substancial da sua capacidade de transfeção. Por último, para avaliar o potencial dos nanossistemas desenvolvidos para mediar uma estratégia antitumoral, foi realizado um ensaio preliminar, usando os políplexos preparados com plasmídeos terapêuticos que codificam os supressores tumorais p53 ou PTEN, tendo-se verificado uma redução significativa da viabilidade celular.

**Palavras-chave:** cancro, carcinoma hepatocelular, terapia génica, sistemas de transporte e entrega da material genético, glicopolímeros, micelas poliméricas, políplexos.



# Abstract

Over the past decades, cancer became one of the major health problems worldwide. Among the most common types of cancers is liver cancer, which includes hepatocellular carcinoma. Hepatocellular carcinoma is the fourth leading cause of cancer-related death, and its incidence has been growing. The currently available treatment options are poorly effective and severely restricted when the disease is advanced. In these cases, systemic chemotherapy is usually applied. However, it is always accompanied by undesired side effects and a high rate of tumor recurrence. Therefore, it is necessary to develop new strategies, able to overcome these limitations.

Gene therapy has been widely studied and has been demonstrating promising results for the treatment of several diseases, including cancer. It consists of the delivery of genetic material to the target cells, inducing a tumor suppressive effect. Even though viral gene delivery systems are most commonly used in the clinical field, non-viral gene delivery systems arise as safer systems and have been widely studied and engineered. Among the various non-viral gene delivery systems, polymeric nanoparticles stand out due to their biocompatibility and versatility. Besides, the techniques used to produce these systems allow a precise control of nanocarriers characteristics and modification of their surface in order to achieve the desired features. Polymeric nanoparticles include, among others, polymeric micelles and polyplexes, that could be synthesized from glycopolymers. These synthetic polymers contain carbohydrate groups in their structure, which promote targeting. Accordingly, glycopolymers containing the monomer LAMA (2-lactobionamidoethyl methacrylate), which has a galactose residue in its structure, were used to produce polymeric micelles and polyplexes. pLAMA is able to bind to the asialoglycoprotein receptor, overexpressed on the surface of HCC cells. Therefore, the main purpose of this work was to develop a polymer-based nanosystem capable of effectively and specifically deliver genetic material into HCC cells.

Taking this into account, initially, polymeric micelles were produced using amphiphilic glycopolymers, PAMA<sub>103-*co*</sub>-PLAMA<sub>19-*b*</sub>-PDEAEMA<sub>63</sub> and PAMA<sub>50-*co*</sub>-PLAMA<sub>10-*b*</sub>-PDEAEMA<sub>16</sub>. These nanosystems were extensively characterized, presenting a size around 70 nm, and were able to condense and protect genetic material. However, the results obtained after transfection of HepG2 cells with the polymeric micelles showed high levels of toxicity and low levels of biological activity. Additionally, the potential of the polymeric nanoparticles for drug delivery was evaluated. PAMA<sub>50-*co*</sub>-PLAMA<sub>10-*b*</sub>-

PDEAEMA<sub>16</sub>-based micelles were loaded with sorafenib, a first-line drug approved for HCC treatment, and the values obtained for loading efficiency and loading capacity was 15 and 4 %, respectively, which are above what has been reported in the literature. However, these micelles resulted in high levels of toxicity in HepG2 cells and, for that reason, another approach was evaluated.

The alternative consisted of the production of polyplexes using the polymer PAMA<sub>73</sub>-*co*-PLAMA<sub>21</sub>. These nanosystems presented a size around 150 nm and, overall, were able to condense and protect genetic material, maintaining their stability along time. The polyplexes were produced at different N/P charge ratios and resulted in great levels of transgene expression in the different hepatocarcinoma cell lines used. Transfection efficiency of these polyplexes prepared at 40/1 N/P charge ratio was evaluated by flow cytometry, showing an increased percentage of transfected cells comparing to the commercial control, PEI, which was confirmed by fluorescence microscopy. Additionally, the specificity of the developed polyplexes towards the asialoglycoprotein receptor was demonstrated by a competition assay, using the natural ligand for this receptor, asialofetuin. The obtained results were confirmed by flow cytometry and fluorescence microscopy. Cellular uptake and intracellular distribution of the polyplexes were assessed by confocal microscopy, showing that some polyplexes were colocalized with endosomes. As an attempt to promote endosomal escape, a microtubule-stabilizing agent, docetaxel, was used, resulting in a substantial increase of transfection activity. At last, to evaluate the potential of the PAMA<sub>73</sub>-*co*-PLAMA<sub>21</sub>-based polyplexes to mediate an antitumor strategy, a preliminary test was performed, using polyplexes prepared with the therapeutic plasmids encoding p53 or PTEN, having been observed a significant reduction on the cell viability.

**Keywords:** cancer, hepatocellular carcinoma, gene therapy, gene delivery systems, glycopolymers, polymeric micelles, polyplexes.

# Table of Contents

<b>Agradecimientos</b> .....	v
<b>Resumo</b> .....	vii
<b>Abstract</b> .....	ix
<b>Table of Contents</b> .....	xi
<b>List of Figures</b> .....	xiii
<b>List of Tables</b> .....	xv
<b>Abbreviations</b> .....	xvii

## Chapter 1

<b>Introduction</b> .....	1
1 Hepatocellular Carcinoma: a brief introduction.....	1
1.1 Chemotherapy for HCC treatment .....	3
1.1.1 Sorafenib .....	4
2 Gene therapy .....	5
2.1 Molecular targets for HCC gene therapy .....	6
2.1.1 p53 gene .....	7
2.1.2 PTEN gene.....	8
3 Gene delivery systems.....	9
3.1 Viral gene delivery systems.....	10
3.2 Non viral gene delivery systems.....	11
3.2.1 Polymeric nanoparticles.....	13
3.2.2 Cellular uptake and intracellular route.....	22
4 Aim of the present work.....	25

## Chapter 2

<b>Materials and Methods</b> .....	27
1 Synthesis of the glycopolymers.....	27
2 Preparation of polymeric micelles and micelleplexes .....	27
3 Preparation of sorafenib-loaded micelles.....	27
4 Preparation of polymer-DNA complexes.....	28
5 Physicochemical characterization.....	28
5.1 Dynamic light scattering and $\zeta$ potential analysis.....	28
5.2 Agarose gel electrophoresis .....	28

6	Cell culture.....	29
7	Transfection activity.....	29
8	Cell viability.....	30
9	Transfection efficiency.....	31
10	Cellular uptake and intracellular distribution of the polyplexes.....	32

### **Chapter 3**

	<b>Results and Discussion</b> .....	33
1	Polymeric micelles for co-delivery of drugs and genes.....	33
1.1	Polymeric micelles production and physicochemical characterization.....	33
1.2	Micelleplexes physicochemical characterization.....	36
1.3	Evaluation of micelleplexes cytotoxicity.....	37
1.4	Evaluation of micelleplexes transfection activity.....	39
1.5	Polymeric micelles for sorafenib delivery.....	40
2	Polyplexes for gene delivery.....	43
2.1	Polyplexes production and physicochemical characterization.....	43
2.2	Evaluation of polyplexes transfection activity.....	45
2.3	Evaluation of polyplexes cytotoxicity.....	47
2.4	Transfection efficiency of polyplexes.....	48
2.5	Evaluation of polyplexes specificity.....	49
2.6	Cellular uptake and intracellular distribution of polyplexes.....	51
3	Strategies to improve transfection activity.....	53
4	Development of a therapeutic strategy.....	57

### **Chapter 4**

	<b>Conclusions</b> .....	59
--	--------------------------	----

### **Chapter 5**

	<b>References</b> .....	63
--	-------------------------	----

# List of Figures

<b>Figure 1</b>   Incidence and mortality of different types of cancer worldwide.....	1
<b>Figure 2</b>   Mechanism of action of different drugs used for HCC treatment .....	3
<b>Figure 3</b>   Mechanism of action of Sorafenib.....	4
<b>Figure 4</b>   Targeted diseases in gene therapy clinical trials worldwide .....	5
<b>Figure 5</b>   Main functions of p53 gene.....	7
<b>Figure 6</b>   Tumor suppressor role of PTEN .....	8
<b>Figure 7</b>   Types of gene therapy used for HCC treatment .....	9
<b>Figure 8</b>   Representation of different non-viral gene delivery systems, divided into polymeric, inorganic and lipid-based nanocarriers.....	12
<b>Figure 9</b>   Representation of a polymeric micelle formed through the self-assembly of amphiphilic block copolymers .....	14
<b>Figure 10</b>   Chemical structures of the cationic polymers Poly-L-lysine (PLL) and Polyethylenimine (PEI) .....	21
<b>Figure 11</b>   Chemical structures of the cationic polymers Poly(2-(dimethylamino)ethyl methacrylate) (PDMAEMA), Poly( $\beta$ -amino ester) (P $\beta$ AE) and Poly(2-aminoethyl methacrylate) (PAMA) .....	22
<b>Figure 12</b>   Extracellular and intracellular barriers for the effective delivery of genetic material into target cells .....	24
<b>Figure 13</b>   Reaction catalyzed by luciferase .....	30
<b>Figure 14</b>   Chemical structure of PAMA-co-PLAMA-b-PDEAEMA glycopolymers .....	34
<b>Figure 15</b>   Size distribution by intensity.....	35
<b>Figure 16</b>   Size and associated polydispersity (a), zeta potential (b), agarose gel electrophoresis (c), and GreenSafe access (d) to DNA of Micelleplexes 1 .....	37
<b>Figure 17</b>   Viability of HepG2 cells in the presence of Micelleplexes 1 and 2 (a), and Empty micelles 1 and 2 (b).....	38
<b>Figure 18</b>   Luciferase gene expression in HepG2 cells transfected with Micelleplexes 1 and 2 (a) and Polyplexes 1 and 2 (b). .....	40
<b>Figure 19</b>   Effect of Sorafenib concentration and amount of micelles on the viability of HepG2 cells .....	42
<b>Figure 20</b>   Size (a), zeta potential (b), condensation of DNA and resistance to DNase I action(c), of Polyplexes .....	44
<b>Figure 21</b>   Influence of time and environment on the stability of Polyplexes .....	45

<b>Figure 22</b>   Transfection activity of polyplexes in different cell lines: HepG2 (a), Hep3B (b) and Huh-7 (c) .....	46
<b>Figure 23</b>   Effect of the polyplexes on the viability of different cell lines: HepG2 (a), Hep3B (b), and Huh-7 (c).....	47
<b>Figure 24</b>   Effect of the polyplexes composition on the green fluorescent protein gene expression evaluated by flow cytometry (a) and fluorescence microscopy (b), using Huh-7 cells.....	48
<b>Figure 25</b>   Effect of the presence of asialofetuin on the luciferase gene expression in the 3 cell lines: HepG2 (a), Hep3B (b), and Huh-7 (c) .....	50
<b>Figure 26</b>   Effect of the presence of asialofetuin on the green fluorescent protein gene expression evaluated by flow cytometry (a) and fluorescence microscopy (b), using Huh-7 cells.....	51
<b>Figure 27</b>   Effect of the presence of asialofetuin on the intracellular distribution of polyplexes in Huh-7 cells observed by confocal microscopy.....	52
<b>Figure 28</b>   Effect of the different concentrations of docetaxel and the combination with polyplexes on the viability of Huh-7 cells .....	53
<b>Figure 29</b>   Effect of the pre-treatment of Huh-7 cells with docetaxel on the luciferase gene expression (a), and green fluorescent protein gene expression evaluated by flow cytometry (b) and fluorescence microscopy (c).....	54
<b>Figure 30</b>   Effect of the pre-treatment with docetaxel on the intracellular distribution of polyplexes in Huh-7 cells observed by confocal microscopy.....	56
<b>Figure 31</b>   Effect of the polyplexes prepared with p53, PTEN and pLUC, and the combination of polyplexes with docetaxel, on the viability of Huh-7 cells, (a) 48 h and (b) 72 h after transfection, and (c) on the luciferase gene expression in Huh-7 cells, 48 and 72 h after transfection .....	58

# List of Tables

<b>Table 1</b>   Altered tumour suppressor and oncogenes identified in HCC patients .....	6
<b>Table 2</b>   Advantages and disadvantages of the main viral vectors .....	10
<b>Table 3</b>   Advantages and disadvantages of the main classes of non-viral gene delivery vectors.....	13
<b>Table 4</b>   Gene therapy studies involving polymeric micelles for co-delivery of drugs and genes.....	16
<b>Table 5</b>   Advantages and disadvantages of different methods to produce polymeric micelles .....	18
<b>Table 6</b>   Gene therapy studies involving polyplexes for cancer treatment.....	19
<b>Table 7</b>   Molecular weight parameters of PAMA-co-PLAMA-b-PDEAEMA glycopolymers.....	34
<b>Table 8</b>   Characterization of polymeric Micelles 1 and Micelles 2 through DLS .....	35
<b>Table 9</b>   Characterization of sorafenib-loaded polymeric Micelles 2.....	41
<b>Table 10</b>   Capacity and efficiency of loading of sorafenib into polymeric Micelles. ....	41
<b>Table 11</b>   Molecular weight parameters of PAMA <sub>73</sub> -co-PLAMA <sub>21</sub> glycopolymer .....	43





# Abbreviations

- ABC – Amphiphilic block copolymer
- ASGPR – Asialoglycoprotein receptor
- ATRP - Atom transfer radical polymerization
- BSA - Bovine serum albumin
- CLSM - Confocal laser scanning microscopy
- CMC – Critical micelle concentration
- DLS – Dynamic light scattering
- DMEM - Dulbecco's modified Eagle's medium
- DNA – Deoxyribonucleic Acid
- EMA – European Medicines Agency
- ERK - Extracellular signal-regulated kinase
- FBS - Fetal bovine serum
- FTTC - Fluorescein isothiocyanate
- GCV - Gancyclovir
- GFP - Green fluorescent protein
- HCC – Hepatocellular Carcinoma
- HSVtk - Herpes simplex virus thymidine kinase
- MEK – Mitogen-activated protein kinase
- Mn – Molecular weight
- mRNA - Messenger RNA
- mTOR – Mechanistic target of rapamycin
- N/P ratio – Nitrogen/Phosphate ratio
- NP – Nanoparticle

PAMA - Poly(2-aminoethyl methacrylate)

PBS - Phosphate-buffered saline solution

PDEAEMA – Poly(2-(diethylamino)ethyl methacrylate)

PEG - Polyethylene glycol

PEI – Polyethylenimine

pGFP – Plasmid DNA encoding for GFP

PI3K – Phosphatidylinositol-3-kinase

PI3K – Phosphoinositide 3-kinases

PIP3 – Phosphatidylinositol (3,4,5)-trisphosphate

PLAMA - Poly(2-lactobionamidoethyl methacrylate)

pLUC - Plasmid DNA encoding for luciferase

PTEN - Phosphatase and tensin homolog

RAF – Rapidly accelerated fibrosarcoma

RAFT - Reversible addition-fragmentation chain transfer

RLU - Relative light units

RNA - Ribonucleic acid

siRNA - Small interfering RNA

TBE - Tris/Borate/EDTA

TFE - Trifluoroethanol

TP53 – Tumour protein 53

Wnt - Wingless-related integration site

# Chapter 1

## Introduction

### 1 Hepatocellular Carcinoma: a brief introduction

Cancer is a leading cause of death worldwide. To add to the existing burden, the number of cancer cases and deaths is expected to increase as populations grow, age, and adopt lifestyle behaviors that increase cancer risk. Many lifestyle risk factors, such as tobacco use, physical inactivity, excess body weight, and reproductive patterns, are becoming increasingly common.<sup>1</sup>

Liver cancer is one of the few neoplasms with a steadily increasing incidence, being predicted that could be one million cases by 2030.<sup>2</sup> According to the International Agency for Research on Cancer, more than 900 000 new cases of liver cancer were registered in 2020, which represents almost 5 % of the total of new cancer cases. The estimated number of deaths related to liver cancer is equally worrying, accounting for more than 800 000 worldwide (**Figure 1**). In Portugal, liver cancer is among the 11 most common cancers, representing 2.6 % of the new cancer cases, and 5 % of the cancer related-deaths, in 2020.<sup>3</sup>

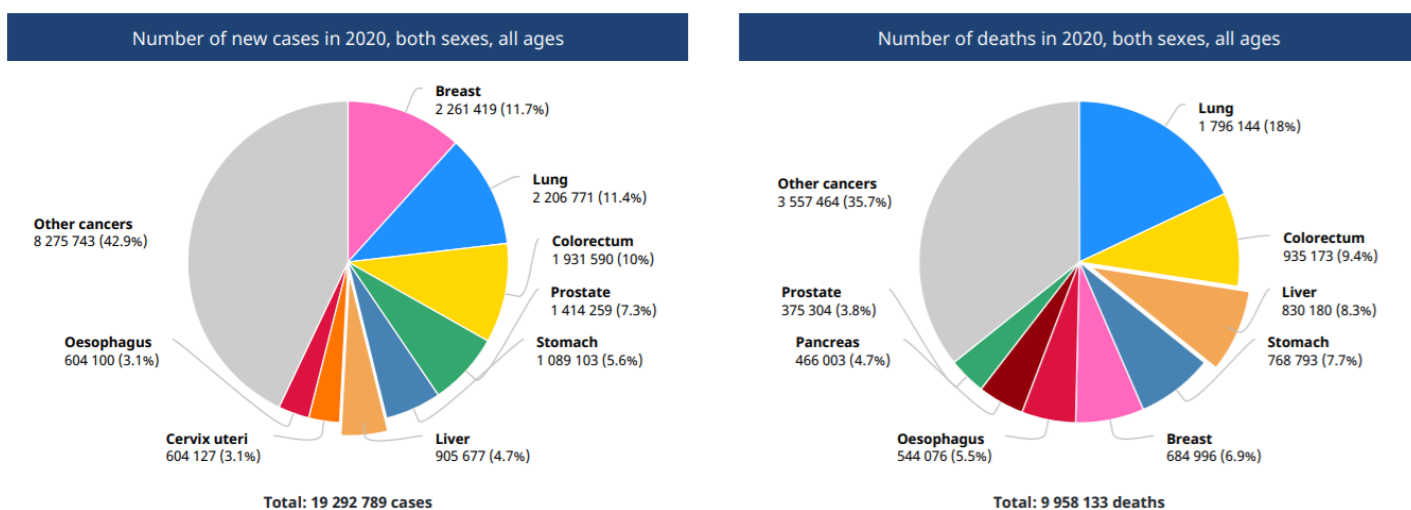


Figure 1 | Incidence and mortality of different types of cancer worldwide. Data from 2020, registered by the International Agency for Cancer Research.<sup>3</sup>

Liver cancer comprises a heterogeneous group of malignant tumors, with different histological features and an unfavorable prognosis, that range from hepatocellular carcinoma (HCC) and intrahepatic cholangiocarcinoma (iCCA) to mixed hepatocellular cholangiocarcinoma (HCC-CCA), fibrolamellar HCC (FL-HCC), and the pediatric neoplasm hepatoblastoma.<sup>2</sup>

Hepatocellular carcinoma represents about 90% of primary liver cancers<sup>4,5</sup> and is the fourth leading cause of cancer-related death worldwide.<sup>5,6</sup> HCC is considered a significant health problem because of its effect on the physiological functions of the liver, high lethality, and the growing incidence, which is associated with several risk factors.<sup>7</sup> Chronic hepatitis B and C viral infection, chronic alcohol consumption, aflatoxin-contaminated food intake, liver cirrhosis and some hereditary diseases are considered risk factors for HCC development in Asian and African countries, while in the developed countries, the epidemiological evidence connecting the pathologies are type 2 diabetes, obesity, metabolic disorders and non-alcoholic steatohepatitis (NASH) as part of non-alcoholic fatty liver diseases (NAFLD).<sup>4,8,9</sup>

Like other liver tumors, HCC is characterized by a high degree of molecular heterogeneity, which is one of the main factors harming the achievement of an effective treatment strategy.<sup>2</sup> As an attempt to overcome this major problem, several studies have been conducted to provide a better understanding of the molecular alterations in HCC, enabling the identification of key driving pathways.<sup>10</sup> Among the most altered pathways are: TP53, PI3K-mTOR, Wnt/ $\beta$ -catenin and RAS/RAF/MEK/ERK.<sup>10-12</sup> The phosphatidylinositol-3-kinase (PI3K)/AKT/mammalian target of rapamycin (mTOR) signaling pathway is involved in cell growth and angiogenesis. Oncogenic activation of PI3K- mTOR signaling was found to affect approximately 45 % of patients with HCC.<sup>10</sup> The RAS pathway is also frequently activated in HCC and has been associated with a poor prognosis. Ras targets RAF and MEK downstream, controlling growth, proliferation, and migration of cancer cells.<sup>12</sup>

Despite the efforts in investigations, HCC remains as a human tumor for which currently available therapeutic approaches are poorly effective.<sup>13</sup> In the early stages, HCC can be treated with surgical modalities, which offers an option for cure, such as liver transplantation and resection, or radiological techniques, as radiofrequency ablation, microwave ablation, percutaneous ethanol or acetic acid ablation and transarterial chemoembolization (TACE).<sup>14,15</sup> However, HCC is characterized by a lack of symptoms in the early stages and, consequently, diagnosis is often made when the disease is advanced.<sup>14</sup> Management of advanced HCC is particularly challenging because of decreased liver

function, making it impossible to apply the strategies mentioned above.<sup>16</sup> In these stages, systemic chemotherapy and molecularly targeted therapies are usually applied.<sup>4,14</sup>

## 1.1 Chemotherapy for HCC treatment

Targeted agents based on improved molecular characterization of HCC have been developed in order to improve patient survival.<sup>17</sup> These small molecule drugs are used to target different signaling pathways (**Figure 2**).<sup>8</sup> Presently, the approved drugs used for systemic treatment of HCC in Europe are multikinase inhibitors, such as sorafenib and lenvatinib, as the first-line therapeutics and, regorafenib and cabozantinib, as second-line therapeutics.<sup>4,17</sup>

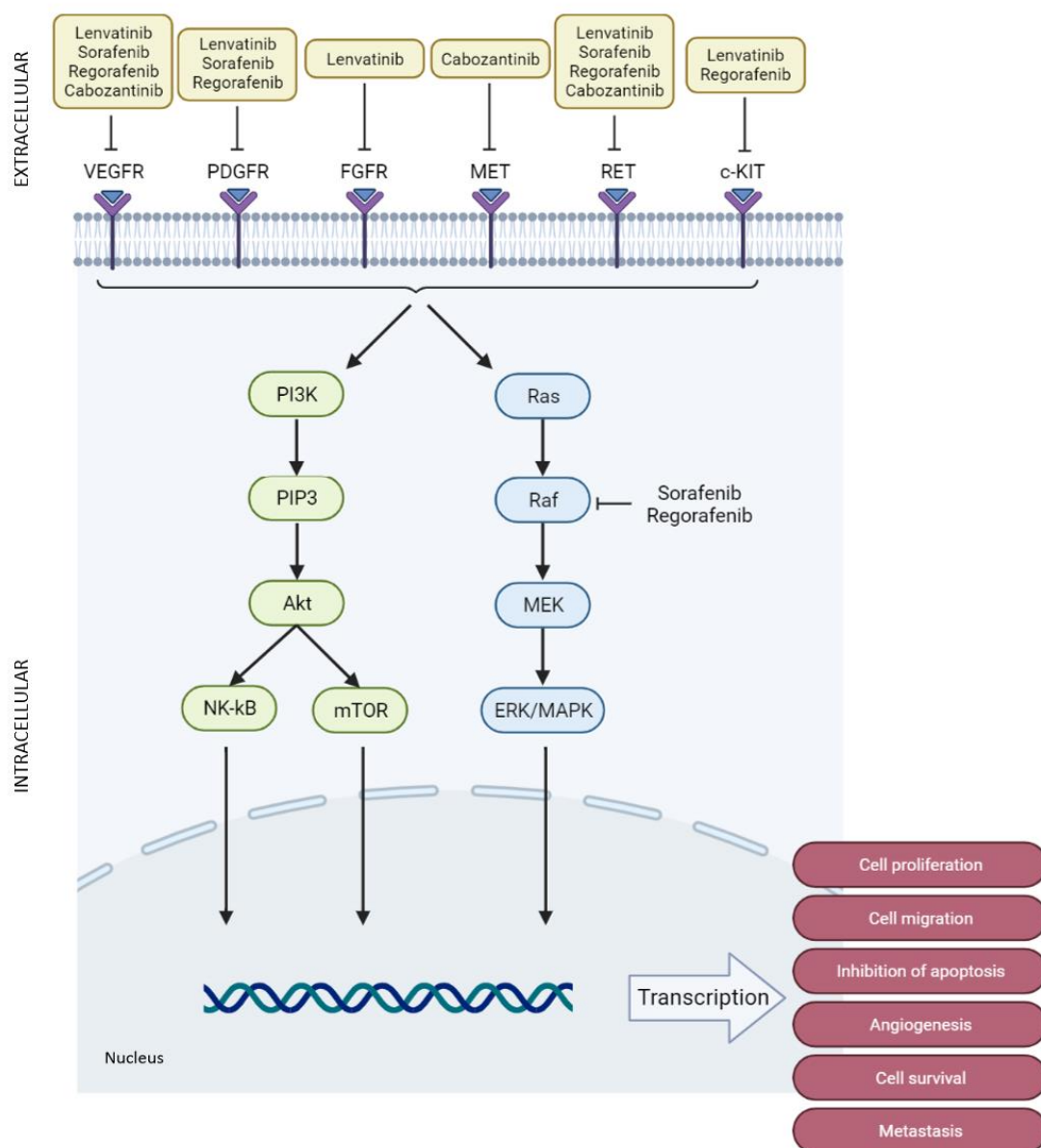
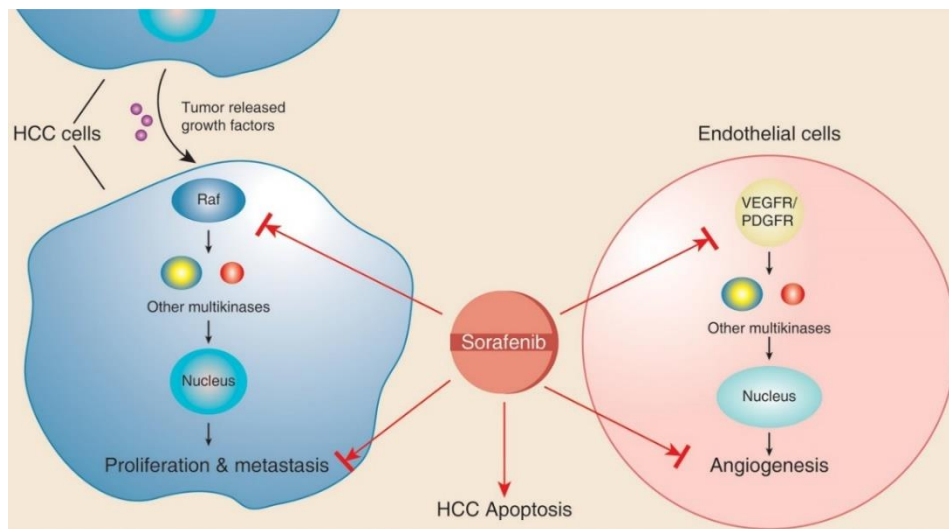


Figure 2 | Mechanism of action of different drugs used for HCC treatment.

### 1.1.1 Sorafenib

Sorafenib was the first drug demonstrating a survival benefit in patients with advanced HCC.<sup>4,17,18</sup> This molecule inhibits several cell surface tyrosine kinases [e.g. vascular endothelial growth factor receptor (VEGFR)-1, (VEGFR)-2, (VEGFR)-3, platelet-derived growth factor receptor (PDGFR)- $\beta$ ] and downstream intracellular serine/threonine kinases in the MAPK cascade, contributing to tumor cell death (**Figure 3**). Besides, sorafenib was found to affect multiple tumor-related signaling pathways, such as those involved in angiogenesis, tumor proliferation, and cell apoptosis (e.g. the PI3K/AKT/mTOR, Wnt/ $\beta$ -catenin, cMET and IGF pathways). Since these pathways are dysregulated in HCC, promoting initiation and progression of this cancer, the use of sorafenib could be advantageous for treatment.<sup>18–22</sup>



**Figure 3 | Mechanism of action of Sorafenib** (adapted).<sup>22</sup>

Moreover, sorafenib appears to have immunomodulatory effects. It affects the immune synapse by modulation of multiple effectors, contributing to an enhanced specific antitumor immune response and reducing suppressive immune populations.<sup>23,24</sup>

Sorafenib has been widely used for adjuvant therapy after surgical resection and ablation.<sup>8</sup> However, besides the survival improvement and delay in progression of advanced HCC, only a limited number of patients have experienced a real and long-term benefit. As sorafenib, chemotherapeutic strategies in general, are associated with dose-limiting toxicity, high rate of tumor recurrence, development of multidrug resistance (MDR) and undesired side-effects, which further restrict their use in the clinical field and constitute a crucial problem in HCC management.<sup>17,18</sup> Therefore, it was necessary to develop new strategies able to overcome these limitations.

## 2 Gene therapy

Over the past decades, gene therapy has been extensively studied to treat several diseases.<sup>25</sup> In general, it refers to the delivery of genetic material to the target cells with a specific purpose, such as to induce a tumor suppressive effect, contributing to the treatment of a particular genetic condition at a sub-molecular level, modifying gene expression, or altering the biological properties of living cells.<sup>26–28</sup>

In the 1990s, Blaese *et al.* conducted the first gene therapy clinical trial in humans, using retroviral-mediated transfer of the adenosine deaminase gene into the T cells of two children with severe combined immunodeficiency.<sup>29</sup> Gene therapy has been extensively studied since.

To date, more than 3000 gene therapy clinical trials have been completed, are ongoing or have been approved worldwide. Given the elevated incidence of cancer, the majority of clinical trials have addressed the treatment of this disease (67.4 %), followed by monogenic (11.6 %), cardiovascular (5.8 %) and infectious (5.8 %) diseases (**Figure 4**).<sup>30</sup> The different targeted cancers include lung, neurological, skin, hematological and gastrointestinal tumours.<sup>31</sup>

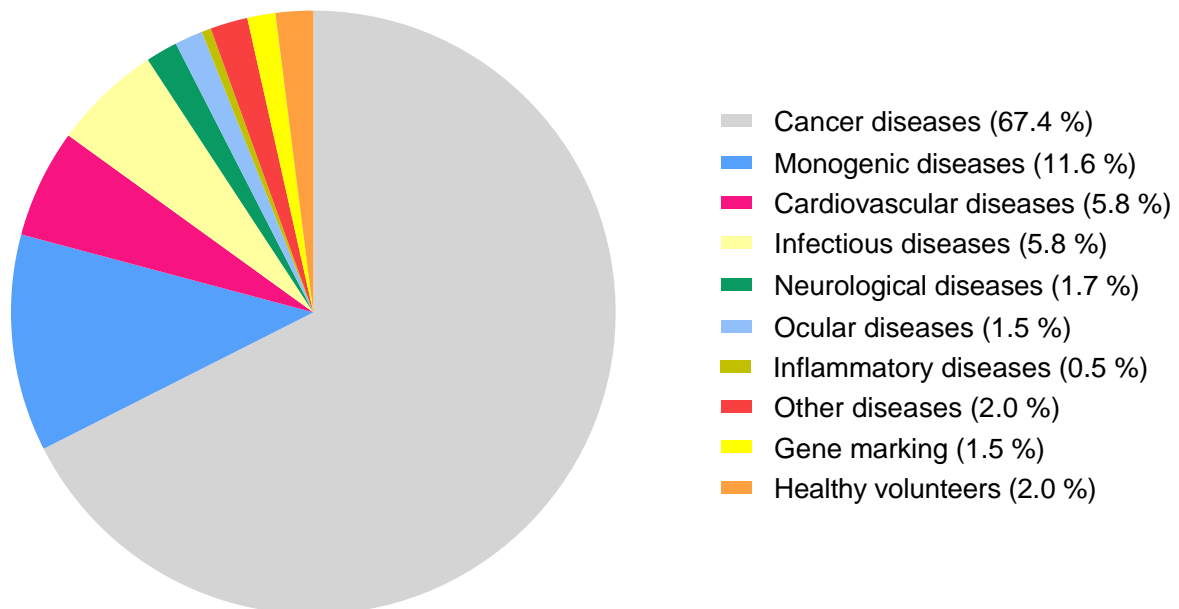


**Figure 4 | Targeted diseases in gene therapy clinical trials worldwide** (adapted).<sup>30</sup>

After several years of investigation, gene therapy was introduced in the market, with the approval of several gene therapy products.<sup>25</sup> Until 2020, EMA (European Medicines Agency) had approved nine gene therapy products, starting in 2012 with the approval of Glybera, a recombinant adeno-associated viral vector, for the treatment of lipoprotein lipase deficiency, followed by Imlygic, in 2015, which uses a genetically modified herpes simplex viral vector to express a human stimulating factor for advanced melanoma treatment, and Strimvelis, in 2016, an *ex vivo* retrovirus-based therapy, for the treatment of adenosine deaminase-deficient severe combined immune deficiency.<sup>32–36</sup>

Given the approval of these medicines, gene therapy demonstrated its high potential, and efforts have been made to apply it to HCC. Numerous preclinical and clinical studies have shown that gene therapy has a positive outcome for HCC patients, being considered a promising strategy to substitute or complement the existing treatments.<sup>27,28</sup>

## 2.1 Molecular targets for HCC gene therapy

Over the past decades, the intensification of mutational analysis in HCC enabled the identification of molecular alterations that represent potential targets for the development of effective gene therapy strategies against this disease. These studies showed that most of the mutations are somatic and occur in tumor suppressor genes or oncogenes.<sup>37</sup> Some of the most altered genes in HCC and their main functions are summarized in **Table 1**. Among them, p53 and PTEN stand out, since their decreased levels of expression were found to be a major contribution for HCC development and progression.

**Table 1 | Altered tumor suppressor and oncogenes identified in HCC patients.**<sup>11,37,38</sup>

Gene	Main Function	Levels of expression in HCC patients
<b>EGFR</b>	Growth factor signaling	Increased
<b>PIK3CA</b>	Proliferation and differentiation	Decreased
<b>PTEN</b>	Tumor suppressor	Decreased
<b>c-myc</b>	Proliferation and differentiation	Increased
<b><math>\beta</math>-Catenin</b>	Proliferation and differentiation	Increased
<b>p53</b>	Cell cycling	Decreased



### 2.1.1 p53 gene

p53 is an endogenous tumor suppressor gene whose functions are crucial for cell maintenance.<sup>39,40</sup> After being activated, tumor suppressor protein p53 has the ability to control cell-cycle arrest, apoptosis, and DNA repair, besides suppressing angiogenesis (Figure 5).<sup>40-43</sup> All of these factors contribute to avoiding cells growth and division, hindering the carcinogenic process.<sup>44,45</sup> This gene could be activated by multiple forms of cellular stress, determining the cell's fate, considering the damage extension and the possibility of reparation.<sup>39,43</sup>

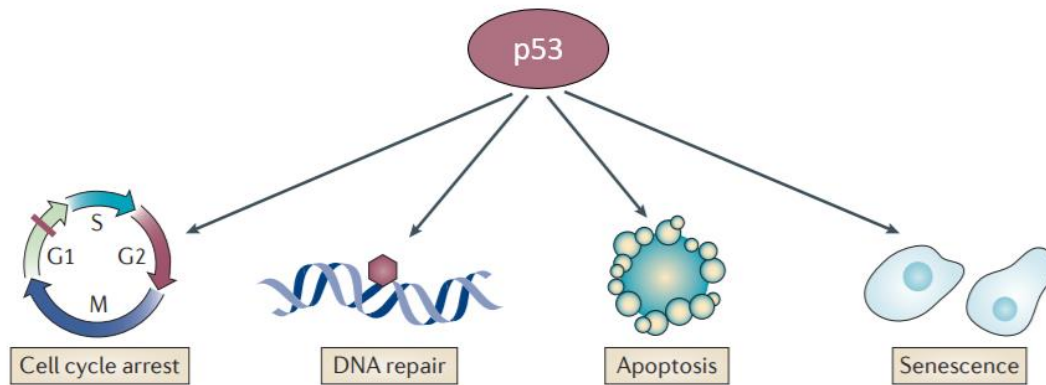


Figure 5 | Main functions of p53 gene (adapted).<sup>46</sup>

Accordingly, tumor development and progression are closely connected to alterations in p53 expression. The majority of human cancers present either abnormal p53 gene or disrupted p53 gene activation pathways, and HCC is not an exception.<sup>43,44,47</sup> The presence of abnormal forms of the protein or the absence of p53 expression has been observed in human HCC-derived cell lines.<sup>43</sup> In fact, a study<sup>48</sup> demonstrated that most of these cell lines present p53 alterations, which suggest that this could be a crucial factor in the transformation of hepatocytes into the malignant phenotype.<sup>49</sup> Furthermore, the p53 gene product mutations were observed in approximately 48% of HCC patients, being associated to a reduced overall survival rate.<sup>50</sup>

The possibility of restoring the normal levels of p53 gene product in cancer cells might be a potential strategy for HCC treatment. This could be achieved through a gene therapy approach mediated by nanoparticles. For example, Kong *et al.* developed a redox-responsive nanoparticle formulation for the effective delivery of p53-encoding synthetic mRNA.<sup>51</sup> The study demonstrated that synthetic p53-mRNA delivered by NPs delayed the growth of p53-null HCC cells, by inducing cell cycle arrest and apoptosis. Furthermore, restoration of p53 levels leads to an increase in sensitivity of tumor cells to everolimus, an

mTOR inhibitor that failed to show clinical benefits in advanced HCC. It was also observed that co-targeting of tumor-suppressing p53 and tumorigenic mTOR signaling pathways results in accentuated antitumor effects *in vitro* and in multiple animal models of HCC.

### 2.1.2 PTEN gene

Phosphatase and tensin homolog (PTEN) is located on human chromosome 10q23 and was first identified as a tumor suppressor gene in 1997.<sup>52,53</sup> PTEN is a dual-specificity phosphatase that presents great ability to dephosphorylate both protein and peptide substrates at tyrosine, serine and threonine sites.<sup>54,55</sup> Lipid phosphatase activity of PTEN is considered the main responsible for its tumor suppressor role since PTEN inhibits PI3K/AKT signaling pathway (**Figure 6**).<sup>56,57</sup> This pathway is involved in cell survival and was found to be frequently dysregulated in several cancers, including HCC.<sup>58,59</sup> PTEN dephosphorylates PIP3 (Phosphatidylinositol (3,4,5)-trisphosphate), a lipid second messenger, preventing its membrane recruitment and, therefore, AKT stimulation.<sup>60</sup> In this case cell death signals are predominant.<sup>59</sup> On the contrary, loss of PTEN contributes to the hyperactivation of AKT, which has been associated with aggressive tumor behaviour.<sup>37,58,59</sup> Loss of PTEN activity was observed in up to 53% of patients diagnosed with HCC, beyond this gene is frequently mutated or even deleted in a smaller proportion of patients.<sup>12,61–63</sup>

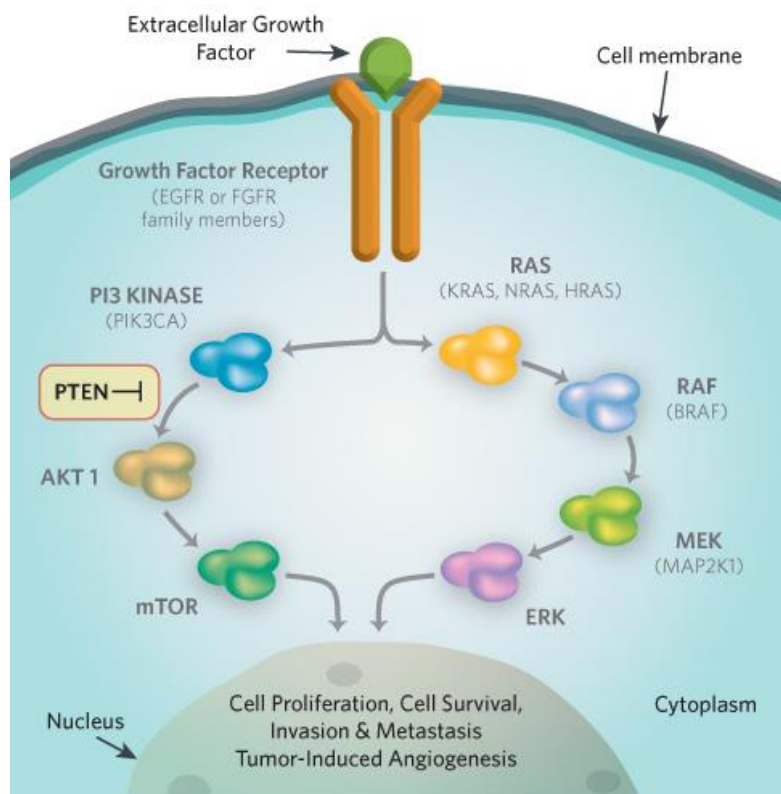


Figure 6 | Tumor suppressor role of PTEN.<sup>64</sup>

### 3 Gene delivery systems

One of the main goals of gene therapy is to correct abnormal gene expression. Therefore, the identification of the main molecular targets in cancer was a major outbreak for the development of gene therapy products, which could offer the possibility to modify the expression profile of these frequently altered genes.<sup>26</sup> For this purpose, several gene delivery systems were developed over decades of investigation.

Gene delivery systems are a crucial part of gene therapy.<sup>26</sup> Contrary to *ex vivo* gene therapy, in which cells are removed from the patient's body, cultured and genetically manipulated outside, and transplanted back into the patients, *in vivo* gene therapy refers to the direct delivery of genetic material into the patient's body in order to induce a therapeutic effect (**Figure 7**). This type of gene therapy takes advantage of the technologies designed to effectively deliver nucleic acids into the target sites, ensuring their stability during circulation.<sup>26,65</sup> The liver is a metabolic organ with a complex vasculature and, therefore, represents a potential target for *in vivo* gene therapy. As a result of its sinusoidal endothelium structure, gene delivery systems could easily be transported from the systemic circulation into the liver parenchyma.<sup>66</sup> These gene delivery systems could be viral or non-viral.<sup>26,65</sup>

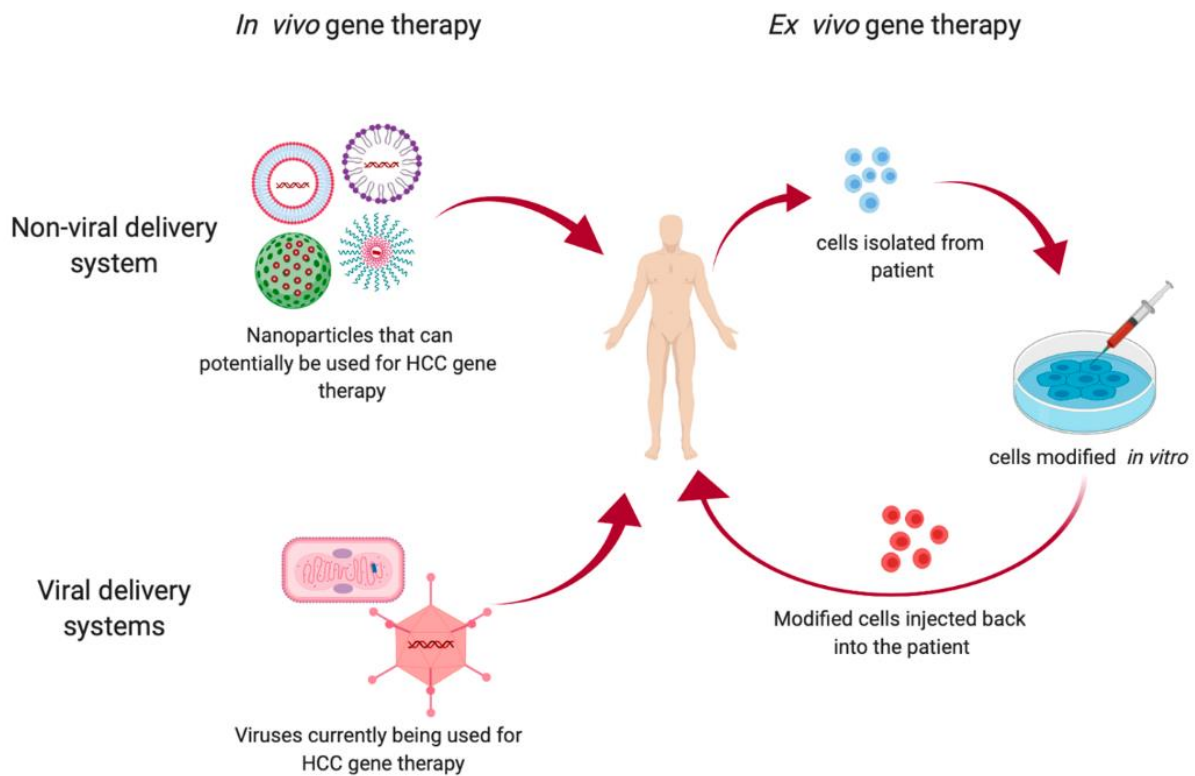


Figure 7 | Types of gene therapy used for HCC treatment.<sup>26</sup>

### 3.1 Viral gene delivery systems

Viral gene delivery systems have been intensively studied over the past decade and include DNA and RNA viruses with single-stranded or double-stranded genomes.<sup>67</sup> These vehicles are used for targeted gene delivery for transient or permanent long-term gene expression.<sup>67,68</sup> Viral gene delivery vectors have the ability to infect and deliver therapeutic genes into the target cells' nucleus.<sup>68</sup>

Some of the main groups of the viral vectors are adenoviruses, adeno-associated viruses, herpes simplex viruses, retroviruses, and lentiviruses. Their advantages and disadvantages are presented at **Table 2**.

**Table 2 | Advantages and disadvantages of the main viral vectors.**<sup>67,69–71</sup>

Viral Vectors	Advantages	Disadvantages
<b>Adenoviruses</b>	<ul style="list-style-type: none"> <li>• Broad host range</li> <li>• Strong immunogenicity</li> <li>• Stability of recombinant vectors</li> <li>• Used in several clinical trials</li> </ul>	<ul style="list-style-type: none"> <li>• Humoral and cellular immune response from high vector doses</li> </ul>
<b>Adeno-associated viruses</b>	<ul style="list-style-type: none"> <li>• Long-term gene expression</li> <li>• Non-pathogenic</li> <li>• Chromosomal integration</li> </ul>	<ul style="list-style-type: none"> <li>• Repeated administration could trigger an immune response</li> <li>• Limited packaging capacity</li> </ul>
<b>Herpes simplex viruses</b>	<ul style="list-style-type: none"> <li>• Broad host range</li> <li>• Long-term gene expression</li> <li>• Low toxicity</li> <li>• Large insert capacity</li> </ul>	<ul style="list-style-type: none"> <li>• Possible residual cytotoxicity</li> <li>• High levels of pre-existing immunity</li> </ul>
<b>Retroviruses</b>	<ul style="list-style-type: none"> <li>• Long-term gene expression</li> <li>• Simple engineering</li> <li>• Low immunogenic</li> </ul>	<ul style="list-style-type: none"> <li>• Random integration</li> <li>• Transduces only dividing cells</li> </ul>
<b>Lentiviruses</b>	<ul style="list-style-type: none"> <li>• Broad host range</li> <li>• Low toxicity</li> <li>• Long-term gene expression</li> <li>• Strong immunogenicity</li> <li>• Transduces dividing and non-dividing cells</li> </ul>	<ul style="list-style-type: none"> <li>• Possible insertional mutagenesis</li> <li>• Packaging construct contains regulatory proteins</li> </ul>

Adenoviruses are the most commonly used viral vectors, mainly because of their flexibility to be genetically modified.<sup>67,72</sup> These viruses consist of non-enveloped double-stranded DNA viruses and have a high capacity for genome insertion, being able to carry therapeutic genes with sizes between 30 and 38 kb.<sup>72</sup> Several oncolytic adenoviruses have been engineered since they can selectively replicate into targeted tumor cells, inducing apoptosis without affecting normal cells.<sup>73</sup> Bai *et al.* developed a novel oncolytic adenovirus containing a Golgi protein promoter and a short hairpin RNA.<sup>73</sup> Transfection of HCC Huh-7 cells showed decreased levels of cell viability and increased apoptotic rate, while no effects were registered in normal human liver cells. In an *in vivo* mouse model, intratumoral injection of this viral vector resulted in a reduction of tumor volume and weight, and prolonged survival time.

Likewise, Li *et al.* constructed a plasmid vector carrying the suicide gene driven by the alpha-fetoprotein promoter to evaluate the cytotoxicity of herpes simplex virus thymidine kinase (HSV-tk)/ gancyclovir (GCV) suicide gene system on hepatocarcinoma cells. HSV-tk can phosphorylate non-toxic GCV, producing phosphorylated products, which can result in cell apoptosis, contributing to tumor cells death. The study demonstrated that the HSVtk gene was effectively expressed in HepG2 cells, showing decreased cell viability and increased cell apoptosis.<sup>74</sup> Accordingly, oncolytic virus therapy is considered one of the major breakthroughs in cancer treatment.<sup>75</sup>

## 3.2 Non-viral gene delivery systems

Besides the several advantages of viral gene delivery vectors and the numerous modifications made aiming to improve their applicability for gene therapy, the use of these vectors is still limited by side effects and safety issues.<sup>76,77</sup> Therefore, non-viral gene delivery systems have been increasingly studied, arising as safer systems.<sup>77</sup> In addition, non-viral vectors are associated with lower immunogenic response and higher gene transport capacity.<sup>76</sup> However, these vectors are associated with lower transfection efficiencies and, therefore, have been engineered in order to overcome this limitation, but also to improve stability and specificity.<sup>76-78</sup>

Contrary to viral vectors, non-viral gene delivery systems are not restricted by the molecular size of the nucleic acid intended to be delivered, having the ability to deliver large genetic payloads.<sup>76,78,79</sup> Considering the treatment purpose, several types of nucleic acids

could be introduced as therapeutic agents using these vectors, such as small interfering RNA (siRNA), which prevents the translation of oncogenic messenger RNA (mRNA) or nucleic acids encoding a downregulated tumor suppressor gene or suicide genes, which lead to cancer cells death.<sup>26,27,80</sup> Nanotechnology-based non-viral delivery systems have been extensively studied for the delivery of these therapeutic agents.<sup>79</sup>

The term nanotechnology includes all aspects of understanding, manipulating, and manufacturing matters into nanoscale, typically within the range of 1–100 nm.<sup>81</sup> A wide variety of nanocarriers, have been developed with different properties and can be divided into polymeric, inorganic and lipid-based nanocarriers (**Figure 8**).<sup>81</sup> To choose the most adequate delivery vector is essential to take into account the properties of the therapeutic agents, as well as the advantages and limitations associated to each category of nanocarriers (**Table 3**).

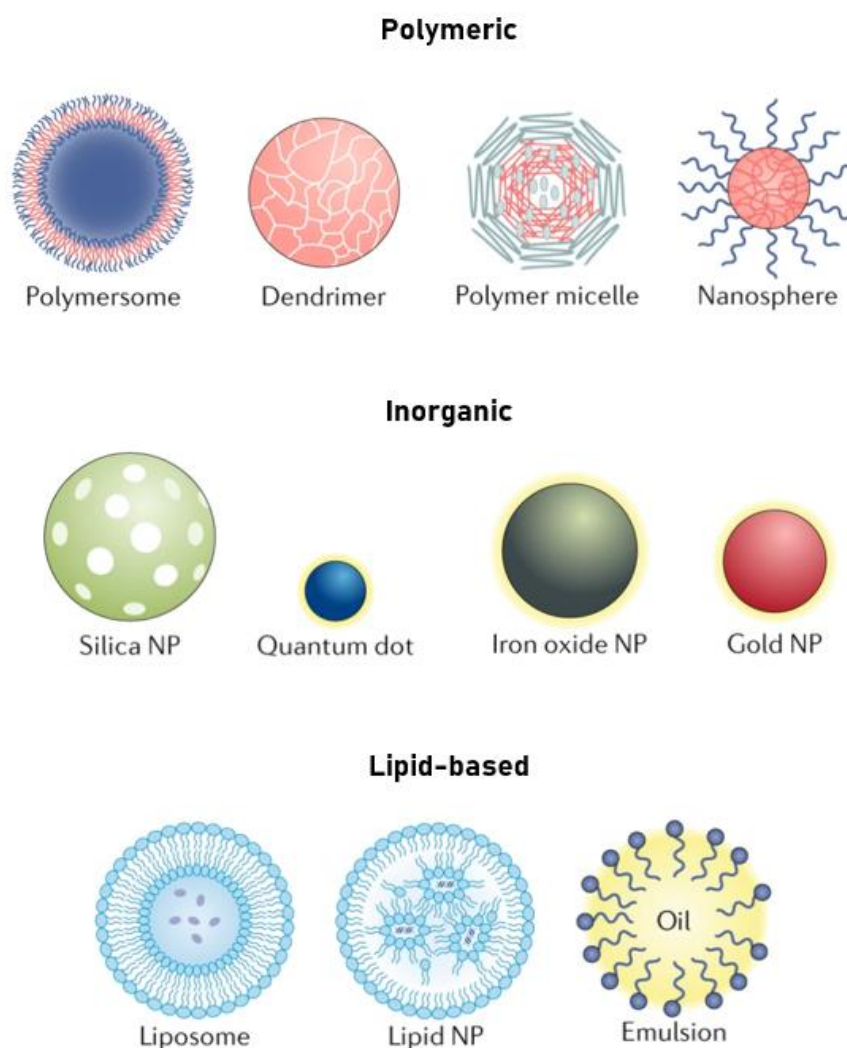


**Figure 8 | Representation of different non-viral gene delivery systems, divided into polymeric, inorganic and lipid-based nanocarriers (adapted).<sup>82</sup>**

**Table 3 | Advantages and disadvantages of the main classes of non-viral gene delivery vectors.**<sup>82</sup>

<b>Non-viral Vectors</b>	<b>Advantages</b>	<b>Disadvantages</b>
<b>Polymeric nanocarriers</b>	<ul style="list-style-type: none"> <li>• Precise control of particle characteristics</li> <li>• Payload flexibility for hydrophilic and hydrophobic cargo</li> <li>• Easy surface modification</li> </ul>	<ul style="list-style-type: none"> <li>• Possibility for aggregation and toxicity</li> </ul>
<b>Inorganic nanocarriers</b>	<ul style="list-style-type: none"> <li>• Unique electrical, optical and magnetic properties</li> <li>• Suitable for theragnostic applications</li> </ul>	<ul style="list-style-type: none"> <li>• Variability in size, structure and geometry</li> <li>• Toxicity and solubility limitations</li> </ul>
<b>Lipid-based nanocarriers</b>	<ul style="list-style-type: none"> <li>• Simple formulation with different physicochemical properties</li> <li>• Payload flexibility</li> <li>• High bioavailability</li> </ul>	<ul style="list-style-type: none"> <li>• Low encapsulation efficiency</li> </ul>

In the context of cancer, nanotechnology can provide a set of tools needed to design and synthesize delivery vehicles that can carry sufficient payloads and efficiently cross physiological barriers to reach target sites, allowing a safe, effective and specific delivery.<sup>81</sup> Particularly, polymeric nanoparticles (NPs) have shown great potential for controlled and sustained co-delivery of drugs and genes, due to many unique features of polymers.<sup>83</sup>

### 3.2.1 Polymeric nanoparticles

Polymeric NPs are polymer-based colloidal macromolecules whose sizes are in the order of nanometres.<sup>84,85</sup> These nanocarriers have been widely used in nanomedicine, namely for targeted drug delivery, sustained release, and as a theragnostic carrier.<sup>84,85</sup> In the context of cancer, besides chemical drugs, many other therapeutic agents, such as nucleic acids, proteins, and photosensitizers, can be loaded into polymeric NPs.<sup>83</sup> These nanocarriers enable prolonged circulation and targeted delivery of the therapeutic agents, resulting in higher therapeutic efficacy and reducing adverse side effects due to alterations in the body distribution.<sup>86</sup>

The unique properties of polymeric NPs are mainly due to specific characteristics of the polymers, such as biocompatibility, tunable chemical structure, controllable molecular weight, and biodegradability. Besides, functional groups could be conjugated for multiple

purposes, highlighting targeting. Therefore, the design of these nanocarriers is easily controlled, making it possible to acquire the desired characteristics.<sup>25,83,87</sup>

Polymeric NPs could be synthesized through various techniques, such as emulsification, nanoprecipitation, microfluids and ionic gelation. Each technique results in a different final product, with different characteristics.<sup>82</sup> Depending on morphology, composition, and physicochemical properties, these nanocarriers are divided into different sub-classes, such as nanocapsules and nanospheres.<sup>82,88,89</sup> While the term nanocapsule refers to cavities surrounded by a polymeric shell, nanospheres consist of systems composed of a solid matrix. Within these classes could be found polymersomes, micelles and dendrimers, according to the shape of the nanocarrier.<sup>82</sup>

### 3.2.1.1 Polymeric micelles

Micelles consist of polymeric particles formed by amphiphilic block copolymers (ABCs) with a size range within 5–100 nm and have been widely studied as nano-scaled drug and gene delivery systems, showing promising results.<sup>90</sup>

Amphiphilic molecules are composed of hydrophilic and hydrophobic groups, which present complete opposite polarities and, consequently, exhibit opposite affinities toward a given solvent. Therefore, polymeric micelles present a hydrophobic inner core, able to protect drugs from degradation, and a hydrophilic outer shell, which can prevent opsonization (**Figure 9**).<sup>81</sup>

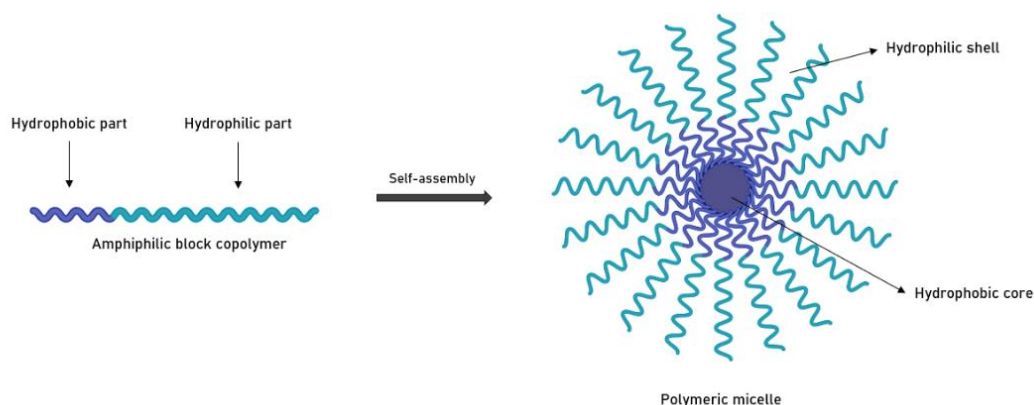


**Figure 9 | Representation of a polymeric micelle formed through the self-assembly of amphiphilic block copolymers.**



The hydrophobic interior of micelles acts as a pool for non-water soluble drugs.<sup>91</sup> The most popular hydrophobic polymers are poly( $\epsilon$ -caprolactone) (PCL), poly(*n*-butyl acrylate) (PnBA), polylactide (PLA) and poly(lactic-*co*-glycolic acid) (PLGA).<sup>91</sup> Another hydrophobic polymer that could be used for the production of polymeric micelles is Poly(2-(diethylamino)ethyl methacrylate) (PDEAEMA). This is a pH-responsive polymer, used to deliver both genes and drugs.  $pK_a$  of PDEAEMA is 7.2, which means that at physiological pH the polymer is hydrophobic. However, in acidic conditions, as the endolysosomal pathway, protonation of amine groups occurs, and the polymer becomes hydrophilic. This allows disintegration of polymeric micelles produced with PDEAEMA, which is an efficient way to release the encapsulated drugs.<sup>92,93</sup> The outer shell is often composed of cationic polymers, that offer the possibility to complex with negatively charged DNA or RNA.<sup>91</sup> Examples of cationic polymers that could be used in the production of polymeric micelles are poly(2-(dimethylamino)ethyl methacrylate) (PDMAEMA), poly( $\beta$ -amino ester) (P $\beta$ AE) and Poly(2-aminoethyl methacrylate) (PAMA).<sup>94-96</sup>

One of the main advantages of polymeric micelles is that they can enhance the solubility of poorly soluble therapeutic agents in aqueous solutions and protect them from enzymatic degradation or elimination.<sup>83</sup> This contributes to increased blood circulation times and improved biodistribution.<sup>83</sup> Delivery of anticancer agents in the form of micelles also ensures reduction in the therapeutic dosage and frequency due to the controlled release properties, resulting in reduced undesired effects in normal tissues.<sup>81</sup>

Importantly, micelles can be tailored according to the molecules that are intended to deliver, altering the molecular weight of the polymer or the chemical structure. These modifications will affect several properties of the polymeric micelles, and consequently the therapeutic effect of the loaded anticancer agents.<sup>12</sup>

However, one of the main advantages of polymeric micelles is the fact that they can be easily functionalized<sup>91</sup>, through the conjugation of targeting groups on the surface.<sup>91,97</sup> These groups could be proteins (antibodies), nucleic acids, peptides, or carbohydrates, and promote active targeting.<sup>97,98</sup> Therefore, the therapeutic agents encapsulated into the polymeric micelles could be effectively delivered into the tumor site, without causing adverse effects to the normal tissues.<sup>98</sup> This is one of the crucial properties of these nanocarriers that make them stand out in the field of co-delivery. Co-delivery of chemical drugs and genes using polymeric micelles can contribute to a synergistic effect, improving the efficacy of

cancer treatments.<sup>83</sup> **Table 4** presents some examples of the use of polymeric micelles to simultaneously deliver drugs and genetic material to different kinds of cancer cells.

**Table 4 | Gene therapy studies involving polymeric micelles for co-delivery of drugs and genes.**

Micelles composition	Delivered agents		Cancer type	Reference
	Drug	Genetic material		
Hyaluronic acid-based amphiphilic conjugate (HA-ss-(OA-g-bPEI), HSOP)	Paclitaxel	AURKA specific siRNA	Breast cancer	99
PDMAEMA-PCL-PDMAEMA triblock copolymers	Paclitaxel	VEGF siRNA	Caucasian prostate adenocarcinoma	100
mPEG- <i>b</i> -PCL- <i>b</i> -PPEEA triblock copolymers	Paclitaxel	Plk1 specific siRNA	Breast cancer	101
Gd-PEG <sub>5k</sub> -PCL <sub>2k</sub> and PEI <sub>2k</sub> -PCL <sub>2k</sub> copolymers	Doxorubicin	miR-34a	Breast cancer	102
Polyethylenimine (PEI) modified by grafting stearic acid (SA)	Doxorubicin	VEGF siRNA	Human hepatoma	103
MPEG-PCL- <i>g</i> -PEI triblock copolymers	Doxorubicin	Msurvivin T34A	Lung cancer	104
Folate-conjugated triblock copolymer (Fa-PEG-PEI-PCL, Fa-PEC)	Temozolomide	Anti-BCL-2 siRNA	Glioma	105
Chitosan-ss-polyethylenimine-urocanic acid (CPU)	Doxorubicin	TLR4-siRNA	Lung cancer	106
POEG-st-Pmor	Doxorubicin	IL-36 $\gamma$ expression plasmid	Lung metastasis and breast cancer	107
PDMA- <i>b</i> -PCL	SN-38	VEGF siRNA	Colorectal cancer	108

For example, Xie *et al.* developed hybrid micelles, based on the amphiphilic diblock copolymers, polyethylenimine-polycaprolactone (PEI-PCL) and diethylenetriaminepentaacetic acid gadolinium (III) (Gd-DTPA)-conjugated polyethyleneglycol-polycaprolactone (Gd-PEG-PCL). These micelles were intended to co-deliver doxorubicin and microRNA-34a (miR-34a) to breast cancer cells. According to the obtained results, the generated micelles deliver the therapeutic agents into the cells via endocytosis. Doxorubicin inhibited cell proliferation, while miR-34a (which expression is

significantly reduced in MDA-MB-231 breast cancer cells, leads to the downregulation of Bcl-2, cyclin D1, CDK6, and Bax expression, consequently inhibiting cell proliferation and migration. In addition, these micelles showed increased accumulation in tumor tissues, improving the combined efficiency of the chemotherapy and gene therapy strategies, as well as magnetic resonance imaging of solid tumors, demonstrating their potential as theragnostic agents.<sup>102</sup>

## Polymeric micelles production

Amphiphilic copolymers contain both hydrophilic and hydrophobic segments in the same macromolecule structure, which leads to a self-assembly behavior since these segments present opposite affinities in an aqueous solvent.<sup>109</sup> When these copolymers are dissolved, in a selective solvent, at a concentration above their critical micelle concentration (CMC), one part of the copolymer could dissolve more easily than the other part. For this reason, hydrophobic segments tend to pack together, forming the hydrophobic core, and the hydrophilic segments tend to exclude each other adjacently for better entropic compensation, forming the hydrophilic shell of the polymeric micelles.<sup>109,110</sup>

Therefore, polymeric micelles can be produced through the self-assembly of amphiphilic copolymers.<sup>111</sup> Numerous techniques have been developed to produce this type of nanocarriers, such as emulsification and solvent evaporation (emulsification), double emulsification and solvent evaporation (double emulsification), nanoprecipitation and film dispersion.<sup>83,109</sup> **Table 5** presents the advantages and disadvantages of each technique mentioned above.

The nanoprecipitation method is the most commonly used to encapsulate hydrophobic bioactive agents. In this case, occurs a rapid desolvation of the amphiphilic copolymer and the drug when the solvent is added to the non-solvent. After the elimination of the organic solvent is usually achieved through evaporation or dialysis. Besides being a simple method, nanoprecipitation allows the preparation of large quantities of polymeric nanocarriers.

Table 5 | Advantages and disadvantages of different methods to produce polymeric micelles.<sup>109</sup>

Method	Emulsification	Double emulsification	Nanoprecipitation	Film dispersion
<b>Advantages</b>	<b>Operation process:</b> <ul style="list-style-type: none"> <li>Rapid reaction.</li> </ul> <b>NPs features:</b> <ul style="list-style-type: none"> <li>Good stability.</li> <li>Small size.</li> <li>Uniform morphology.</li> </ul>	<b>Operation process:</b> <ul style="list-style-type: none"> <li>Rapid reaction.</li> </ul> <b>NPs features:</b> <ul style="list-style-type: none"> <li>Uniform morphology.</li> <li>Slow-release behavior of the drug.</li> <li>Suitable for hydrophobic/hydrophilic bioactive agents.</li> </ul>	<b>Operation process:</b> <ul style="list-style-type: none"> <li>No surfactant and emulsifier.</li> <li>Large quantities preparation.</li> </ul> <b>NPs features:</b> <ul style="list-style-type: none"> <li>Suitable for encapsulation of unstable bioactive agents.</li> </ul>	<b>Operation process:</b> <ul style="list-style-type: none"> <li>Rapid reaction.</li> <li>No surfactant and emulsifier.</li> <li>Simple operation.</li> </ul> <b>NPs features:</b> <ul style="list-style-type: none"> <li>Small size.</li> </ul>
<b>Disadvantages</b>	<b>Operation process:</b> <ul style="list-style-type: none"> <li>Not suitable for unstable bioactive agents.</li> </ul> <b>NPs features:</b> <ul style="list-style-type: none"> <li>Not suitable for encapsulation of hydrophilic drug</li> </ul>	<b>Operation process:</b> <ul style="list-style-type: none"> <li>Complex operation and influencing factors.</li> <li>Not suitable for encapsulation of unstable bioactive agents.</li> </ul> <b>NPs features:</b> <ul style="list-style-type: none"> <li>Larger average size.</li> </ul>	<b>Operation process:</b> <ul style="list-style-type: none"> <li>Long time-consuming.</li> </ul> <b>NPs features:</b> <ul style="list-style-type: none"> <li>Inhomogeneous morphology.</li> </ul>	<b>NPs features:</b> <ul style="list-style-type: none"> <li>Not suitable for encapsulation of hydrophilic bioactive agents.</li> <li>Poor stability.</li> </ul>

### 3.2.1.2 Polyplexes

Polyplexes consist of complexes formed through the electrostatic interactions established between cationic polymers and genetic material.<sup>77,80</sup> These structures are able to condense a great amount of DNA to a high density, since cationic polymers can embed it in major grooves, protecting the genetic material from enzymatic degradation.<sup>112,113</sup> These nanocarriers have been demonstrating their gene delivery potential and proved to be advantageous mainly because they are made from self-assembling and non-immunogenic components.<sup>113</sup> Additionally, physicochemical properties of these nanosystems could also be

manipulated in order to enhance cellular uptake, promote endosomal escape and/or facilitate nuclear import to enhance transgene expression.<sup>114</sup>

Because of these advantages, several gene therapy studies have been conducted using polyplexes for cancer treatment (**Table 6**). For example, Kloeckner *et al.* developed PEI-based polyplexes for gene delivery to hepatocellular carcinoma cells.<sup>115</sup> Linear PEI with a molecular weight of 22 kDa was mixed with various amounts of conjugates composed of murine epidermal growth factor (EGF), PEG and branched PEI (25kDa). While EGF protein binds to EGF receptor (EGFR) on the surface of the cells promoting endocytosis, PEG has the ability to mask polyplex surface charge. DNA complexes were produced using reporter plasmids. Cells were previously treated with amphiphilic photosensitizers, which were activated by light after transfection. The activation of these photosensitizers, located on the membranes of the endocytic vesicles, resulted in the destruction of the endocytic membrane and, consequently the release of the endocytosed polyplexes into the cytosol. This resulted in enhanced and specific transgene expression.<sup>115</sup>

**Table 6 | Gene therapy studies involving polyplexes for cancer treatment.**

Polyplexes composition	Type of genetic material	Cancer type	Reference
mPEG-b-PLA-PHis-ssOEI	siRNA	Breast Adenocarcinoma	116
four-arm PEO-b-PDEAEMA block copolymer	pDNA	Neuroblastoma	93
Lipid-coated PDMAEMA	pDNA	Ovarian Carcinoma	117
PEG-PCD-F copolymer	siRNA	Melanoma and Breast Cancer	118
PEI (22kDa) conjugated with EGF-PEG-PEI (25 kDa)	pDNA	Hepatocellular Carcinoma	115
PVTC and POEGMA	siRNA	Ovarian Carcinoma	119
PEI-PEG-PCP	siRNA	Prostate Cancer	120
Cholesterol-modified HPMA and NAS copolymers	siRNA	Glioblastoma	121
Arginine-rich oligopeptide-grafted bPEI modified with PEG	DNA and siRNA	Breast Cancer	122

### 3.2.1.3 Glycopolymers

Glycopolymers are synthetic polymers containing carbohydrate groups in their structure, added to the polymers to promote targeting, and have attracted attention due to their relevance in biomedical applications, such as drug and gene delivery.<sup>111,123</sup> Accordingly, carbohydrate ligands have been widely used to achieve specific delivery to HCC. Lectins are a group of proteins, which specifically bind to certain sugars, through hydrogen bonding, van der Waals' interactions, and hydrophobic stacking at the molecular level.<sup>123</sup> Low toxicity of these polymers and high expression of these receptors are some of the advantages of exploiting carbohydrate–receptor interactions. One major receptor responsible for this specificity is the asialoglycoprotein receptor (ASGPR), belonging to the lectins group, which is found predominately on the surface of hepatocytes and HCC cells, but minimally on nonhepatic cells.<sup>124</sup> Glycopolymers are able to mimic biological functions of natural oligosaccharides and glycan in recognition processes involving lectins.<sup>123</sup> Some glycoproteins with sugar groups such as galactose and lactose, as well as the sugar derivatives, lactobionic acid and galactosamine, can be used as targeting ligand for ASGPR-mediated drug delivery by following a similar mechanism as the sugar residues. Particularly, the glycoprotein asialofetuin, which is considered the natural ligand for ASGPR, possesses terminal N-acetylgalactosamine residues and exhibits high affinity towards this receptor, promoting the internalization by HCC cells.<sup>125,126</sup>

For example, Li *et al.* developed galactose-based glycopolymers, poly(N-(prop-2-enoyl)- $\beta$ -D-galactopyranosylamine)-b-poly(N-isopropyl acrylamide) (pGal(OH)-b-pNIPAA), which undergo collaborative assembly with hydrophilic doxorubicin hydrochloride. The generated nanoparticles presented uniform size and high efficiency in terms of drug loading and encapsulation. Because they were taken up through an ASGPR-mediated mechanism, these nanosystems resulted in enhanced cellular uptake by HepG2 cells and high antitumor efficacy *in vitro*.<sup>127</sup>

Glycopolymers can be synthesized by polymerization of a monomer containing saccharide functionality or by post-functionalization of presynthesized polymer scaffolds. Controlled polymerization techniques, such as reversible addition-fragmentation chain transfer (RAFT) and atom transfer radical polymerization (ATRP), allow the preparation of polymers with low polydispersity and well-controlled molecular weights, besides different compositions and architectures. Therefore, it is possible to produce adequate polymers according to the target and the molecules that are intended to load.<sup>111</sup>

Compared with other synthetic polymers, glycopolymers stand out because of their biocompatibility and biodegradability. Moreover, these sugar based-materials are nonimmunogenic, making them particularly suitable for *in vivo* therapeutic applications.<sup>111</sup>

### 3.2.1.4 Cationic polymers

On the other hand, polycationic polymers have received increased attention in gene therapy due to their attractive properties. The first cationic polymer used for gene therapy was Poly-L-lysine (PLL). Together with PEI, these are the cationic polymers most commonly applied in the field of gene therapy.<sup>112</sup> The chemical structures of these polymers are presented in **Figure 10**.

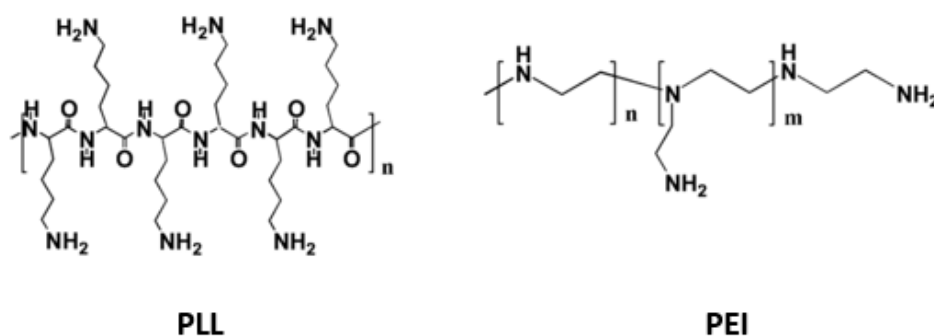


**Figure 10 | Chemical structures of the cationic polymers Poly-L-lysine (PLL) and Polyethylenimine (PEI).**<sup>128</sup>

The structure of cationic polymers could be linear, branched, or dendrimeric and, in opposite to amphiphilic copolymers, do not include hydrophobic groups, making these polymers completely soluble in an aqueous solution.<sup>113,129</sup> On the contrary, includes several amine groups, which  $pK_a$  values are above or near physiological pH, making them positively charged compounds. Therefore, these polymers could electrostatically interact with negatively charged genetic material, forming the polyplexes. Examples of polymers that proved to be effective for transport and delivery of genetic material are PDMAEMA, P $\beta$ AE and PAMA, whose chemical structures are presented in **Figure 11**.<sup>94-96</sup> PDMAEMA is a dual-responsive polymer (temperature and pH)<sup>94</sup>, while P $\beta$ AE stands out because of its biodegradability and biocompatibility.<sup>95</sup> In the case of PAMA, this polymer was found to promote high transfection efficiency, due to its longer polymer chains, since they lead to higher levels of cellular internalization.<sup>130</sup>

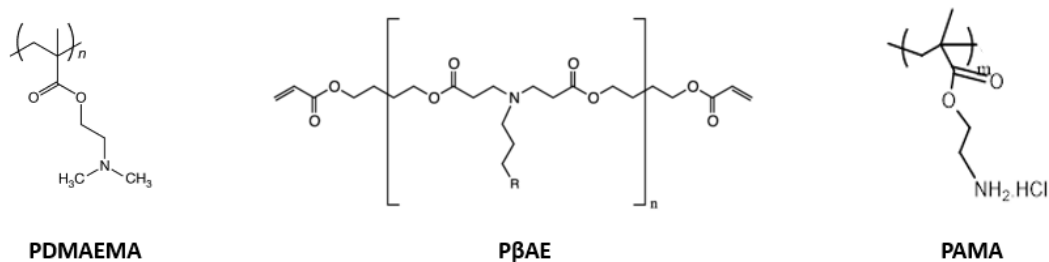


**Figure 11 | Chemical structures of the cationic polymers Poly(2-(dimethylamino)ethyl methacrylate) (PDMAEMA), Poly( $\beta$ -amino ester) (P $\beta$ AE) and Poly(2-aminoethyl methacrylate) (PAMA).**

### 3.2.2 Cellular uptake and intracellular route

Given the fact that for gene therapy to occur, nucleic acids need to penetrate the target cells, it becomes clear that internalization is one of the cellular obstacles that nanocarriers must overcome (**Figure 12**).<sup>113</sup> Along the entire route from the injection point to the target cells, nanocarriers should present low toxicity, preventing adverse side effects, and the ability to avoid elimination by the immune system. Besides, the encapsulated genetic material must be kept stable and protected from enzymatic degradation, so it is possible to achieve the desired effect.<sup>112,113</sup> Understanding the mechanisms underlying cellular uptake and intracellular trafficking is crucial to achieve adequate nanocarriers for a certain purpose, by tuning their physicochemical properties.<sup>131</sup>

Endocytosis is the main uptake process in cells. Besides nutrients and other substances, most nanocarriers are also thought to be taken up by this mechanism, which can be divided into phagocytosis and pinocytosis.<sup>110</sup> Phagocytosis is the most common process for the uptake of large particles, but can only take place in professional phagocytes, such as monocytes, macrophages, neutrophils and dendritic cells, or other cells with lower phagocytic activity, such as fibroblasts, endothelial and epithelial cells. Contrary to phagocytosis, pinocytosis can be performed by nearly all cells and includes clathrin-mediated endocytosis, caveolae-mediated endocytosis, clathrin/caveolae-independent endocytosis and macropinocytosis.<sup>110,132</sup>

Clathrin-mediated endocytosis is believed to be the main process for the polymeric micelles cellular uptake.<sup>132</sup> This pathway takes advantage of the highly expressed surface receptors on cancer cells, which form ligand-receptor complexes on the surface of the cellular membrane.<sup>98,133</sup> These complexes further move to clathrin rich sites and are engulfed



through the formation of clathrin-coated vesicles, which detach from the complexes once they are inside the cell.<sup>133</sup> After attaching to the specific receptors, ligands can mediate the accumulation of the nanosystems inside the tumor site, which increases the cytotoxicity in these tissues and reduces the delivery of the payloads to normal tissues.<sup>98</sup>

Cellular uptake of polyplexes also involves endocytosis, which is promoted by the interactions between the cationic surface charge and the anionic cell-surface proteoglycans.<sup>112,134</sup> These electrostatic and non-specific interactions promote internalization through adsorptive endocytosis.<sup>80,134</sup> The successful internalization depends on the cell type and the polymer used. However, it has been reported that this process not only involves the electrostatic binding of the nanocarrier to the cellular membrane but also the aid of syndecan molecules.<sup>113,114,134</sup> These molecules are transmembrane proteins that form a cluster and trigger protein kinase C. This results in the actin-binding to the cytoplasmic tail of the syndecan molecule, following polyplex engulfment.<sup>114</sup>

When these nanocarriers possess ligands that bind to ASGPR, the interactions between the ligands and the receptor take place in clathrin-coated vesicles of the membrane. This means that these nanocarriers are internalized via clathrin-mediated endocytosis.<sup>124</sup>

Once inside the cell, both nanosystems are targeted to degradative lysosomes. First, they will be transported into early endosomes (pH ~ 6), which takes the cargo to the target sites, losing part of it to the plasma membrane via recycling endosomes. Early endosomes further mature into late endosomes (pH ~ 5), which will fuse with prelysosomal vesicles to form lysosomes. Lysosomes have an acidic (pH ~ 4–5) and enzyme-rich environment to promote degradation. In the case of polymeric micelles, this microenvironment could be utilized to release the drug after degradation of the carrier, but only when the drugs are stable under these harsh conditions.<sup>110</sup> Several strategies have been engineered to promote the dissociation of these nanosystems. For example, some polymers could be degraded by responding to intracellular stimuli, such as pH, temperature or light.<sup>134</sup> In the case of polyplexes, the pH decrease along the endolysosomal pathway leads to the successive protonation of the polymer amine groups, depending on their pKa.<sup>135</sup> This increases the influx of chloride ions and water, resulting in vesicle swelling, consisting of the so-called “proton sponge effect”. This process was initially believed to induce the rupture of the vesicles and release of polyplexes content into the cytosol. More recently, this process of endolysosomal escape has been associated to a direct destabilization of the phospholipid membrane, caused by the pH-triggered increase of cationic charge density.<sup>113,135</sup>

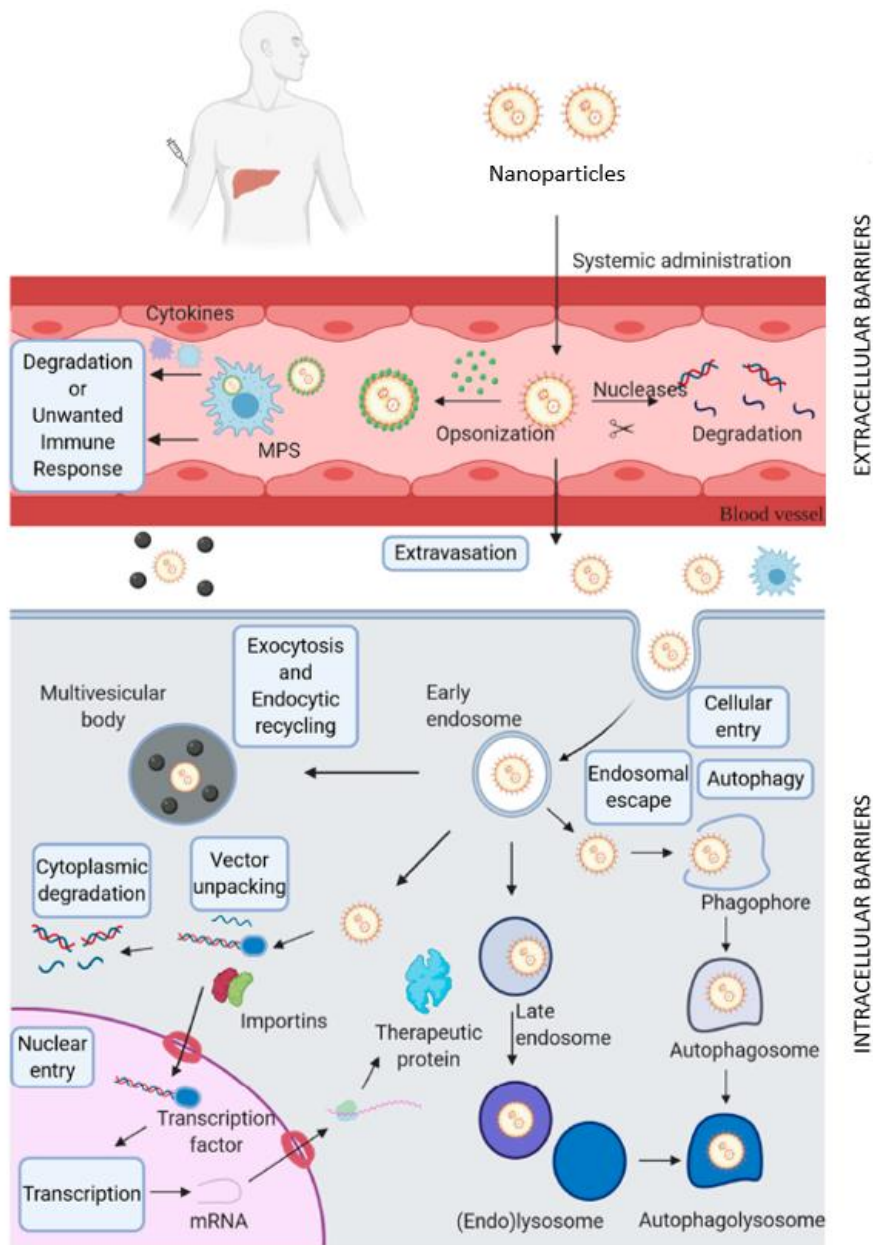


**Figure 12 | Extracellular and intracellular barriers for the effective delivery of genetic material into target cells (adapted).<sup>136</sup>**

After avoiding lysosomal degradation, the released genetic material needs to enter the cell nucleus. It has been reported that DNA enters the nucleus in a passive manner, when the nuclear membrane is disassembled during the process of cell division, or via active transport through the nuclear pores. This culminates in the genetic material expression and the obtention of the pretended therapeutic effect.<sup>134</sup>

## 4 Aim of the present work

Hepatocellular Carcinoma is considered a major health problem and represents the fourth leading cause of cancer-related deaths worldwide. The existing treatment options include surgical modalities, which are often discarded due to advanced stage of the disease and reduced liver function, and systemic chemotherapy, which do not represent a long-term benefit and is always accompanied by undesired side effects.

On the other hand, gene therapy has been demonstrating its potential for the treatment of several diseases. The application of gene therapy in the clinical field takes advantage of the development of gene delivery systems. Among the different vectors, non-viral gene delivery systems arise as safer systems and, particularly, polymeric nanocarriers have been standing out because they enable prolonged circulation and targeted delivery of the therapeutic agents.

Taking this into account, the main purpose of this work was to develop a new polymer-based nanosystem able to effectively deliver genetic material into hepatocellular carcinoma cells, in a specific manner. Copolymers used for the preparation of the nanosystems were synthesized through a controlled polymerization method, which offers the possibility to obtain polymers with well-defined properties. Different polymeric nanocarriers were developed, extensively characterized, and evaluated as gene delivery systems to HCC cells. Moreover, some strategies to improve transgene expression were applied, with the final objective of developing a therapeutic approach for HCC treatment.



# Chapter 2

## Materials and Methods

### 1 Synthesis of the glycopolymers

The glycopolymers used to prepare the different nanosystems were previously synthesized in the Polymer Synthesis and Characterization group, PolySyc, at the Chemical Engineering Department of FCTUC. The synthesis process followed an atom transfer radical polymerization (ATRP) method and then the molecular weight parameters were measured through nuclear magnetic resonance spectroscopy ( $^1\text{H}$  RMN).

### 2 Preparation of polymeric micelles and micelleplexes

Polymeric micelles were produced through the nanoprecipitation method, using two amphiphilic glycopolymers, PAMA<sub>103-*co*</sub>-PLAMA<sub>19-*b*</sub>-PDEAEMA<sub>63</sub> (Polymer 1) and PAMA<sub>50-*co*</sub>-PLAMA<sub>10-*b*</sub>-PDEAEMA<sub>16</sub> (Polymer 2). Briefly, these glycopolymers were dissolved in the organic solvent, TFE (trifluoroethanol) (Fisher Scientific, NH, USA), for one hour at 30°C, and then, were added dropwise to carbonate buffer pH 10. This solution was kept under stirring for 30 minutes, at 30°C. Afterwards, the organic solvent was removed using the rotary evaporator and the colloidal solution was left in dialysis, overnight, against water.

These polymeric micelles were used to produce micelleplexes according to the pretended polymer/DNA (N/P, +/-) charge ratio. For this purpose, 1  $\mu\text{g}$  of the genetic material, a plasmid that codes for luciferase, pLUC, was added to the micelles colloidal solution, followed by a 15 minutes incubation at room temperature. Micelleplexes were immediately used after preparation.

### 3 Preparation of sorafenib-loaded micelles

As polymeric micelles are intended to be used for drug delivery, sorafenib was loaded into the micelles produced as described above. In parallel with the dissolution of the glycopolymers, 1 mg of sorafenib was dissolved in TFE, in the same conditions, and the

solutions were mixed. The final solution was kept under stirring for 2 hours, at 30°C. After that, the same procedure as described to produce empty micelles was followed.

In order to determine loading efficiency and loading capacity, the loaded micelles were lyophilized overnight. These parameters were calculated using a calibration curve of absorbance based on the concentrations of free sorafenib in TFE, through the formulas presented below.

$$\text{Loading efficiency (\%)} = \frac{\text{Weight of the drug in nanoparticles}}{\text{Weight of the feeding drugs}} \times 100$$

$$\text{Loading capacity (\%)} = \frac{\text{Weight of the drug in nanoparticles}}{\text{Weight of the nanoparticles}} \times 100$$

## 4 Preparation of polymer-DNA complexes

To produce polymer-DNA complexes, the so-called polyplexes, the polymer PAMA<sub>73-60</sub>-PLAMA<sub>21</sub> (Polymer 3) was used. This polymer was dissolved in water at pH 3 and 1 µg of pLUC was added, in slow and circular motions, to the desired amount of polymer according to the required polymer/DNA (N/P, +/-) charge ratio. The mixture was incubated at room temperature, for 15 minutes, and polyplexes were used immediately after.

## 5 Physicochemical characterization

### 5.1 Dynamic light scattering and ζ potential analysis

Dynamic light scattering (DLS) measurements were performed in Zetasizer Nano-ZS (Malvern Instruments Ltd., UK). The particle size distribution (in intensity) and average hydrodynamic particle size average were both determined with Zetasizer 7.02 software. Measurements were made at 25 °C and a backward scattering angle of 173°.

The same equipment, Zetasizer Nano-ZS (Malvern Instruments Ltd., UK), coupled to laser Doppler electrophoresis, was also used to measure ζ potential. Polyplexes were prepared immediately before analysis.

### 5.2 Agarose gel electrophoresis

The evaluation of the condensation degree of the DNA into the polymeric nanosystems was performed using agarose gel electrophoresis. The gel was prepared using

1% (m/v) of agarose in TBE solution and allowed to polymerize before the addition of the nanosystems. Nanosystems were prepared using 1  $\mu\text{g}$  of pLUC at the indicated polymer/DNA N/P ratios.

For polyplexes, the evaluation of the resistance to DNase I action was performed in parallel. The samples were mixed with 10 units of the enzyme, followed by a 10-minute incubation, at 37 °C. Free plasmid DNA was used as a control. All samples were placed in the gel immediately after preparation and the electrophoresis was set to 45 minutes at 80 mV. Samples visualization took place in a GelDoc system (BioRad, USA).

## 6 Cell culture

The cytotoxicity and biological activity of the different nanosystems were evaluated in various human hepatocellular carcinoma cell lines: HepG2, Hep3B and Huh-7. These cells were maintained at 37 °C, under 5% CO<sub>2</sub>, in Dulbecco's modified Eagle's medium (DMEM) (Sigma–Aldrich, MO, USA) supplemented with 10% (v/v) heat-inactivated fetal bovine serum (FBS) (Sigma–Aldrich, MO, USA), penicillin (100 U/ml) and streptomycin (100 mg/ml). Cells were grown in a monolayer and were detached by treatment with trypsin solution (Sigma, St. Louis, MO), two times per week, for sub-cultivation purposes.

## 7 Transfection activity

To evaluate transfection activity of the polymeric micelles, micelleplexes and sorafenib-loaded micelles, HepG2 cells ( $8 \times 10^4$  cells/well), at approximately 70% confluence, were seeded onto 48-well culture plates, 24 hours before the addition of nanosystems. In the case of polyplexes, three cell lines were used, HepG2 ( $4,5 \times 10^4$  cells/well), Hep3B ( $2,5 \times 10^4$  cells/well) and Huh-7 ( $2,5 \times 10^4$  cells/well), also at 70% confluence, that were seeded onto 48-well culture plates, 48 hours before the addition of polyplexes.

After the addition of the different nanosystems, cells were incubated for 4 hours, at 37 °C, in 5% CO<sub>2</sub> and then the incubation medium was replaced by DMEM containing 10% (v/v) FBS and antibiotics. Cells were further incubated again for 48 hours to allow internalization and gene expression.

After this period, biological activity was determined by luminescence 48 hours post-transfection with the different nanosystems containing 1  $\mu\text{g}$  of pLUC, used as a reporter gene. Briefly, cells were washed twice with phosphate-buffered saline solution (PBS) and 100  $\mu\text{L}$  of lysis buffer were added to each well. The plates were frozen for at least 10 minutes, to promote lysis, and after that the content of each well was transferred to identified eppendorfs, followed by centrifugation for 5 minutes, at 10 000 rpm. The quantification of luciferase expression in the cell lysates was using a SPECTRAmax iD3 luminometer (Molecular Devices, USA). During the measurement, the equipment injects luciferin and ATP into each well. The luciferase gene encodes a 61-kDa enzyme that oxidizes luciferin in the presence of ATP, yielding a fluorescent product, oxyluciferin, that can be quantified by measuring the released light, at 560 nm (**Figure 13**). Then it is possible to correlate the quantity of release light with the quantity of luciferase, by quantifying the protein of the lysates, using bovine serum albumin (BSA) as a standard, by the DC Protein Assay kit (Biorad, CA, USA). Results are expressed as relative light units (RLU) of luciferase per mg of total cell protein.

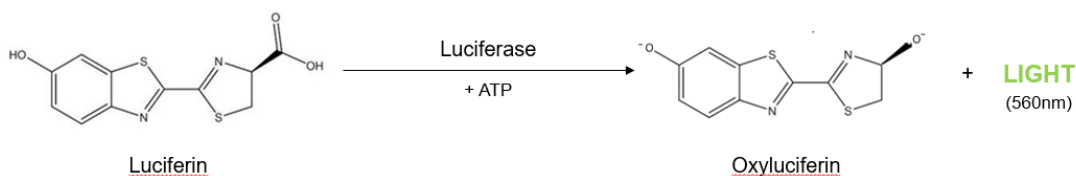


**Figure 13 | Reaction catalyzed by luciferase.**

## 8 Cell viability

Cell viability under different experimental conditions was assessed by the Alamar Blue Assay, 48 hours after transfection, performed as described above. Cells were incubated at 37 °C with 0.3 mL of DMEM containing 10% (v/v) of Alamar Blue dye, from a 0.1 mg/mL stock solution. This blue dye, called resazurin, is reduced by mitochondrial and cytoplasmic enzymes, present in metabolically active cells, turning into a fluorescent pink product, resorufin.

After observing the color exchange in the untreated control cells, the assay was stopped, meaning that 180  $\mu\text{L}$  of each well was transferred to a transparent 96-well plate, and absorbance was measured, at 570 and 600 nm, using a SPECTRAmax PLUS 384 spectrophotometer (Molecular Devices, USA). Cell viability for each condition was



calculated, as a percentage of untreated control cells, according to the formula presented below.

$$\text{Cell viability (\% of control)} = \frac{(A_{570} - A_{600}) \text{ of treated cells}}{(A_{570} - A_{600}) \text{ of control cells}} \times 100$$

## 9 Transfection efficiency

In order to evaluate the transfection efficiency of the generated polyplexes, the green fluorescent protein (GFP) expression was assessed by flow cytometry. Briefly, Huh-7 cells ( $1 \times 10^5$  per well in 4 mL of DMEM) were seeded on 12-well plates, and 48 hours later, polyplexes corresponding to 4  $\mu$ g of plasmid encoding GFP (pGFP) per well were added to the cells. After 4 hours of incubation (at 37 °C, 5% CO<sub>2</sub>), the transfection medium was replaced by DMEM containing 10% (v/v) FBS and antibiotics, followed by incubation for 48 hours.

After, cells were washed twice with PBS and trypsin was used to detach them, following incubation for approximately 2 minutes, at 37 °C. Then, to inhibit trypsin action, avoiding toxicity, culture medium was added and the content of each well was transferred to cytometry tubes, followed by centrifugation, at 950 rpm, for 5 minutes, at 4 °C. Centrifugation was repeated twice, washing the pellets with PBS. At last, cells were resuspended in PBS and kept at 4 °C, until measurement, using FACSCalibur flow cytometer (Becton Dickinson, Franklin Lakes, NJ, USA). Live cells were gated by forward/side scattering from a total of 20 000 events, and data were analyzed using FlowJo software.

The transfection activity of the generated nanosystems was evaluated qualitatively by fluorescence microscopy. For that purpose, polyplexes were prepared with pGFP, at 40/1 N/P ratio. Huh-7 cells ( $6,5 \times 10^4$  per well in 2 mL of DMEM) were seeded onto 24-well plates containing coverslips and, 48 hours later, the polyplexes were added. After incubation, for 4 hours (at 37 °C, 5% CO<sub>2</sub>), the transfection medium was replaced by new culture medium, followed by another incubation for 48 hours. After, cells were washed twice with PBS and fixed with 4% paraformaldehyde solution, for 15 minutes, at room temperature, under stirring. After washing again with PBS, cells were mounted in Fluoroshield and images were taken in Zeiss LSM 510 Meta microscope (Zeiss, Göttingen, Germany) with Plan-Apochromat 63 $\times$ /1.4 oil DIC M27 objective at excitation wavelength of 488 nm for GFP (green).

## 10 Cellular uptake and intracellular distribution of the polyplexes

Cellular uptake and intracellular distribution of the polyplexes, containing 2% of the fluorescein-labelled polymer and prepared at 40/1 N/P ratio, was assessed through confocal laser scanning microscopy (CLSM). Huh-7 cells were seeded in 12-well culture plates ( $6,5 \times 10^4$  cells per well in 4 mL of DMEM) 48 hours before the addition of polyplexes. Cells were incubated with the nanosystems (at 37 °C, 5% CO<sub>2</sub>), for 4 hours. Then, the transfection medium was removed, cells were washed twice with PBS and incubated for 30 minutes with 200 nM of LysoTrack Red, which presents the ability to label acidic compartments of living cells. Cells were washed once again with PBS and fixed with 4% paraformaldehyde solution, for 15 minutes, at room temperature, under stirring. Nuclei labelling was achieved through 5 minutes of incubation with the fluorescent DNA binding dye DAPI (1 µg/mL). Cells were mounted in Fluoroshield and images were taken in Zeiss LSM 510 Meta microscope (Zeiss, Göttingen, Germany) with Plan-Apochromat 63×/1.4 oil DIC M27 objective at excitation wavelengths of 405 nm for DAPI (blue), 488 nm for FITC (green), and 561 nm for LysoTrack (red).

# Chapter 3

## Results and Discussion

In this chapter, it is presented and discussed the results obtained during the present work. With the aim of producing a novel polymeric nanosystem able to effectively and specifically deliver genetic material to hepatocarcinoma cells, new copolymers containing pLAMA, Poly(lactobion-amidoethyl methacrylate), were developed in order to target a receptor overexpressed on the surface of these cells. Therefore, the first main section of this chapter refers to the ability of polymeric micelles, produced with amphiphilic glycopolymers, to co-deliver drugs and genes in HCC cells. In the following section, the ability of polyplexes, produced with a cationic glycopolymer, to deliver genetic material in different hepatocarcinoma cell lines was evaluated. Additionally, the implementation of a strategy to improve the transfection activity of the formed polyplexes was also investigated. In the last section of this chapter, it was analyzed the potential of the generated polyplexes to mediate a therapeutic approach for HCC treatment.

### 1 Polymeric micelles for co-delivery of drugs and genes

#### 1.1 Polymeric micelles production and physicochemical characterization

Initially, polymeric micelles were produced using two amphiphilic glycopolymers, PAMA<sub>103-*co*</sub>-PLAMA<sub>19-*b*</sub>-PDEAEMA<sub>63</sub> and PAMA<sub>50-*co*</sub>-PLAMA<sub>10-*b*</sub>-PDEAEMA<sub>16</sub>, which were coded as Polymer 1 and Polymer 2, respectively, for simplification purposes. These polymers were previously synthesized following an ARGET ATRP method, and their molecular weight parameters and chemical structure are presented in **Table 7** and **Figure 14**, respectively. This method allows the obtention of the most adequate polymers according to the type of nanosystems that are intended to produce, since it is possible to control the final characteristics of the polymers, such as molecular weight, composition, and architecture.<sup>111</sup>

Both polymers are composed of a monomer containing galactose, obtained from lactobionic acid, LAMA (Lactobion-amidoethyl methacrylate). Since PLAMA contains this sugar group, it will be able to bind to ASGPR, which was found to be overexpressed on the

surface of hepatocarcinoma cells, allowing the specific targeting of these cells.<sup>124,137</sup> On the other hand, PAMA is a cationic polymer, which allows the complexation/ condensation of genetic material and whose long polymer chains were found to potentiate transfection efficiency, due to higher levels of cellular internalization and nuclear uptake of DNA plasmid.<sup>96,130</sup> Along with PLAMA, this polymer form the hydrophilic part of polymeric micelles, consisting of the outer shell. The hydrophobic part of the glycopolymer is composed of PDEAEMA, which constitutes the core of the micelles, in which it is possible to encapsulate hydrophobic drugs. PDEAEMA is a pH-responsive polymer and presents a  $pK_a$  of 7.2, which means that in acidic conditions, as in the endocytic pathway, protonation makes the polymer hydrophilic. This fact promotes the disintegration of the polymeric micelles and, therefore, contributes to the specific release of their content.<sup>92</sup>

Table 7 | Molecular weight parameters of PAMA-*co*-PLAMA-*b*-PDEAEMA glycopolymers.

Composition	Glycopolymer architecture	$M_n^{th} \times 10^3$ (g/mol)	$M_n^{SEC} \times 10^3$ (g/mol)	$\bar{D}$	Code
PAMA <sub>103</sub> - <i>co</i> -PLAMA <sub>19</sub> - <i>b</i> -PDEAEMA <sub>63</sub>	Random-block	37.9	34.4	1.2	Polymer 1
PAMA <sub>50</sub> - <i>co</i> -PLAMA <sub>10</sub> - <i>b</i> -PDEAEMA <sub>16</sub>	Random-block	16.1	*	*	Polymer 2

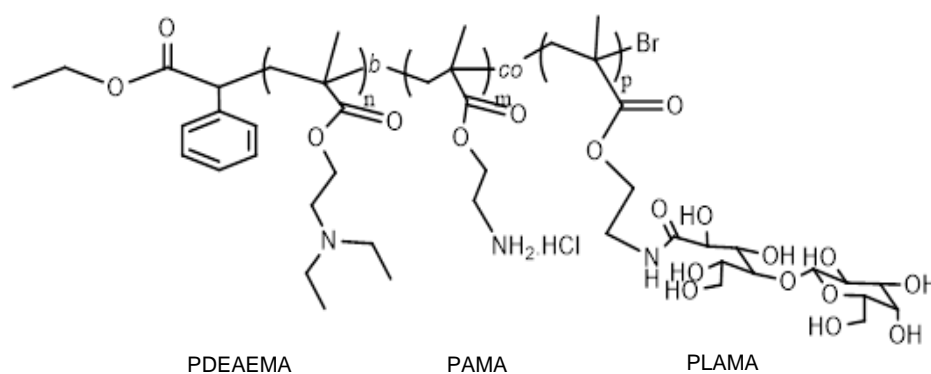


Figure 14 | Chemical structure of PAMA-*co*-PLAMA-*b*-PDEAEMA glycopolymers.

Polymeric micelles were produced using both polymers, as described in “Materials and Methods” chapter. After, these micelles were characterized through DLS, which provides the values for the hydrodynamic diameter and respective polydispersity index, and in terms of zeta potential. The obtained results are presented in **Table 8**. Hydrodynamic

diameter refers to the size of the polymeric micelles and was about 70 nm for both formulations. Both polymers originated polymeric micelles with reduced polydispersity, as could be confirmed in the size distribution by intensity presented in **Figure 15**. Zeta potential, which refers to the surface charge of the nanosystems, was positive for both micelle formulations. The positive charge of the formed micelles is advantageous not only to electrostatically bind negatively charged genetic material but could also promote internalization through the electrostatic interaction between these nanosystems and cellular membranes.<sup>92</sup>

**Table 8 | Characterization of polymeric Micelles 1 and Micelles 2 through DLS.** Results correspond to the medium value of 3 independent measurements.

Code	Polymer	Hydrodynamic diameter (nm)	Polydispersity index	Zeta potential (mV)
Micelles 1	<b>PAMA<sub>103</sub>-<i>co</i>-PLAMA<sub>19</sub>-<i>b</i>-PDEAEMA<sub>63</sub></b>	73,42	0,184	+ 11,2
Micelles 2	<b>PAMA<sub>50</sub>-<i>co</i>-PLAMA<sub>10</sub>-<i>b</i>-PDEAEMA<sub>16</sub></b>	61,19	0,216	+ 28,3

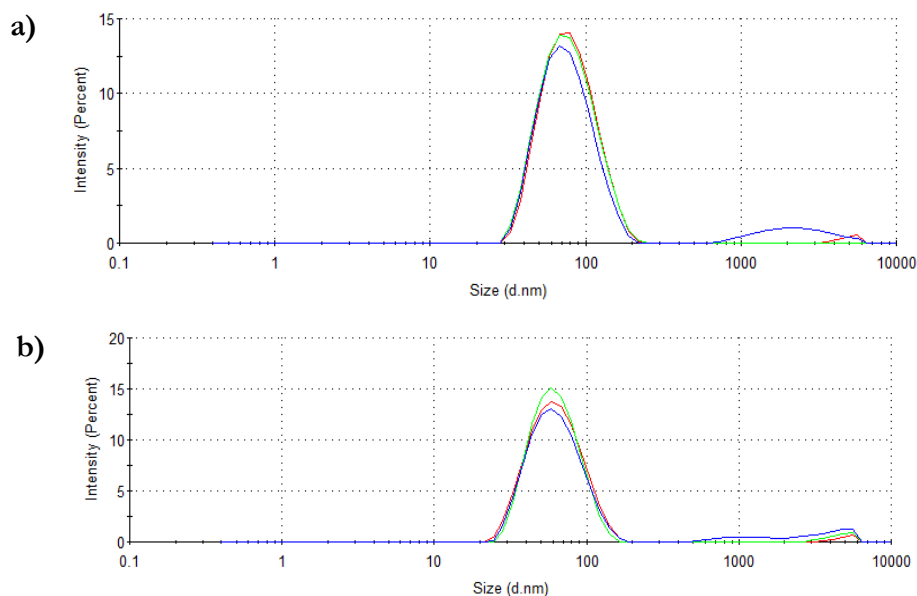


**Figure 15 | Size distribution by intensity.** a) Polymeric Micelles 1. b) Polymeric Micelles 2. The different lines correspond to 3 independent measurements.

Polymer 2 presents a smaller hydrophilic block and, therefore, it could be expected that the surface charge would be inferior for Micelles 2, comparing to Micelles 1. However, the opposite was observed. This could be not only due to a rearrangement of the molecules inside the polymeric micelle but also to the hydrophobic/hydrophilic ratio. This ratio is 30/70 for Polymer 1 and 20/80 for Polymer 2, meaning that Polymer 2 presents a higher proportion of hydrophilic segments than Polymer 1, which could explain the superior zeta potential in Micelles 2. Besides, Polymer 1 contains more PLAMA monomers and, consequently, more sugar groups, which could mask positive charge and justify the inferior zeta potential.

## 1.2 Micelleplexes physicochemical characterization

Since polymeric micelles were intended to be used for gene delivery, micelleplexes were produced as described in “Materials and Methods”, using Micelles 1. A plasmid encoding for luciferase (pLUC) was complexed with the micelles, at different polymer/DNA N/P charge ratios.

These nanosystems were characterized through DLS and the obtained results show a hydrodynamic diameter between 150 and 200 nm, which is within what was expected for this type of nanosystems (**Figure 16 a**). A size increase was registered compared to empty micelles, which indicates that, in fact, genetic material was complexed. In terms of zeta potential, no obvious alterations were observed compared to empty micelles and the measurements indicated a positively charged surface that was around 15 mV for all N/P charge ratios (**Figure 16 b**).

The condensation and protection of the genetic material by the nanoparticle was as well evaluated, using electrophoresis in agarose gel (**Figure 16 c**) and a GreenSafe assay (**Figure 16 d**), respectively. The agarose gel showed no migration of the DNA complexed by the micelles, independently of the charge ratio, demonstrating that the condensation of the genetic material successfully occurred. On the other hand, results from the GreenSafe assay showed that probe access occurred solely for superior ratios (50/1, 75/1, and 100/1), increasing with the increase of polymer quantity. It is unlikely that the observed fluorescence is the result of the intercalation of GreenSafe with the DNA encapsulated into the micelleplexes, and this could be confirmed with the results of the electrophoresis in agarose gel. This fact could be due to an interaction between the probe and the polymer, causing an increase of fluorescence in agreement with the increase of the amount of polymer. In any

case, even considering the observed GreenSafe access to DNA, it is possible to state that the genetic material was condensed and protected by the formed micelles.

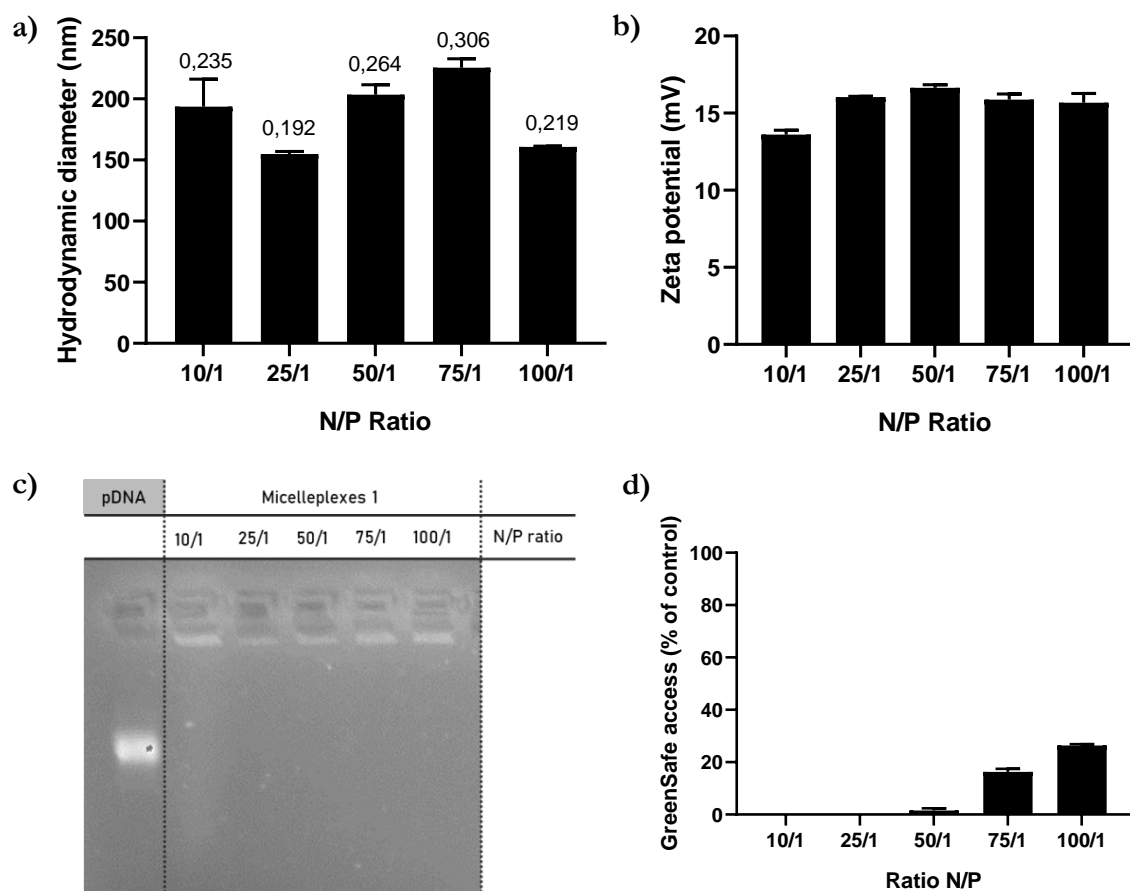


**Figure 16 | Size and associated polydispersity (a), zeta potential (b), agarose gel electrophoresis (c), and GreenSafe access (d) to DNA of Micelleplexes 1.** The micelleplexes were prepared with 1  $\mu\text{g}$  of pLUC at the indicated polymer/DNA N/P ratios. Hydrodynamic diameter is expressed in nanometers (mean  $\pm$  SEM, n=3) and zeta potential in mV (mean  $\pm$  SEM, n=3). The hydrodynamic diameter graph shows the associated polydispersity for each value.

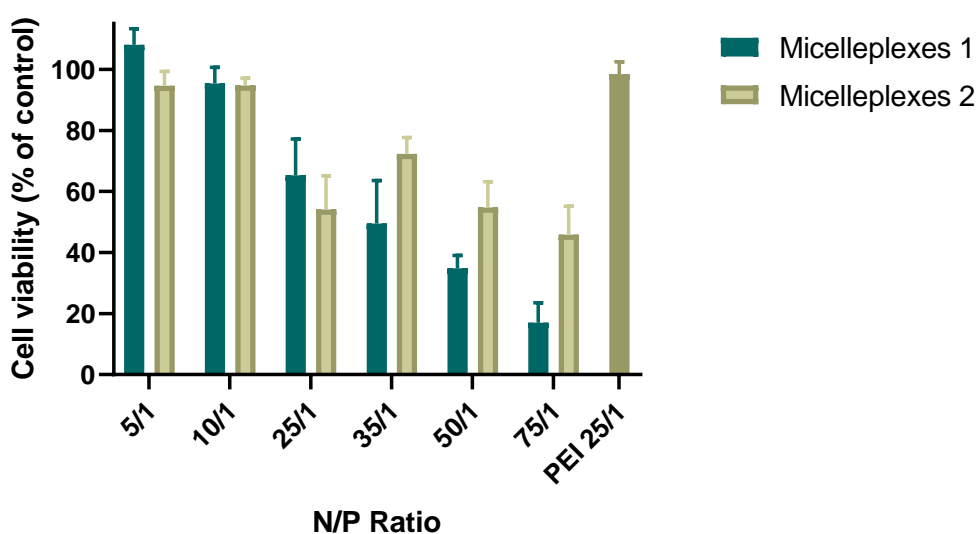
### 1.3 Evaluation of micelleplexes cytotoxicity

To apply the developed nanosystems in gene therapy the evaluation of their safety and toxicity is crucial. Despite it has been reported that the electrostatic interactions, established between the cationic surface of nanosystems and the anionic cell surface, can promote the internalization of cationic polymeric-based gene delivery systems, these interactions with cell membranes or intracellular organelles could also cause cytotoxicity, which often limits these nanosystems *in vivo* application.<sup>138</sup>

Accordingly, the cytotoxicity of Micelleplexes 1 and 2, prepared at different polymer/DNA N/P ratios, was evaluated in HepG2 cells by the Alamar blue assay. For the

ratios 5/1 and 10/1, promising results were obtained, the values for cell viability being above 90%. However, the results showed that cell viability decreased along with the increase of the N/P ratio and, for the highest ones, cell viability is around 60% or below (**Figure 17 a**). Several studies have been shown that cationic polymeric based-gene delivery systems strongly interact with cellular membranes, causing a structural destabilization.<sup>103,139</sup> Accordingly, for superior N/P charge ratios, it can be stated that the registered cytotoxicity is due to the destabilization of cytoplasmatic membranes caused by the addition of higher quantities of polymer to the cells.

a)



b)

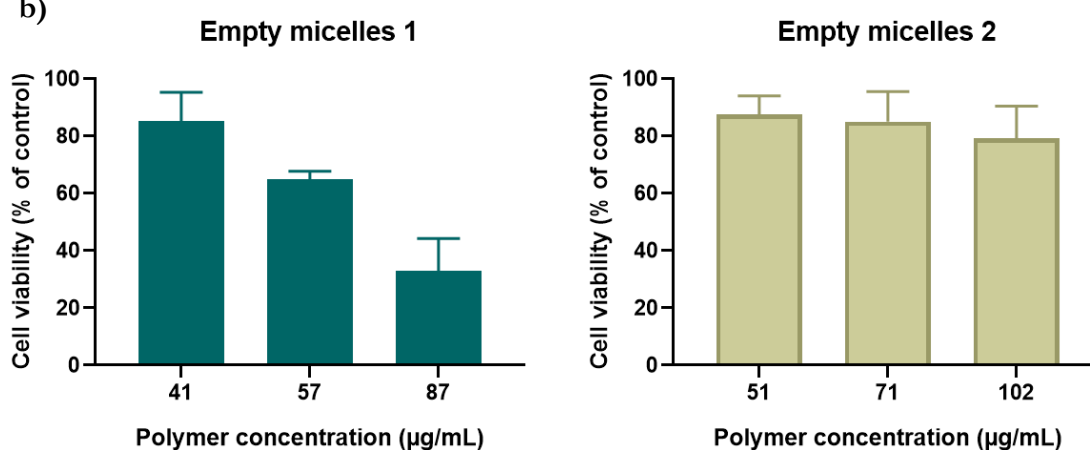


**Figure 17 | Viability of HepG2 cells in the presence of Micelleplexes 1 and 2 (a), and Empty micelles 1 and 2 (b).** The micelleplexes were prepared with 1 µg of pLUC at the indicated polymer/DNA N/P ratios. The concentrations of polymer used in Empty micelles 1 and 2 correspond to the amounts used to produce Micelleplexes 1 and 2 at 25/1, 35/1 and 50/1 charge ratios. Cell viability is expressed as a percentage of untreated control cells (mean ± SEM, obtained from triplicates) and was measured through the Alamar blue assay. The results are representative of 3 independent experiments.



To determine if the registered toxicity was related to the nanosystem by itself, empty micelles were also incubated with cells, using polymer concentrations corresponding to the ratios 25/1, 35/1, and 50/1 of the micelleplexes (**Figure 17 b**). The obtained results showed superior values of cell viability registered with empty micelles, compared to that observed with micelleplexes in the respective ratio, particularly using Polymer 2, demonstrating the biocompatibility of this formulation. The cytotoxicity profile of the empty micelles is different for the two polymers. A proportionality relationship between the high molecular weight of cationic polymers and their toxicity to the cells has been reported.<sup>140</sup> Taking this into account and knowing that the molecular weight of Polymer 1 is more than the double of Polymer 2, it was confirmed the expected higher cytotoxicity of Micelles 1.

#### **1.4 Evaluation of micelleplexes transfection activity**

In addition to the safety and non-toxic characteristics of nanosystems, it is essential that they effectively deliver the genetic material in the target cells, in order to achieve a therapeutic effect. Accordingly, transfection activity of Micelleplexes 1 and 2 was evaluated, for different N/P ratios, using a plasmid encoding for luciferase. The transgene expression on HepG2 cells was measured following a luminescence assay. The obtained results showed that none of the micelleplexes formulations present significant transfection activity, being practically null compared to the commercial control, PEI (**Figure 18 a**). However, since the DNA plasmid is complexed (**Figure 16**), the absence of signal is possibly due to the inability of the plasmid to be released from the nanosystem, making it impossible to be expressed. Furthermore, the cationic polymeric based-gene delivery systems can cause a structural destabilization of cytoplasmatic membranes, resulting in higher levels of cytotoxicity. This could also affect the metabolic capacity of the cells, leading to lower levels of transfection activity.<sup>139</sup>

Given these results, polyplexes were produced using the same polymers and the luminescence assay was performed with those nanosystems. Nevertheless, no luciferase expression was registered, confirming that neither micelleplexes nor polyplexes present biological activity (**Figure 18 b**).

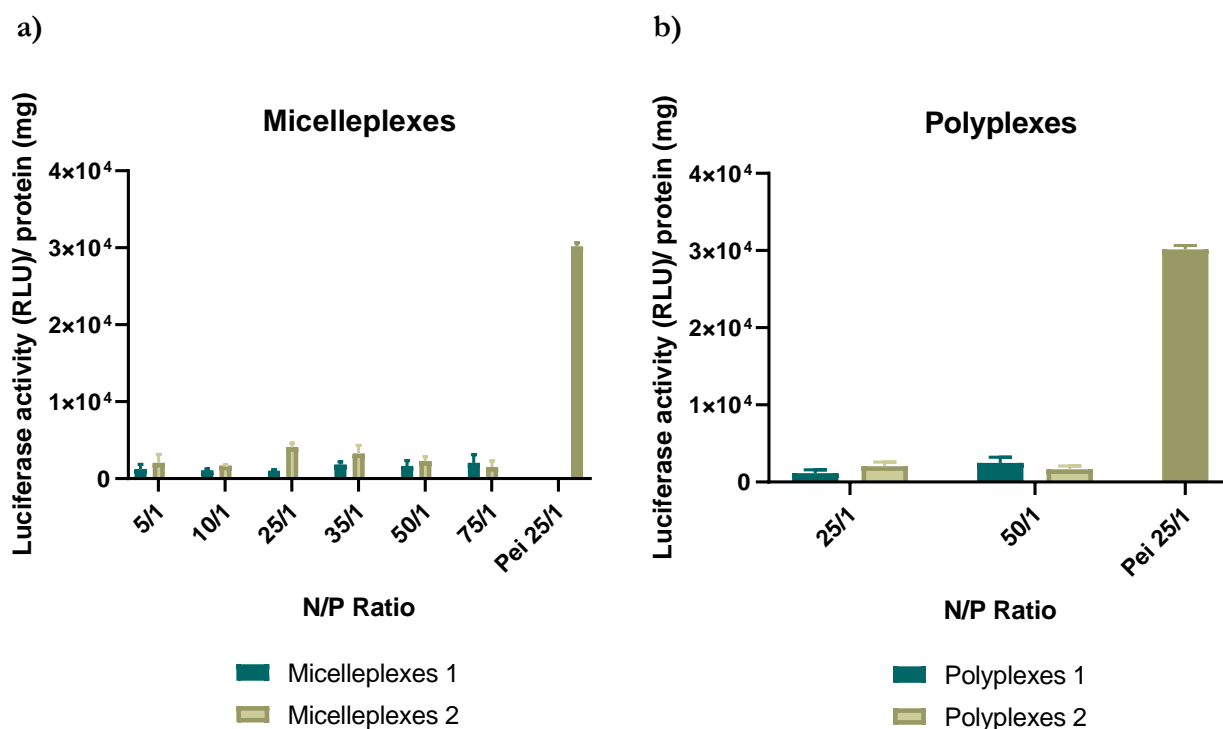


**Figure 18 | Luciferase gene expression in HepG2 cells transfected with Micelleplexes 1 and 2 (a) and Polyplexes 1 and 2 (b).** The micelleplexes and polyplexes were prepared with 1  $\mu\text{g}$  of pLUC at the indicated polymer/DNA N/P ratios. Levels of gene expression are expressed as RLU of luciferase per mg of total cell protein (mean  $\pm$  SEM, obtained from triplicates) and was determined as described in “Materials and Methods”. The results are representative of 3 independent experiments.

### 1.5 Polymeric micelles for sorafenib delivery

As previously mentioned, polymeric micelles could be used for drug delivery since their hydrophobic core can be used to encapsulate hydrophobic agents, protecting them, avoiding their degradation, and transporting them from the injection site to the target cells. Therefore, sorafenib, a first-line drug used for HCC treatment, was encapsulated into Micelles 2, produced with the polymer PAMA<sub>50-co</sub>-PLAMA<sub>10-b</sub>-PDEAEMA<sub>16</sub>. These micelles were chosen due to their lower levels of toxicity, comparing to Micelles 1. The new nanosystems were physicochemically characterized through DLS and the results showed a slight increase of approximately 10 nm in the hydrodynamic diameter, compared to empty micelles (**Table 9**). This suggests that the drug encapsulation had no obvious effect on the self-assembly of the polymer when micelles were produced. In terms of zeta potential, it was observed a decrease comparing to empty micelles.

**Table 9 | Characterization of sorafenib-loaded polymeric Micelles 2.** Hydrodynamic diameter is expressed in nanometers (mean  $\pm$  SEM, n=3) and zeta potential in mV (mean  $\pm$  SEM, n=3).

Code	Polymer	Hydrodynamic diameter (nm)	Polydispersity	Zeta potential (mV)
Micelles SF	PAMA <sub>50</sub> - <i>co</i> -PLAMA <sub>10</sub> - <i>b</i> -PDEAEMA <sub>16</sub>	82.68	0,193	- 14.00

After lyophilization of the micelles containing sorafenib, micelles were dissolved in TFE and a calibration curve depending on the concentration of the drug in the same organic solvent was constructed. Based on this, the loading efficiency and loading capacity were determined (**Table 10**). The results for loading capacity reported in the literature with micelles are usually below 10 %, given the limited encapsulation capacity of this type of nanosystems.<sup>100,103</sup> Therefore, the obtained value for loading capacity, 4 %, was in agreement with the expected.

**Table 10 | Capacity and efficiency of loading of sorafenib into polymeric Micelles 2.** Sorafenib concentration into micelles was calculated after lyophilization and is expressed in mg of drug per mL of organic solvent. Loading efficiency and loading capacity were calculated as described in “Materials and Methods” and are expressed in percentage.

Code	SF concentration (mg/mL)	Loading efficiency (%)	Loading capacity (%)
Micelles SF	0.50	15.00	4.00

To evaluate the cytotoxicity of the micelles an Alamar blue assay was performed. These nanosystems were added to HepG2 cells, as well as the free drug, in order to obtain final concentrations of 1, 5, and 10  $\mu$ M of the drug. Empty micelles were also used as control in order to obtain the same concentration of polymer used with Micelles SF. It was observed that the levels of toxicity of these new nanosystems, prepared with or without drug, were effectively higher than the levels produced by the free drug (**Figure 19**). In fact, when comparing the results using micelles loaded with sorafenib and empty micelles, it can be observed similar levels of cytotoxicity, which means that the concentration of polymer added to the cells was extremely elevated, resulting in lower levels of cell viability. Overall, the obtained results showed the limitations of these nanosystems that further restrict their application for drug delivery purposes.

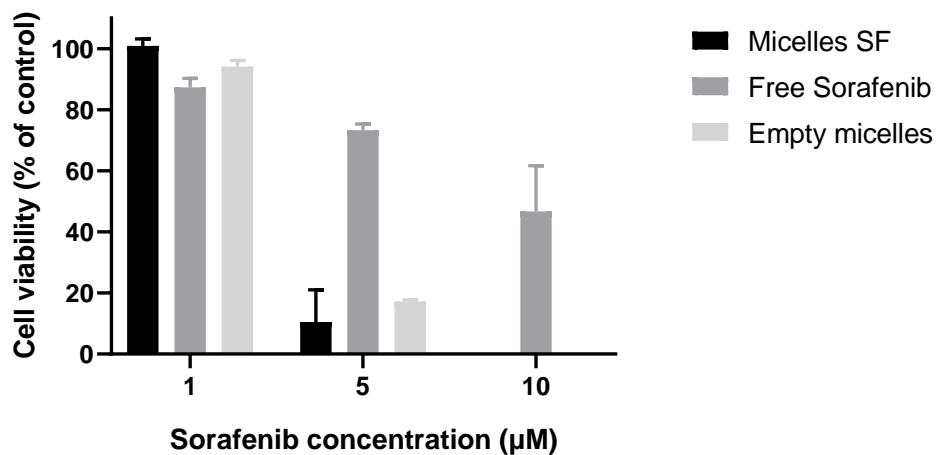


**Figure 19 | Effect of Sorafenib concentration and amount of micelles on the viability of HepG2 cells.**

Micelles SF were produced as described in “Materials and Methods” using 1 mg of Sorafenib. The appropriate concentration of Micelles SF was used so that the final concentration of the drug was the indicated (1, 5, and 10 µM). As control, free sorafenib at the indicated concentrations and Empty micelles were used. Empty micelles were used in the same concentrations as Micelles SF. Cell viability is expressed as a percentage of untreated control cells (mean ± SEM, obtained from triplicates) and was measured through an Alamar blue assay.

## 2 Polyplexes for gene delivery

The results presented in the previous section, regarding the development and production of polymeric micelles for the co-delivery of drugs and genes, showed a major limitation of these nanosystems, their cytotoxicity. It has been reported that hydrophobic polymers, such as PDEAEMA, usually present high electropositivity, because of the existence of amine groups, resulting in increased toxicity.<sup>141</sup> However, the monomers constituting the hydrophilic part of the glycopolymers used to produce the polymeric micelles, AMA and LAMA, have been involved in studies showing promising results in the field of gene delivery. AMA is a cationic monomer that has been used for the production of polyplexes showing a high transfection efficiency, which was found to be directly related to the polymer chain length.<sup>96</sup> On the other hand LAMA is a carbohydrate monomer with the ability to promote targeting to the hepatocytes, through the binding to the ASGPR, resulting in the specific delivery of the nanosystems content.<sup>126</sup> Additionally, this type of monomers can contribute to the increase of hydrophilicity, resulting in highly biocompatible nanosystems.<sup>111</sup>

### 2.1 Polyplexes production and physicochemical characterization

Taking this into account, polyplexes were produced using a new glycopolymer, PAMA<sub>73-co</sub>-PLAMA<sub>21</sub>, coded as Polymer 3. This polymer contains the cationic monomer, AMA, and the carbohydrate monomer, LAMA, abdicating from the hydrophobic part present in the previously used polymers (**Table 11**).

**Table 11 | Molecular weight parameters of PAMA<sub>73-co</sub>-PLAMA<sub>21</sub> glycopolymer.**

Composition	Glycopolymer architecture	Mn <sup>th</sup> x 10 <sup>3</sup> (g/mol)	Mn <sup>SEC</sup> x 10 <sup>3</sup> (g/mol)	Đ	Code
PAMA <sub>73-co</sub> -PLAMA <sub>21</sub>	Random	22.0	19.8	1.30	Polymer 3

Polyplexes were produced at different polymer/DNA N/P charge ratios, following the procedure described in “Materials and Methods” chapter. These nanosystems were characterized through DLS and laser doppler electrophoresis, and the values obtained for hydrodynamic diameter and zeta potential, respectively, are presented in **Figure 20**.

Polyplexes diameter is around 150 nm, and no obvious differences were registered between ratios. The surface charge is near +40 mV, indicating that most probably no genetic material was exposed.

To evaluate the condensation of the genetic material complexed by the polyplexes and its resistance to DNase I, an electrophoresis in agarose gel was performed. For polyplexes prepared at ratio 10/1 incubated with inactive DNase I a very tenuous band is visible when compared to the one observed with the control (free DNA incubated with inactive DNase I), suggesting that most, but not all, of the genetic material is condensed (**Figure 20 c**). For the remaining ratios, both in the presence or absence of DNase I, no bands were observed, showing that DNA had been completely complexed by the polyplexes. This was an expected result since the quantity of polymer increases with the N/P ratio, resulting in a higher degree of condensation of DNA for higher ratios.

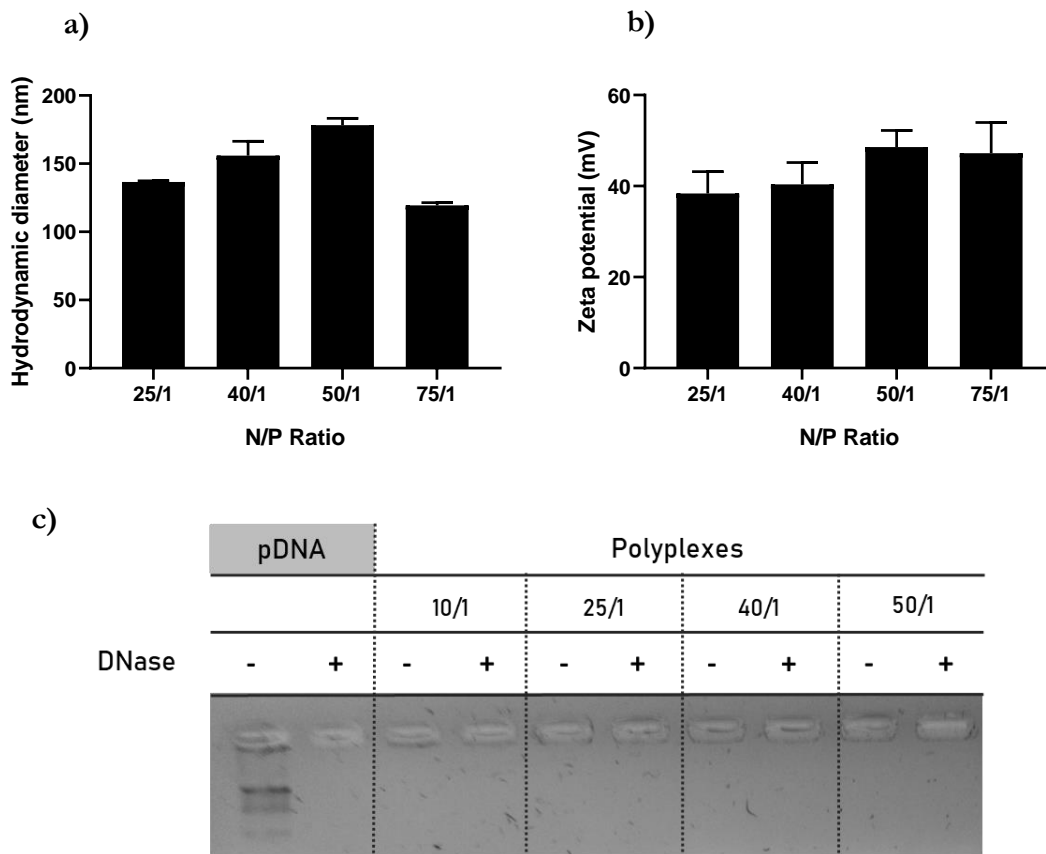


**Figure 20 | Size (a), zeta potential (b), condensation of DNA and resistance to DNase I action(c), of Polyplexes.** The polyplexes were prepared with 1 µg of pLUC at the indicated polymer/DNA N/P ratios. Hydrodynamic diameter is expressed in nanometers (mean ± SEM, n=3) and zeta potential in mV (mean ± SEM, n=3). Agarose gel electrophoresis and digestion with DNase I was performed as described in “Materials and Methods”.

Additionally, the hydrodynamic diameter was measured through DLS over time, for 4 hours, at 1-hour intervals, in order to evaluate the stability of the generated polyplexes at 40/1 charge ratio in culture medium, DMEM. The objective was to evaluate polyplexes stability mimicking physiological conditions during the incubation period used in the transfection assays. As expected, a size increase was registered, since the culture medium contains serum proteins (FBS), which are negatively charged. These proteins will electrostatically interact with the formed polyplexes, affecting their stability and causing structural changes, such as aggregation.<sup>96</sup> A hydrodynamic diameter increase, from approximately 150 to 600 nm, was observed (**Figure 21**). However, polyplexes remain this size for 4 hours.

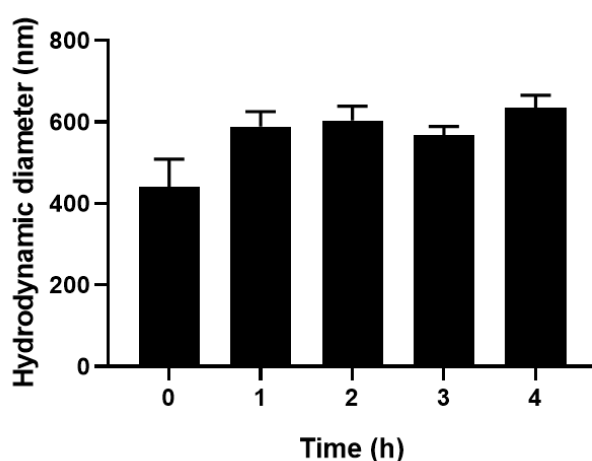


**Figure 21 | Influence of time and environment on the stability of Polyplexes.** The polyplexes were prepared with 1  $\mu\text{g}$  of pLUC at 40/1 N/P ratio and diluted in DMEM. Hydrodynamic diameter is expressed in nanometers (mean  $\pm$  SEM, n=3) and was measured at 1-hour intervals for 4 h.

## 2.2 Evaluation of polyplexes transfection activity

To evaluate the transfection activity, polyplexes were produced at different N/P charge ratios using a plasmid encoding for luciferase and were incubated with three hepatocarcinoma cell lines, HepG2, Hep3B, and Huh-7. After, the levels of luciferase expression were measured by a luminescence assay. The obtained results demonstrated that these nanosystems had the ability to efficiently transfect the different cell lines, resulting in a similar profile of transfection activity (**Figure 22**). It was also observed that transgene expression increased along with the N/P charge ratio, which was consistent in all cell lines. For higher N/P ratios, the amount of polymer is bigger and, therefore, the density of positive

charges is also higher. Not only these polyplexes will interact more strongly with cellular membranes, promoting internalization, but also this high density of positive charges will provide them the capability to overcome the neutralization promoted by serum proteins, that most probably occurred at inferior N/P ratios.<sup>96</sup> This results in higher levels of transgene expression for superior ratios. For Hep3B and Huh-7 cells, a decrease of biological activity at the 75/1 N/P ratio was registered, which is probably due to cell damage caused by superior amounts of polymer.<sup>142</sup> Overall, the results showed great levels of biological activity, particularly in Huh-7 cells.

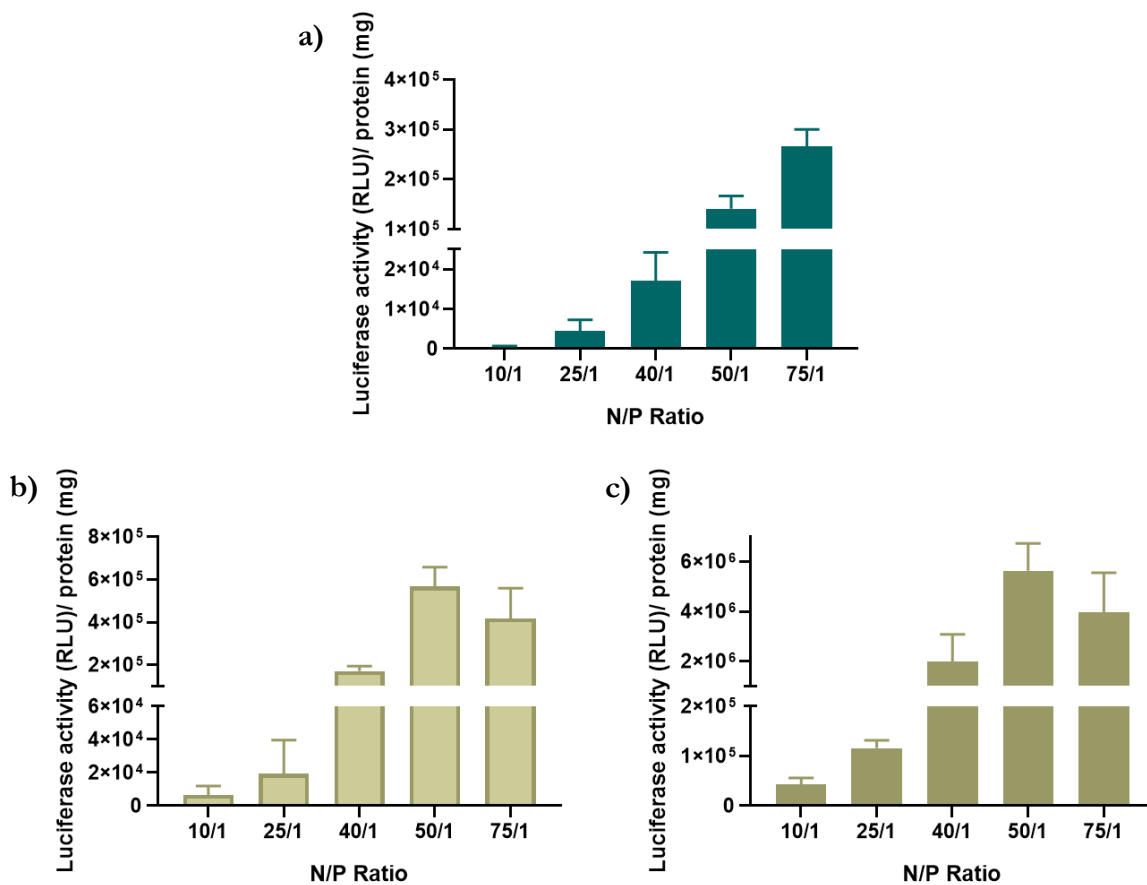


**Figure 22 | Transfection activity of polyplexes in different cell lines: HepG2 (a), Hep3B (b) and Huh-7 (c).** The polyplexes were prepared with 1  $\mu$ g of pLUC at the indicated polymer/DNA charge N/P ratios. Levels of gene expression are expressed as RLU of luciferase per mg of total cell protein (mean  $\pm$  SEM, obtained from triplicates) and were determined as described in “Materials and Methods”. The results are representative of 3 independent experiments.



### 2.3 Evaluation of polyplexes cytotoxicity

Cytotoxicity of cationic polymers is one of the major limitations to the application of cationic polymer-based nanosystems in the clinical field. To overcome this limitation, several strategies have been developed, such as PEGylation<sup>96</sup> and the addition of carbohydrate groups. Carbohydrates, such as LAMA, were found to be involved not only in the binding and cellular internalization of nanosystems, but also in the condensation of genetic material through hydrogen bonding, reducing the need of using an excess of cationic polymer, consequently reducing the toxicity.<sup>143</sup>

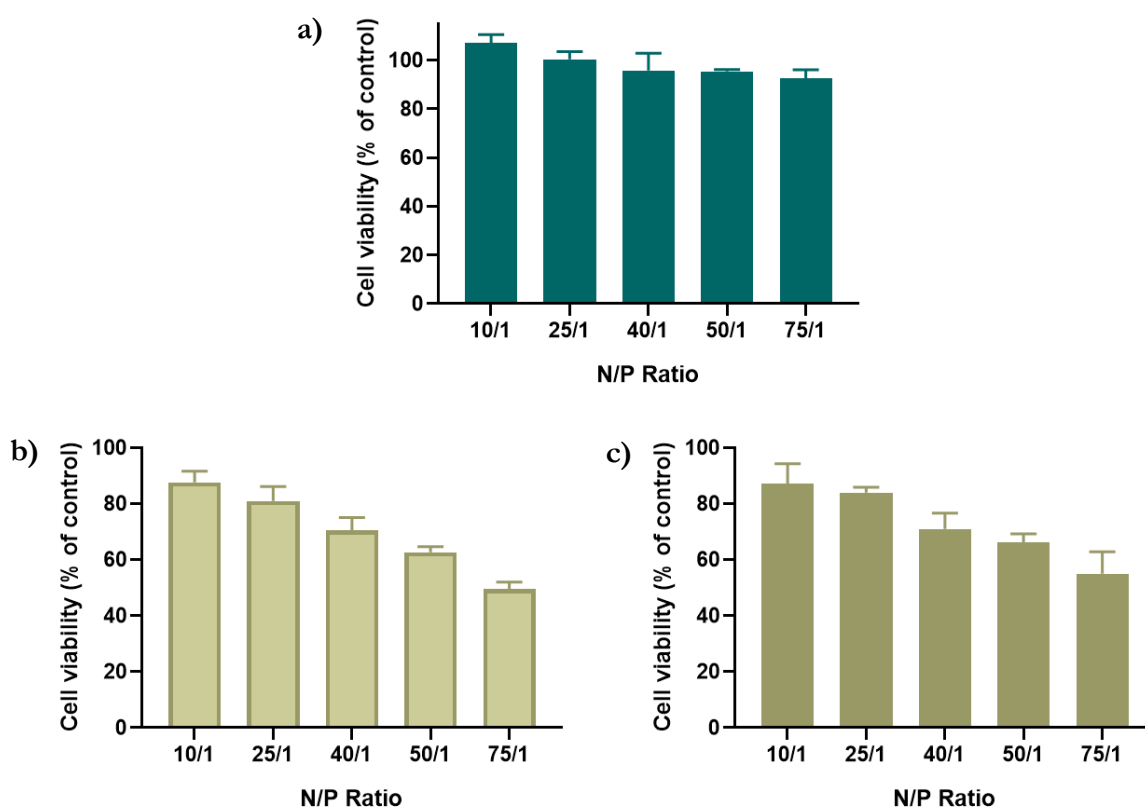


**Figure 23 | Effect of the polyplexes on the viability of different cell lines: HepG2 (a), Hep3B (b), and Huh-7 (c).** The polyplexes were prepared with 1  $\mu\text{g}$  of pLUC at the indicated polymer/DNA N/P charge ratios. Cell viability is expressed as a percentage of untreated control cells (mean  $\pm$  SEM, obtained from triplicates) and was measured through an Alamar blue assay. The results are representative of 3 independent experiments.

Taking this into account, evaluation of polyplexes cytotoxicity was performed in the different cell lines, using the Alamar blue assay. Cytotoxicity was not significant in HepG2 cells, while on the other cell lines, Hep3B and Huh-7, the levels of cell viability are substantially reduced beyond the 40/1 N/P charge ratio (**Figure 23**).

Overall, a similar profile was observed for these two cell lines, in which cell viability decreased along with the increase of the N/P charge ratio. This is due to the fact that at superior N/P charge ratios, the quantity of polymer added to the cells is higher, resulting in excessive positive charges that can structurally destabilize cellular membranes, causing cell damage.

## 2.4 Transfection efficiency of polyplexes

Flow cytometry and fluorescence microscopy were used to evaluate the transfection efficiency of the polyplexes, in a quantitative and qualitative manner, respectively. These assays were performed using Huh-7 cells since in this cell line polyplexes presented greater levels of biological activity. Polyplexes prepared with a plasmid encoding for GFP at 40/1 N/P charge ratio were used in these transfection experiments. This N/P charge ratio was chosen given the balance between biological activity and cytotoxicity observed in the previous luminescence and Alamar blue assays, respectively. In other words, this N/P ratio provides high levels of transgene expression without substantially compromising the viability of the cells.

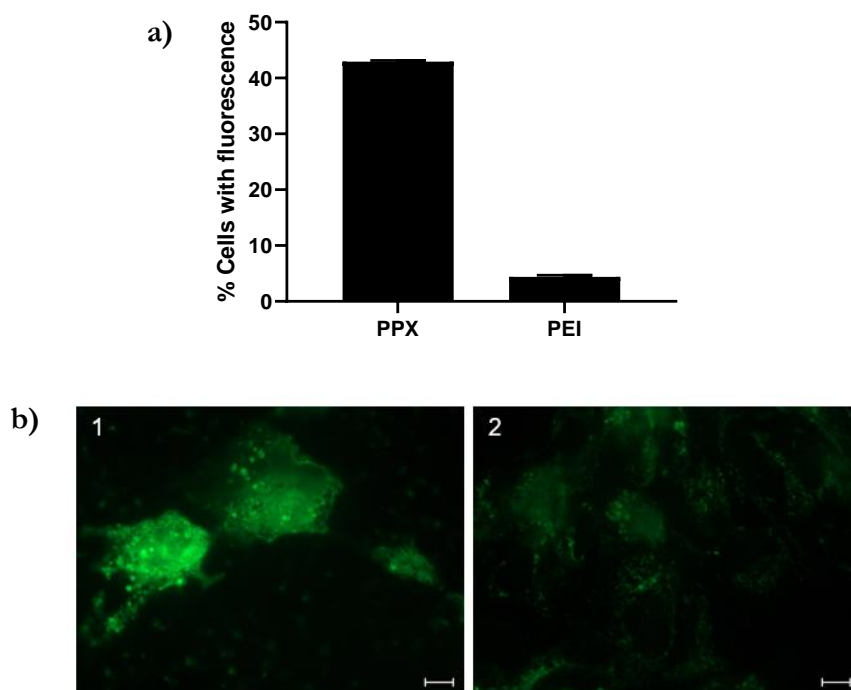


**Figure 24 | Effect of the polyplexes composition on the green fluorescent protein gene expression evaluated by flow cytometry (a) and fluorescence microscopy (b), using Huh-7 cells.** PAMA-co-PLAMA-based polyplexes were prepared with 4  $\mu\text{g}$  of pGFP, at the 40/1 N/P charge ratio, while PEI-based polyplexes were prepared with 4  $\mu\text{g}$  of pGFP, at the 25/1 N/P charge ratio. (a) Data are expressed as a percentage of transfected cells. (b) Fluorescence microscopy images: (1) cells treated with polyplexes and (2) cells treated with PEI-based polyplexes (scale bar = 10  $\mu\text{m}$ ).

Flow cytometry provided the percentage of fluorescent Huh-7 cells after transfection with polyplexes produced with PAMA-co-PLAMA or PEI. The results showed that, after transfection with the PAMA-co-PLAMA-based polyplexes, the percentage of cells with fluorescence was approximately 40%. This represents a transfection efficiency 10 times superior than that obtained with polyplexes produced with PEI, which is considered a gold standard (**Figure 24 a**). The results were confirmed through fluorescence microscopy, which showed that the intensity of fluorescence after transfection with the PAMA-co-PLAMA-based polyplexes is visibly superior than after transfection with PEI-based polyplexes (**Figure 24 b**).

## 2.5 Evaluation of polyplexes specificity

In an attempt to identify if the developed polyplexes were internalized in a specific manner, a competition assay was performed in the different hepatocarcinoma cell lines. Cells were incubated with asialofetuin, the natural ligand of ASGPR, before the addition of polyplexes, followed by a luminescence assay to evaluate transfection activity. It was expected a decrease of transgene expression in the presence of asialofetuin, since this protein presents a higher affinity towards ASGPR than PAMA-co-PLAMA copolymer, blocking polyplexes binding to the receptor on the cell membrane, and consequently decreasing their internalization. The results showed almost complete inhibition, resulting in very reduced levels of luciferase expression in the presence of asialofetuin, when compared to the levels in the absence of the protein (**Figure 25**). As previously mentioned, for superior ratios, it would be expected that polyplexes internalization occurred mainly through electrostatic interactions with the negatively charged membranes, given the higher concentration of polymer and, therefore, superior positive charge density. However, this assay showed that, independently of the N/P charge ratio, polyplexes are mainly internalized through the receptor.

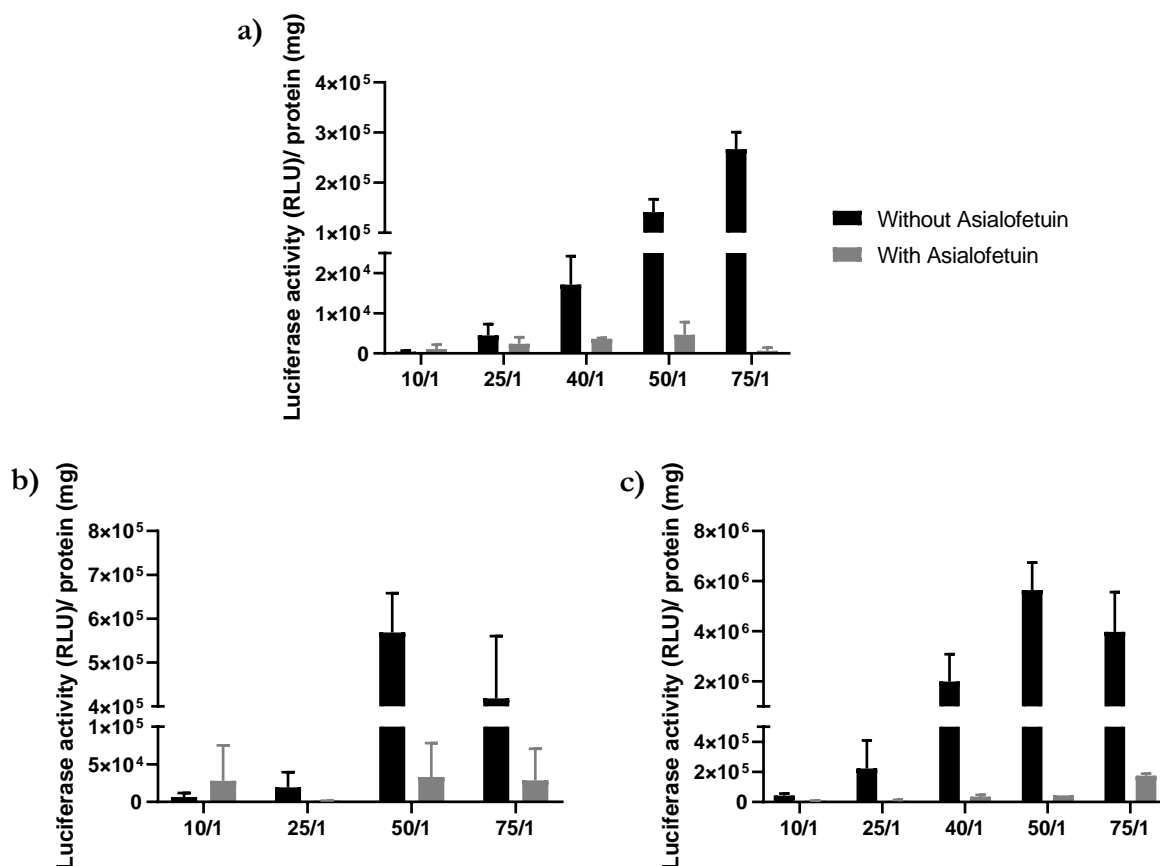


**Figure 25 | Effect of the presence of asialofetuin on the luciferase gene expression in the 3 cell lines: HepG2 (a), Hep3B (b), and Huh-7 (c).** The polyplexes were prepared with 1  $\mu\text{g}$  of pLUC at the indicated polymer/DNA N/P ratios. For the conditions in the presence of asialofetuin, cells were preincubated with DMEM containing 1 mg of asialofetuin. Levels of gene expression are expressed as RLU of luciferase per mg of total cell protein (mean  $\pm$  SEM, obtained from triplicates) and were determined as described in “Materials and Methods”. The results are representative of the remaining experiments. The results are representative of 3 independent experiments.

These results were confirmed through flow cytometry and fluorescence microscopy, using Huh-7 cells, and PAMA-*co*-PLAMA-based polyplexes prepared with a plasmid encoding for GFP, at 40/1 N/P charge ratio. The flow cytometry assay showed that the percentage of cells with fluorescence, after transfection with these polyplexes in the presence of asialofetuin, is approximately 10 times lower than that observed in the absence of the glycoprotein. Fluorescence microscopy showed decreased intensity of fluorescence after transfection with polyplexes in the presence of asialofetuin. Overall, the obtained results showed reduced levels of transgene expression after transfection with PAMA-*co*-PLAMA-based polyplexes in the presence of asialofetuin, demonstrating the specificity of the generated nanosystems towards ASGPR.

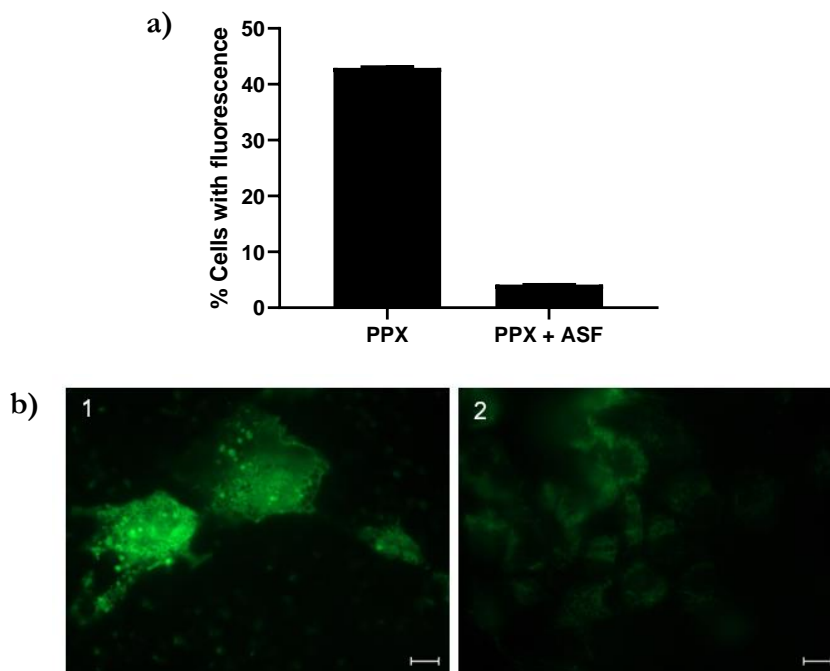


**Figure 26 | Effect of the presence of asialofetuin on the green fluorescent protein gene expression evaluated by flow cytometry (a) and fluorescence microscopy (b), using Huh-7 cells.** The polyplexes (N/P charge ratio = 40/1) were prepared with 4  $\mu$ g of pGFP. For the conditions in the presence of asialofetuin, cells were preincubated with DMEM containing 4 mg of asialofetuin. (a) Data are expressed as a percentage of transfected cells. (b) Fluorescence microscopy images: (1) cells treated with polyplexes and (2) cells treated with polyplexes in the presence of asialofetuin (scale bar = 10  $\mu$ m).

## 2.6 Cellular uptake and intracellular distribution of polyplexes

In order to effectively result in a therapeutic effect, the genetic material transported by the nanosystems needs to reach the nucleus of the target cells, in which it would be transcribed. Therefore, nanosystems should promote binding to the cellular membrane and cellular internalization, and then, should avoid degradation and clearance, which mainly happens in the endocytic vesicles.

Taking this into account, the intracellular distribution of the PAMA-*co*-PLAMA-based polyplexes, in the presence or absence of asialofetuin, was observed in Huh-7 cells by confocal laser scanning microscopy (**Figure 27**). In the case of the cells pre-incubated with asialofetuin it is possible to visualize a clear decrease in the amount of polyplexes (labelled in green) inside the cells. Asialofetuin presents a high affinity towards ASGPR, competing with the polyplexes, which resulted in an almost complete inhibition of their binding to the receptor on the cell surface, hindering their internalization. Therefore, it is possible to state that the lower levels of transgene expression observed by luminescence assay (**Figure 25**), in the presence of asialofetuin, are due to the accentuated decrease of polyplexes internalization.

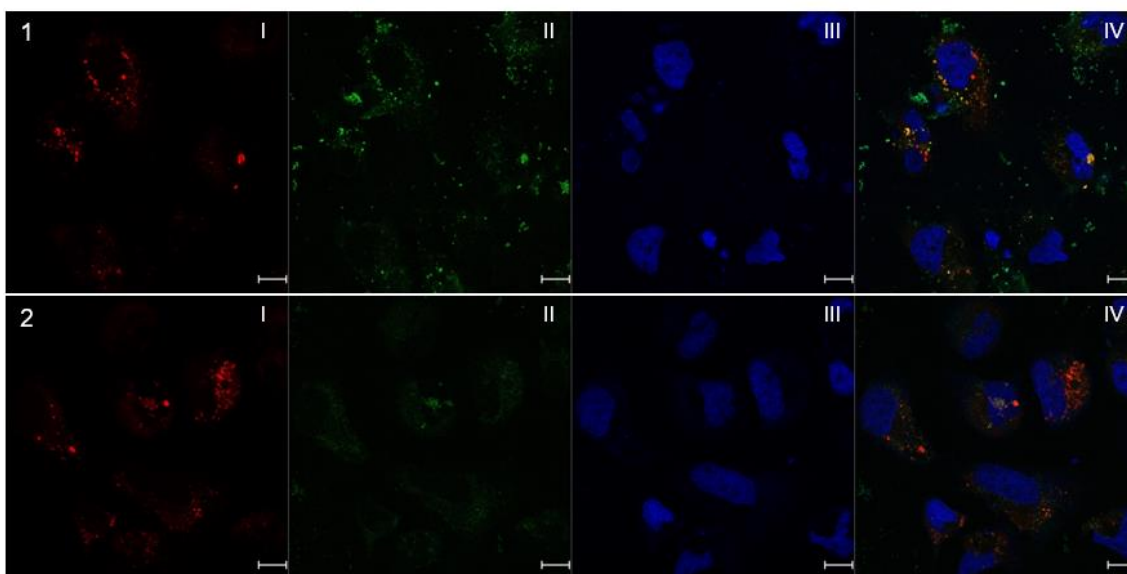


**Figure 27 | Effect of the presence of asialofetuin on the intracellular distribution of polyplexes in Huh-7 cells observed by confocal microscopy.** The polyplexes were prepared with 2% of the fluorescein-labelled polymer, at a 40/1 N/P charge ratio with pLUC. For the conditions in the presence of asialofetuin, cells were preincubated with DMEM containing 4 mg of asialofetuin for 1 h. After, cells were labelled and fixed as described in “Materials and Methods”. (1) Cells treated with polyplexes and (2) cells treated with polyplexes in the presence of asialofetuin. (I) red fluorescent image of acidic compartments labelled with LysoTracker Red DND-99; (II) green fluorescent image of polyplexes prepared with fluorescein-labelled polymer; (III) blue fluorescent image of cell nucleus stained by DAPI; (IV) overlay image of images I–III (scale bar = 10  $\mu$ m).

Acidic compartments were stained with LysoTracker (red) to determine lysosomal localization during polyplex trafficking. The obtained images showed that polyplexes seem to be evenly distributed throughout the cytoplasm and some of them are co-localized with the acidic compartments, which leads to the appearance of small yellow dots in the overlaying images. This demonstrates the need to further promote endosomal escape, in order to avoid degradation of the polyplexes into the endocytic vesicles and enhance gene delivery efficiency.

This assay demonstrated that the main form of PAMA-*co*-PLAMA-based polyplexes internalization is through the ASGPR and confirmed the specificity of these nanosystems towards this receptor. Additionally, it was observed that some of the internalized polyplexes are being targeted for degradation, demonstrating the need to promote endosomal escape.

### 3 Strategies to improve transfection activity

In an attempt to increase the transfection activity and promote the endosomal escape of the PAMA-*co*-PLAMA-based polyplexes, it was evaluated the effect of the presence of docetaxel, a microtubule-stabilizing taxane. This type of drug was found to affect the transport from early to late endosomes and, therefore, could have a direct impact on the intracellular trafficking of polyplexes.<sup>144</sup> Combining the developed polyplexes with docetaxel could facilitate the endosomal escape of the genetic material and its transportation to the nucleus, enhancing transfection efficiency.<sup>145,146</sup>

Taking this into account, polyplexes prepared with pLUC at 40/1 N/P charge ratio were added to Huh-7 cells after pre-incubation with different concentrations of docetaxel. Cell viability was assessed by Alamar blue assay, and the obtained results were compared with the cell viability registered in the presence of the docetaxel alone. It was possible to observe that the different concentrations tested of docetaxel caused a similar impact on cell viability and that the addition of the drug to polyplexes promotes a decrease of around 20% in cell viability (Figure 28). Furthermore, there were no significant differences between the presence and absence of polyplexes in the toxicity.

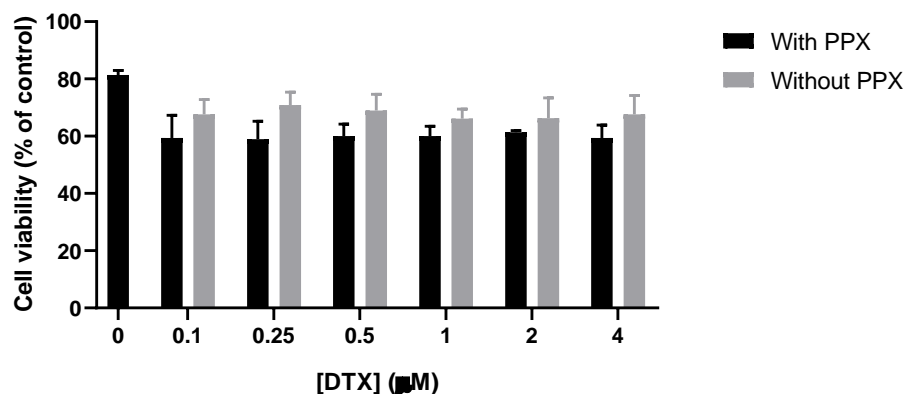


**Figure 28 | Effect of the different concentrations of docetaxel and the combination with polyplexes on the viability of Huh-7 cells.** Cells were preincubated with DMEM with or without different concentrations of docetaxel (0.1, 0.25, 0.5, 1, 2, and 4 µM). The polyplexes (N/P charge ratio = 40/1) were prepared with 1 µg of pLUC (conditions identified with “With PPX”). Cell viability is expressed as a percentage of untreated control cells (mean ± SEM, obtained from triplicates) and was measured through an Alamar blue assay.

Biological activity was also assessed using these polyplexes, in the same conditions, by a luminescence assay. The obtained results showed a slight increase of transfection activity in the presence of docetaxel, which proved to be independent of the tested concentrations. Therefore, the minimum concentration (0.1 µM) was used to evaluate the impact of the drug

on the percentage of transfected cells with polyplexes prepared with a plasmid encoding for GFP, by flow cytometry. The percentage of cells with fluorescence was approximately 40% for both conditions, cells transfected with polyplexes alone or transfected with polyplexes in the presence of docetaxel. It was concluded that the pre-incubation of the cells with docetaxel does not lead to an increase of the percentage of transfected cells. However, and according to the literature, the main advantage of the use of microtubule-stabilizing taxanes is the promotion of the polyplexes endosomal escape and not necessarily the increase of the percentage of transfected cells.<sup>145</sup>

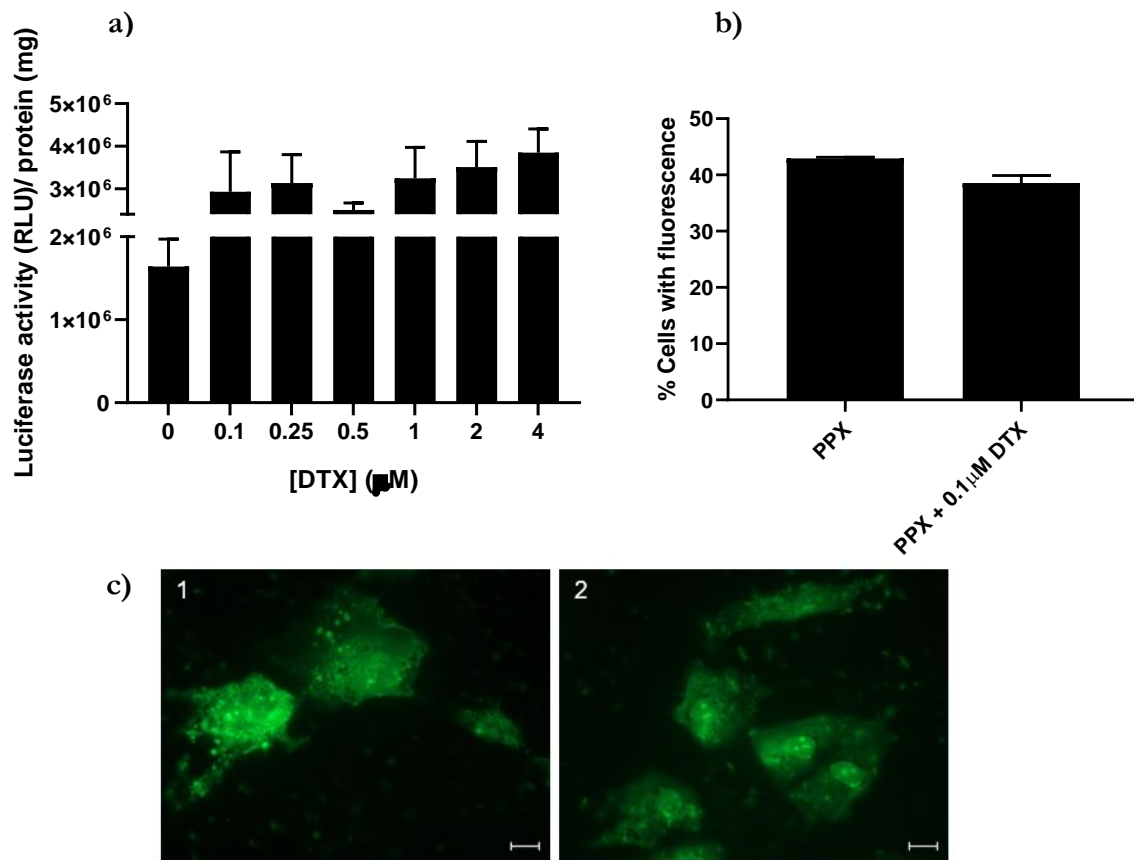


**Figure 29 | Effect of the pre-treatment of Huh-7 cells with docetaxel on the luciferase gene expression (a), and green fluorescent protein gene expression evaluated by flow cytometry (b) and fluorescence microscopy (c).** (a) The polyplexes (N/P charge ratio = 40/1) were prepared with 1 μg of pLUC. Cells were preincubated with DMEM with or without different concentrations of docetaxel (0.1, 0.25, 0.5, 1, 2, and 4 μM). Levels of gene expression are expressed as RLU of luciferase per mg of total cell protein (mean ± SEM, obtained from triplicates) and were determined as described in “Materials and Methods”. (b, c) The polyplexes (N/P charge ratio = 40/1) were prepared with 4 μg of pGFP. Cells were preincubated with DMEM with or without 0.1 μM of docetaxel. (b) Data are expressed as a percentage of transfected cells. (c) Fluorescence microscopy images: (1) cells treated with polyplexes and (2) cells treated with polyplexes in the presence of 0.1 μM of docetaxel (scale bar = 10 μm)



In order to confirm the flow cytometry results, fluorescence microscopy was performed using polyplexes prepared with the plasmid encoding for GFP, at the 40/1 N/P charge ratio. The obtained images showed no significant differences in the fluorescence intensity of the cells transfected with the polyplexes and the cells transfected after pre-incubation with 0.1  $\mu$ M of docetaxel, opposite to what was observed in terms of luciferase expression.

As previously mentioned, microtubule-stabilizing drugs could influence the intracellular trafficking of polyplexes.<sup>145</sup> As components of the cytoskeleton, microtubules are involved in the vesicles and organelles transport, including the endocytic pathway and nuclear migration.<sup>146</sup> Therefore, the use of these therapeutics can promote polyplexes endosomal escape, by avoiding the fusion between the late endosomes and lysosomes.<sup>145</sup> After polyplexes escape from the endocytic pathway, avoiding degradation, they can effectively migrate to the nucleus, which provides the necessary machinery for transcription of the delivered genetic material, leading to transgene expression enhancement. .<sup>145</sup>

In order to prove this hypothesis, confocal laser scanning microscopy was performed after transfection with solely the polyplexes and the polyplexes in the presence of 0.1 $\mu$ M of docetaxel. Polyplexes were prepared with 2% of the fluorescein-labelled polymer and pLUC, at 40/1 N/P charge ratio. The obtained results showed a slight increase of yellow dots in the overlaying images, which means that the co-localization of the polyplexes (green) with the acidic compartments (red) increased after pre-incubation of the cells with docetaxel (**Figure 30**). Since docetaxel inhibits the fusion of endosomes with lysosomes, the polyplexes could be inside the endosome, but will not necessarily be degraded. Therefore, docetaxel could still be promoting polyplexes endosomal escape, which would explain the increase of transgene expression, registered in the luminescence assay (**Figure 29 a**).

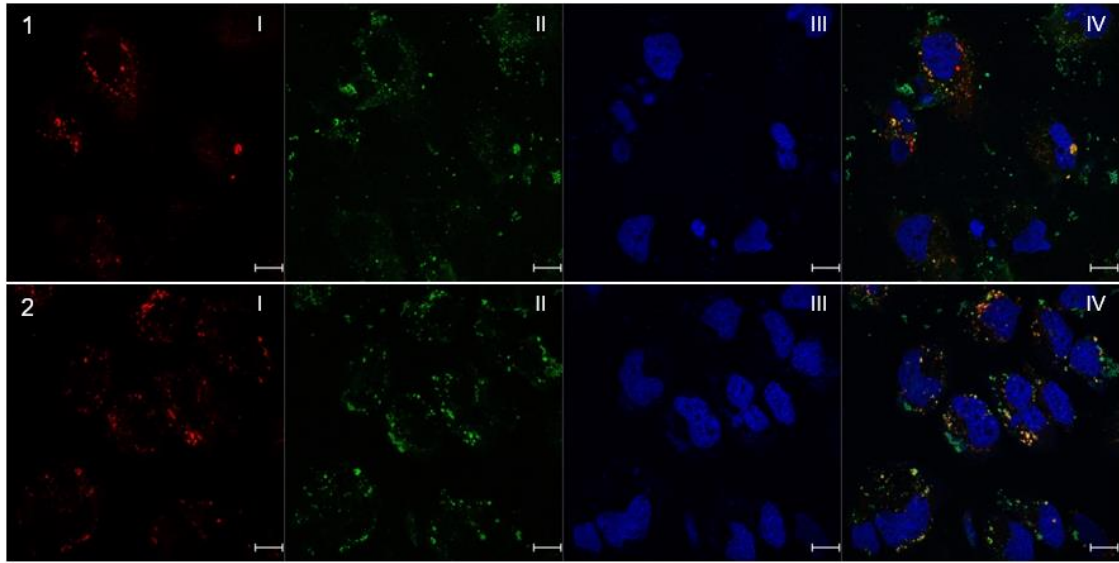


**Figure 30 | Effect of the pre-treatment with docetaxel on the intracellular distribution of polyplexes in Huh-7 cells observed by confocal microscopy.** The polyplexes were prepared with 2% of the fluorescein-labelled polymer, at a 40/1 N/P charge ratio with pLUC. Cells were preincubated with DMEM with or without 0.1  $\mu\text{M}$  of docetaxel. After, cells were labelled and fixed as described in “Materials and Methods”. (1) Cells treated with polyplexes and (2) cells treated with polyplexes in the presence of 0.1  $\mu\text{M}$  of docetaxel. (I) red fluorescent image of acidic compartments labelled with Lysotracker Red DND-99; (II) green fluorescent image of polyplexes prepared with fluorescein-labelled polymer; (III) blue fluorescent image of cell nucleus stained by DAPI; (IV) overlay image of images I–III (scale bar = 10  $\mu\text{m}$ ).

## 4 Development of a therapeutic strategy

p53 is an endogenous tumor suppressor gene that presents the ability to control cell-cycle arrest, apoptosis, and DNA repair, besides suppressing angiogenesis.<sup>40-43</sup> Likewise, PTEN, a dual-specificity phosphatase, acts as a tumor suppressor by inhibiting PI3K/AKT signaling pathway, involved in cell survival.<sup>56,57</sup> Both genes were found to be dysregulated in several cancers, including HCC.<sup>43,58,59</sup>

In order to evaluate the potential of the PAMA-co-PLAMA-based polyplexes to mediate an antitumor strategy, a preliminary test was performed using polyplexes at 40/1 N/P charge ratio, prepared with DNA plasmids encoding p53 or PTEN. The objective was to restore the normal levels of expression of these genes. Cell viability of Huh-7 cells was measured 48 and 72 hours after transfection and the results were compared to the ones obtained in the presence of polyplexes prepared with pLUC, in the same conditions.

The obtained results showed that the polyplexes prepared with these plasmids lead to a similar profile of toxicity in Huh-7 cells. In fact, at 48 hours of incubation, polyplexes containing the plasmid encoding p53 or PTEN did not lead to an increase of toxicity when compared with polyplexes prepared with pLUC (**Figure 31 a**).

This means that there was no antitumor effect. It was also observed that the drug by itself does not present high toxicity (70 % of cell viability). However, when combined with the polyplex formulation, cell viability decreases to 54 %. In terms of the combination of docetaxel with the polyplexes prepared with the therapeutic plasmids, the obtained results showed no significant antitumor effect, since the decrease in cell viability was less than 10 % when compared with the results obtained with the combination of docetaxel with polyplexes prepared with pLUC.

On the other hand, after 72 hours of incubation, it was observed a decrease of cell viability from 80 %, in the presence of the formulation prepared with pLUC, to 59%, after transfection with polyplexes prepared with the therapeutic plasmids (**Figure 31 b**). Here, the effect of the therapeutic genes on cell viability was more notorious, probably due to the increase of incubation time, which enabled a more extended expression of these genes, enhancing the antitumor effect. In what concerns the combination with docetaxel, it was observed that the levels of cell viability after transfection with the formulation in the presence of docetaxel are close to the ones obtained with the drug alone.

Overall, the results demonstrated that the developed formulation can effectively deliver the therapeutic plasmids, p53 and PTEN, resulting in a decrease of cell viability, 72 hours after transfection. The antitumor effect obtained after transfection with polyplexes prepared with the plasmid encoding p53 or PTEN was similar. The obtained results did not allow to show an evident benefit of combining the formed polyplexes with docetaxel, since 72 hours after transfection the observed cell damage was mostly caused by the drug. Despite the transgene expression enhancement registered using polyplexes prepared with pLUC in the presence of docetaxel (**Figure 31 c**) the strong impact of this drug on cell viability restricts the application of this combination.

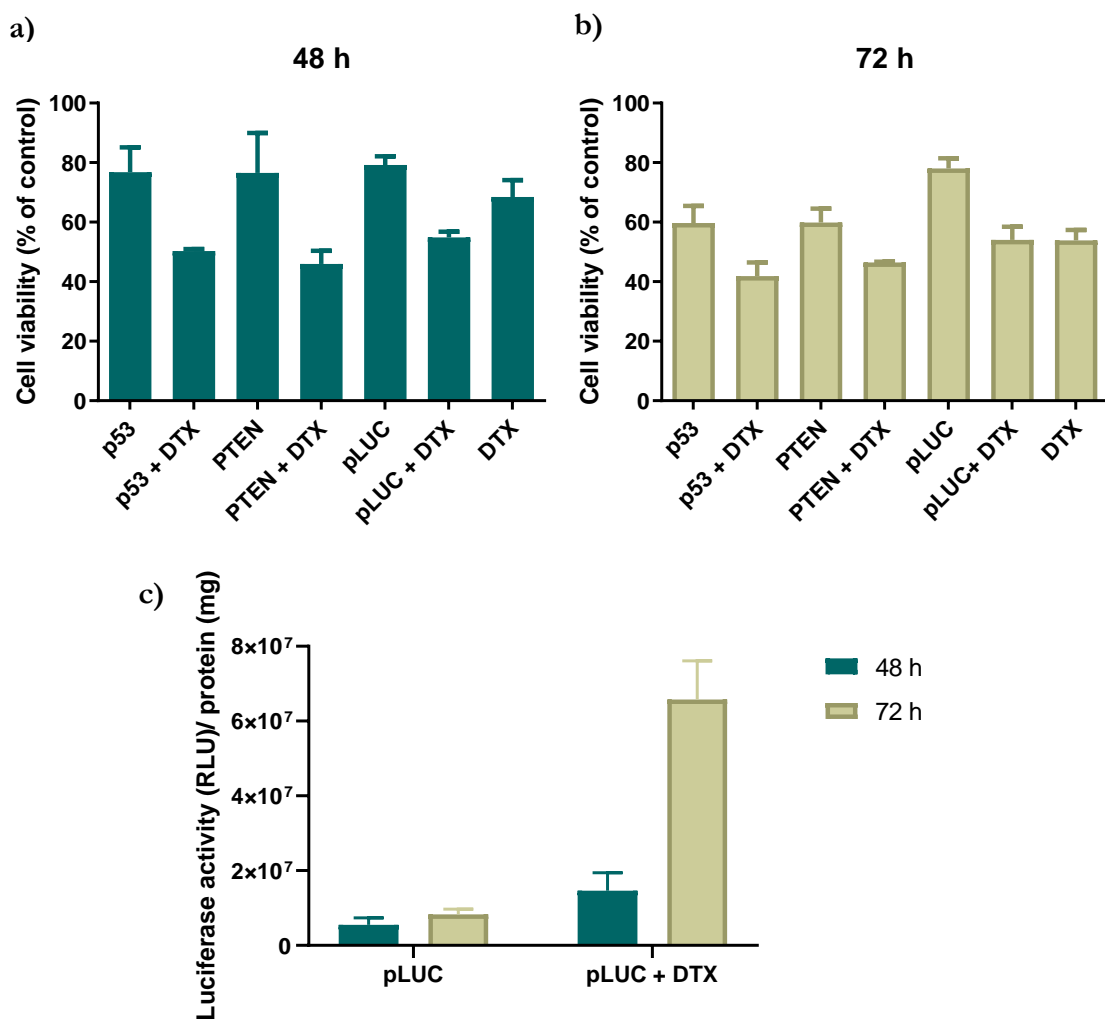


**Figure 31 | Effect of the polyplexes prepared with p53, PTEN and pLUC, and the combination of polyplexes with docetaxel, on the viability of Huh-7 cells, (a) 48 h and (b) 72 h after transfection, and (c) on the luciferase gene expression in Huh-7 cells, 48 and 72 h after transfection.** The polyplexes were prepared with 1  $\mu$ g of the indicated plasmids at a 40/1 N/P charge ratio. Cells were preincubated with DMEM containin or not 0.1  $\mu$ M of docetaxel. Cell viability is expressed as a percentage of untreated control cells (mean  $\pm$  SEM, obtained from triplicates) and was measured through an Alamar blue assay. Levels of gene expression are expressed as RLU of luciferase per mg of total cell protein (mean  $\pm$  SEM, obtained from triplicates) and was determined as described in “Materials and Methods”.

# Chapter 4

## Conclusions

Gene therapy has been extensively studied to treat, prevent or even eliminate several diseases, including cancer. In this regard, it refers to the delivery of genetic material to the target cells to induce an antitumor effect, preventing adverse side effects, which are a major limitation of the traditional systemic chemotherapy. Over the years, several gene delivery systems have been developed and engineered and, despite viral gene delivery systems being most commonly used, non-viral gene delivery systems stand out due to their safety and versatility. This type of delivery systems includes polymeric nanoparticles, which present several advantages making them extremely attractive. In the context of cancer, polymeric nanoparticles are suitable not only for gene delivery but also for the delivery of other therapeutic agents, such as drugs and proteins, allowing prolonged circulation times and targeted delivery, resulting in higher therapeutic efficacy. The unique properties of these nanosystems are mainly due to specific characteristics of the polymers, including biocompatibility, controllable molecular weight, and tunable chemical structure.

Taking this into account, the main purpose of this study was to develop a new polymer-based nanosystem able to effectively and specifically deliver genetic material into hepatocellular carcinoma cells. Accordingly, the copolymers used for the preparation of these nanosystems were synthesized through a controlled polymerization method, ARGET ATRP, which offers the possibility to obtain polymers with well-defined properties. Moreover, these copolymers contained LAMA, a monomer with galactose, able to target ASGPR, overexpressed in the surface of hepatocarcinoma cells, allowing the specific targeting of these cells.

Initially, polymeric micelles were prepared using amphiphilic glycopolymers, PAMA<sub>103-*co*</sub>-PLAMA<sub>19-*b*</sub>-PDEAEMA<sub>63</sub> and PAMA<sub>50-*co*</sub>-PLAMA<sub>10-*b*</sub>-PDEAEMA<sub>16</sub>, and extensively characterized through DLS and zeta potential, demonstrating that both micelle formulations presented a size around 70 nm and positive surface charge. To produce micelleplexes, a DNA plasmid encoding luciferase was complexed with the micelles, which proved to effectively condense and protect the genetic material. The cytotoxicity of these nanosystems was evaluated and the obtained results showed that superior N/P charge ratios were associated with higher levels of cytotoxicity, given the increased amount of polymer.

After, the ability of these nanosystems to deliver genetic material into HepG2 cells was evaluated. Transfection activity results showed that none of the formulations present significant transgene expression. Therefore, despite the polymeric micelles ability to condense and protect the genetic material, their application is limited most probably due to the plasmid inability to be released from the nanosystem, which makes it impossible to be expressed. At last, to evaluate the potential of the polymeric micelles for drug delivery, sorafenib was loaded into PAMA<sub>50-*co*</sub>-PLAMA<sub>10-*b*</sub>-PDEAEMA<sub>16</sub>-based micelles, resulting in high levels of cytotoxicity caused by the high amount of polymer, which showed another major limitation of these nanosystems, restricting their application for drug delivery.

In the second approach, PAMA<sub>73-*co*</sub>-PLAMA<sub>21</sub>-based polyplexes were produced and characterized through DLS, presenting a size around 150 nm and a positive surface charge. Moreover, these nanosystems proved to effectively condense and protect genetic material (pLUC), maintaining their stability over time. The ability of these polyplexes to deliver genetic material into different hepatocellular carcinoma cell lines (HepG2, Hep3B and Huh-7) was evaluated, and the obtained results showed great levels of transgene expression, particularly in Huh-7 cells. For the tested charge ratios, transgene expression increased along with the N/P charge ratio, since for these cases the high amount of polymer and, consequently, high density of positive charges, contribute to overcoming the neutralization promoted by the interaction with negatively charged serum proteins. In terms of cytotoxicity, the obtained data showed a similar profile in all cell lines, demonstrating that superior N/P charge ratios caused higher levels of cytotoxicity, resulting from the high amount of positive charges, which can structurally destabilize cellular membranes, causing cell damage. Transfection efficiency of the PAMA<sub>73-*co*</sub>-PLAMA<sub>21</sub>-based polyplexes, evaluated by flow cytometry, resulted in a 10-fold increase of the percentage of transfected cells comparing to the commercial control, PEI. After, a competition assay performed with the natural ligand for the ASGPR, asialofetuin, demonstrated that these nanosystems interact specifically with these cells, since the presence of this protein blocked the internalization of the polyplexes, resulting in no expression of the transgene.

The ability of the nanosystems to escape from endocytic vesicles is a major step to avoid degradation and clearance, enhancing gene delivery efficiency. Since cellular uptake and intracellular distribution analysis by confocal microscopy showed that some polyplexes were co-localized with acidic compartments, docetaxel, a microtubule-stabilizing taxane was used to promote endosomal escape. Different concentrations of this drug were tested and

the preincubation of Huh-7 cells with docetaxel before transfection with the generated polyplexes showed increased levels of transgene expression.

At last, in order to evaluate the potential of PAMA<sub>73-*l*0</sub>-PLAMA<sub>21</sub>-based polyplexes to mediate an antitumor strategy, a preliminary assay showed a decrease of cell viability after transfection of Huh-7 cells with polyplexes prepared with the therapeutic plasmids encoding p53 or PTEN, comparing to the result obtained after transfection with polyplexes prepared with pLUC. These results demonstrated that the polyplex formulation could effectively deliver the therapeutic plasmids, resulting in a similar profile of toxicity in Huh-7 cells. Levels of toxicity were also assessed in the presence of docetaxel, showing that the strong impact of the drug in cell viability restricts the application of the combined strategy in the tested experimental conditions.





# Chapter 5

## References

1. Torre, L. A., Siegel, R. L., Ward, E. M. & Jemal, A. Global cancer incidence and mortality rates and trends - An update. *Cancer Epidemiol. Biomarkers Prev.* **25**, 16–27 (2016).
2. Sia, D., Villanueva, A., Friedman, S. L. & Llovet, J. M. Liver Cancer Cell of Origin, Molecular Class, and Effects on Patient Prognosis. *Gastroenterology* **152**, 745–761 (2017).
3. Global Cancer Observatory. (2020).
4. Galle, P. R. *et al.* EASL Clinical Practice Guidelines: Management of hepatocellular carcinoma. *J. Hepatol.* **69**, 182–236 (2018).
5. Kabashima, A. *et al.* Molecular and Immunological Paradigms of Hepatocellular Carcinoma: Special Reference to Therapeutic Approaches. *J. Hepatobiliary. Pancreat. Sci.* 0–2 (2020) doi:10.1002/jhbp.874.
6. Singal, A. G., Lampertico, P. & Nahon, P. Epidemiology and surveillance for hepatocellular carcinoma: New trends. *J. Hepatol.* **72**, 250–261 (2020).
7. Chew, S. A., Moscato, S., George, S., Azimi, B. & Danti, S. Liver cancer: Current and future trends using biomaterials. *Cancers (Basel)*. **11**, (2019).
8. Dutta, R. & Mahato, R. I. Recent advances in hepatocellular carcinoma therapy. *Pharmacol. Ther.* **173**, 106–117 (2017).
9. Fitzmaurice, C. *et al.* The burden of primary liver cancer and underlying etiologies from 1990 to 2015 at the global, regional, and national level results from the global burden of disease study 2015. *JAMA Oncol.* **3**, 1683–1691 (2017).
10. Hung, M. H. & Wang, X. W. Molecular Alterations and Heterogeneity in Hepatocellular Carcinoma. 293–316 (2019) doi:10.1007/978-3-030-21540-8\_14.
11. Colombino, M. *et al.* BRAF and PIK3CA genes are somatically mutated in hepatocellular carcinoma among patients from South Italy. *Cell Death Dis.* **3**, (2012).
12. Akula, S. M. *et al.* RAS/RAF/MEK/ERK, PI3K/PTEN/AKT/mTORC1 and TP53 pathways and regulatory miRs as therapeutic targets in hepatocellular carcinoma. *Expert Opin. Ther. Targets* **23**, 915–929 (2019).
13. Yang, J. D. *et al.* HHS Public Access prevention and management. **16**, 589–604 (2019).
14. Kim, D. W., Talati, C. & Kim, R. Hepatocellular carcinoma (HCC): Beyond sorafenib-chemotherapy. *J. Gastrointest. Oncol.* **8**, 256–265 (2017).
15. Zhang, T. *et al.* Neoadjuvant therapy and immunotherapy strategies for hepatocellular carcinoma. *Am. J. Cancer Res.* **10**, 1658–1667 (2020).
16. Medavaram, S. & Zhang, Y. Emerging therapies in advanced hepatocellular carcinoma. *Exp. Hematol. Oncol.* **7**, 1–9 (2018).
17. De Mattia, E. *et al.* Pharmacogenetics of the systemic treatment in advanced hepatocellular carcinoma. *World J. Gastroenterol.* **25**, 3870–3896 (2019).
18. Fan, G., Wei, X. & Xu, X. Is the era of sorafenib over? A review of the literature. *Ther. Adv. Med. Oncol.* **12**, 1–21 (2020).
19. Keating, G. M. Sorafenib: A Review in Hepatocellular Carcinoma. *Target. Oncol.* **12**, 243–253 (2017).

20. Swamy, S. G. *et al.* Targeting multiple oncogenic pathways for the treatment of hepatocellular carcinoma. *Target. Oncol.* **12**, 1–10 (2017).
21. Liu, L. *et al.* Sorafenib blocks the RAF/MEK/ERK pathway, inhibits tumor angiogenesis, and induces tumor cell apoptosis in hepatocellular carcinoma model PLC/PRF/5. *Cancer Res.* **66**, 11851–11858 (2006).
22. Daher, S., Massarwa, M., Benson, A. A. & Khoury, T. Current and future treatment of hepatocellular carcinoma: An updated comprehensive review. *J. Clin. Transl. Hepatol.* **6**, 69–78 (2018).
23. Harding, J. J., El Dika, I. & Abou-Alfa, G. K. Immunotherapy in hepatocellular carcinoma: Primed to make a difference? *Cancer* **122**, 367–377 (2016).
24. Chen, M. L. *et al.* Sorafenib relieves cell-intrinsic and cell-extrinsic inhibitions of effector T cells in tumor microenvironment to augment antitumor immunity. *Int. J. Cancer* **134**, 319–331 (2014).
25. Younis, M. A., Khalil, I. A. & Harashima, H. Gene Therapy for Hepatocellular Carcinoma: Highlighting the Journey from Theory to Clinical Applications. *Adv. Ther.* **3**, 2000087 (2020).
26. Reghupaty, S. C. & Sarkar, D. Current status of gene therapy in hepatocellular carcinoma. *Cancers (Basel)*. **11**, (2019).
27. Duan, F. & Lam, M. G. E. H. Delivery approaches of gene therapy in hepatocellular carcinoma. *Anticancer Res.* **33**, 4711–4718 (2013).
28. Wang, X., Tai, Z., Zhang, W. & Gao, S. Current Status of Gene Therapy for Hepatocellular Carcinoma, with a Focus on Gene Delivery Approaches. *Curr. Gene Ther.* **15**, 120–141 (2015).
29. Blaese, R. M. *et al.* T lymphocyte-directed gene therapy for ADA-SCID: Initial trial results after 4 years. *Science (80-. ).* **270**, 475–480 (1995).
30. Gene Therapy Clinical Trials Worldwide. *The Journal of Gene Medicine* <https://a873679.fmphost.com/fmi/webd/GTCT> (2021).
31. Ginn, S. L., Amaya, A. K., Alexander, I. E., Edelstein, M. & Abedi, M. R. Gene therapy clinical trials worldwide to 2017: An update. *J. Gene Med.* **20**, 1–16 (2018).
32. Nidetz, N. F. *et al.* Adeno-associated viral vector-mediated immune responses: Understanding barriers to gene delivery. *Pharmacol. Ther.* **207**, 107453 (2020).
33. Gaudet, D. *et al.* Efficacy and long-term safety of alipogene tiparvovec (AAV1-LPL S447X) gene therapy for lipoprotein lipase deficiency: An open-label trial. *Gene Ther.* **20**, 361–369 (2013).
34. Keeler, A. M., ElMallah, M. K. & Flotte, T. R. Gene Therapy 2017: Progress and Future Directions. *Clin. Transl. Sci.* **10**, 242–248 (2017).
35. Andtbacka, R. H. I. *et al.* Patterns of Clinical Response with Talimogene Laherparepvec (T-VEC) in Patients with Melanoma Treated in the OPTiM Phase III Clinical Trial. *Ann. Surg. Oncol.* **23**, 4169–4177 (2016).
36. Gruntman, A. M. & Flotte, T. R. The rapidly evolving state of gene therapy. *FASEB J.* **32**, 1733–1740 (2018).
37. Villanueva, A., Newell, P., Chiang, D. Y., Friedman, S. L. & Llovet, J. M. Genomics and signaling pathways in hepatocellular carcinoma. *Semin. Liver Dis.* **27**, 55–76 (2007).
38. Stephanie C. Casey, Ling Tong, Yulin Li, Rachel Do, Susanne Walz, Kelly N. Fitzgerald, Arvin Gouw, Virginie Baylot, Ines Gutgemann, Martin Eilers, and D. W. F. MYC Regulates the Anti-Tumor Immune Response through CD47 and PD-L1. *Science (80-. ).* **176**, 100–106 (2016).
39. Pollutri, D., Gramantieri, L., Bolondi, L. & Fornari, F. TP53/MicroRNA interplay in hepatocellular carcinoma. *Int. J. Mol. Sci.* **17**, 1–20 (2016).

40. C. G. Ferreira, C. T. & G. G. p53 and chemosensitivity. *Ann. Oncol.* **10**, 1011–1021 (1999).
41. Bálint, É. & Vousden, K. H. Activation and activities of the p53 tumour suppressor protein. *Br. J. Cancer* **85**, 1813–1823 (2001).
42. Xu, G. W. *et al.* Tissue-specific growth suppression and chemosensitivity promotion in human hepatocellular carcinoma cells by retroviral-mediated transfer of the wild-type p53 gene. *Hepatology* **24**, 1264–1268 (1996).
43. Guan, Y. S., La, Z., Yang, L., He, Q. & Li, P. p53 gene in treatment of hepatic carcinoma: Status quo. *World J. Gastroenterol.* **13**, 985–992 (2007).
44. Kountouras, J., Zavos, C. & Chatzopoulos, D. Apoptotic and anti-angiogenic strategies in liver and gastrointestinal malignancies. *J. Surg. Oncol.* **90**, 249–259 (2005).
45. Couri, T. & Pillai, A. Goals and targets for personalized therapy for HCC. *Hepatol. Int.* **13**, 125–137 (2019).
46. Biegging, K. T., Mello, S. S. & Attardi, L. D. Unravelling mechanisms of p53-mediated tumour suppression. *Nat. Rev. Cancer* **14**, 359–370 (2014).
47. Wang, W., Rastinejad, F. & El-Deiry, W. S. Restoring p53-dependent tumor suppression. *Cancer Biol. Ther.* **2**, (2003).
48. Yaginuma, Y. & Westpha, H. Abnormal Structure and Expression of the p53 Gene in Human Ovarian Carcinoma Cell Lines. *Cancer Res.* **52**, 4196–4199 (1992).
49. Nagao, M. *et al.* The alteration of Fas receptor and ligand system in hepatocellular carcinomas: How do hepatoma cells escape from the host immune surveillance in vivo? *Hepatology* **30**, 413–421 (1999).
50. Kabashima, A. *et al.* Molecular and immunological paradigms of hepatocellular carcinoma: Special reference to therapeutic approaches. *J. Hepatobiliary. Pancreat. Sci.* **28**, 62–75 (2021).
51. Kong, N. *et al.* Synthetic mRNA nanoparticle-mediated restoration of p53 tumor suppressor sensitizes p53-deficient cancers to mTOR inhibition. *Sci. Transl. Med.* **11**, 1–32 (2019).
52. Li, J. *et al.* PTEN, a putative protein tyrosine phosphatase gene mutated in human brain, breast, and prostate cancer. *Science (80-. )*. **275**, 1943–1947 (1997).
53. Peter A. Steck, Mark A. Pershouse, Samar A. Jasser, W.K. Alfred Yung, Huai Lin, Azra H. Ligon, Lauren A. Langford, Michelle L. Baumgard, Thomas Hattier, Thaylon Davis, Cheryl Frye, Rong Hu, Bradley Swedlund, D. H. R. T. & S. V. T. Identification of a candidate tumour suppressor gene, MMAC1, at chromosome 10q23.3 that is mutated in multiple advanced cancers. *Nat. Genet.* **15**, 57–61 (1997).
54. Myers, M. P. *et al.* P-TEN, the tumor suppressor from human chromosome 10q23, is a dual-specificity phosphatase. *Proc. Natl. Acad. Sci. U. S. A.* **94**, 9052–9057 (1997).
55. Naderali, E. *et al.* Regulation and modulation of PTEN activity. *Mol. Biol. Rep.* **45**, 2869–2881 (2018).
56. Brito, M. B., Goulielmaki, E. & Papakonstanti, E. A. Focus on PTEN regulation. *Front. Oncol.* **5**, 1–15 (2015).
57. Myers, M. P. *et al.* The lipid phosphatase activity of PTEN is critical for its tumor suppressor function. *Proc. Natl. Acad. Sci. U. S. A.* **95**, 13513–13518 (1998).
58. Cervello, M. *et al.* New landscapes and horizons in hepatocellular carcinoma therapy. *Aging (Albany. NY)*. **12**, 3053–3094 (2020).
59. Wang, Q., Chen, X. & Hay, N. Akt as a target for cancer therapy: More is not always better (lessons from studies in mice). *Br. J. Cancer* **117**, 159–163 (2017).

60. Maehama, T. & Dixon, J. E. The tumor suppressor, PTEN/MMAC1, dephosphorylates the lipid second messenger, phosphatidylinositol 3,4,5-trisphosphate. *J. Biol. Chem.* **273**, 13375–13378 (1998).
61. Subbiah, I. M. *et al.* Exploring response signals and targets in aggressive unresectable hepatocellular carcinoma: An analysis of targeted therapy phase 1 trials. *Oncotarget* **6**, 28453–28462 (2015).
62. Khemlina, G., Ikeda, S. & Kurzrock, R. The biology of Hepatocellular carcinoma: Implications for genomic and immune therapies. *Mol. Cancer* **16**, 1–10 (2017).
63. Zucman-Rossi, J., Villanueva, A., Nault, J. C. & Llovet, J. M. Genetic Landscape and Biomarkers of Hepatocellular Carcinoma. *Gastroenterology* **149**, 1226-1239.e4 (2015).
64. Tumor Suppressor Protein - PTEN. *Targeted Cancer Care* <https://targetedcancercare.massgeneral.org/My-Trial-Guide/Diseases/Lung-Cancer/PTEN.aspx> (2020).
65. Kulkarni, J. A. *et al.* The current landscape of nucleic acid therapeutics. *Nat. Nanotechnol.* **16**, 630–643 (2021).
66. Xia, D., Zhang, M.-M. & Yan, L.-N. Recent advances in liver-directed gene transfer vectors. *Hepatobiliary Pancreat. Dis. Int* **3**, 332–336 (2004).
67. Slade, N. Viral vectors in gene therapy. *Period. Biol.* **103**, 139–143 (2018).
68. Shahryari, A., Burtcher, I., Nazari, Z. & Lickert, H. Engineering Gene Therapy: Advances and Barriers. *Adv. Ther.* **2100040**, 2100040 (2021).
69. Ura, T., Okuda, K. & Shimada, M. Developments in viral vector-based vaccines. *Vaccines* **2**, 624–641 (2014).
70. Warnock, J. N., Daigre, C. & Al-Rubeai, M. Introduction to viral vectors. *Methods Mol. Biol.* **737**, 1–25 (2011).
71. Vannucci, L., Lai, M., Chiuppesi, F., Ceccherini-Nelli, L. & Pistello, M. Viral vectors: A look back and ahead on gene transfer technology. *New Microbiol.* **36**, 1–22 (2013).
72. Abudoureyimu, M. *et al.* Oncolytic Adenovirus—A Nova for Gene-Targeted Oncolytic Viral Therapy in HCC. *Front. Oncol.* **9**, (2019).
73. Bai, Y. huan *et al.* A novel oncolytic adenovirus inhibits hepatocellular carcinoma growth. *J. Zhejiang Univ. Sci. B* **20**, 1003–1013 (2019).
74. Li, Y. F. *et al.* HSVtk/GCV system on hepatoma carcinoma cells: Construction of the plasmid pcDNA3.1-pAFP-TK and targeted killing effect. *Mol. Med. Rep.* **16**, 764–772 (2017).
75. Fukuhara, H., Ino, Y. & Todo, T. Oncolytic virus therapy: A new era of cancer treatment at dawn. *Cancer Sci.* **107**, 1373–1379 (2016).
76. Patil, S. *et al.* The development of functional non-viral vectors for gene delivery. *Int. J. Mol. Sci.* **20**, 1–23 (2019).
77. Kuşcu, L. & Sezer, A. D. Future prospects for gene delivery systems. *Expert Opin. Drug Deliv.* **14**, 1205–1215 (2017).
78. Shim, G. *et al.* Nonviral Delivery Systems For Cancer Gene Therapy: Strategies And Challenges. *Curr. Gene Ther.* **18**, 3–20 (2018).
79. Li, L., He, Z. Y., Wei, X. W., Gao, G. P. & Wei, Y. Q. Challenges in CRISPR/CAS9 Delivery: Potential Roles of Nonviral Vectors. *Hum. Gene Ther.* **26**, 452–462 (2015).
80. Mohammadinejad, R., Dehshahri, A. & Madamsetty, V. S. In vivo gene delivery mediated by non-viral vectors for cancer therapy. (2020).

81. Baig, B., Halim, S. A., Farrukh, A., Greish, Y. & Amin, A. Current status of nanomaterial-based treatment for hepatocellular carcinoma. *Biomed. Pharmacother.* **116**, 108852 (2019).
82. Mitchell, M. J. *et al.* Engineering precision nanoparticles for drug delivery. *Nat. Rev. Drug Discov.* **20**, 101–124 (2021).
83. Li, Y., Thambi, T. & Lee, D. S. Co-Delivery of Drugs and Genes Using Polymeric Nanoparticles for Synergistic Cancer Therapeutic Effects. *Adv. Healthc. Mater.* **7**, (2018).
84. Guo, X., Wang, L., Wei, X. & Zhou, S. Polymer-based drug delivery systems for cancer treatment. *J. Polym. Sci. Part A Polym. Chem.* **54**, 3525–3550 (2016).
85. Choudhury, H., Gorain, B., Pandey, M., Khurana, R. K. & Kesharwani, P. Strategizing biodegradable polymeric nanoparticles to cross the biological barriers for cancer targeting. *Int. J. Pharm.* **565**, 509–522 (2019).
86. Zhou, Q., Zhang, L. & Wu, H. Nanomaterials for cancer therapies. *Nanotechnol. Rev.* **6**, 473–496 (2017).
87. Dang, Y. & Guan, J. Nanoparticle-based drug delivery systems for cancer therapy. *Smart Mater. Med.* **1**, 10–19 (2020).
88. Khan, I., Saeed, K. & Khan, I. Nanoparticles: Properties, applications and toxicities. *Arab. J. Chem.* **12**, 908–931 (2019).
89. Werfel, T. & Duvall, C. *Polymeric nanoparticles for gene delivery. Polymers and Nanomaterials for Gene Therapy* (Elsevier Ltd., 2016). doi:10.1016/B978-0-08-100520-0.00007-2.
90. Wei, H., Zhuo, R. X. & Zhang, X. Z. Design and development of polymeric micelles with cleavable links for intracellular drug delivery. *Prog. Polym. Sci.* **38**, 503–535 (2013).
91. Kang, L., Gao, Z., Huang, W., Jin, M. & Wang, Q. Nanocarrier-mediated co-delivery of chemotherapeutic drugs and gene agents for cancer treatment. *Acta Pharm. Sin. B* **5**, 169–175 (2015).
92. Yang, Y. Q. *et al.* PH-sensitive micelles self-assembled from multi-arm star triblock co-polymers poly( $\epsilon$ -caprolactone)-b-poly(2-(diethylamino)ethyl methacrylate)-b-poly(poly(ethylene glycol) methyl ether methacrylate) for controlled anticancer drug delivery. *Acta Biomater.* **9**, 7679–7690 (2013).
93. He, E. *et al.* Polyplex formation between four-arm poly(ethylene oxide)-b-poly(2-(diethylamino)ethyl methacrylate) and plasmid DNA in gene delivery. *J. Biomed. Mater. Res. - Part A* **91**, 708–718 (2009).
94. Santo, D. *et al.* Combination of Poly[(2-dimethylamino)ethyl methacrylate] and Poly( $\beta$ -amino ester) Results in a Strong and Synergistic Transfection Activity. *Biomacromolecules* **18**, 3331–3342 (2017).
95. Cordeiro, R. A., Serra, A., Coelho, J. F. J. & Faneca, H. Poly( $\beta$ -amino ester)-based gene delivery systems: From discovery to therapeutic applications. *J. Control. Release* **310**, 155–187 (2019).
96. Santo, D. *et al.* Poly(ethylene glycol)- block-poly(2-aminoethyl methacrylate hydrochloride)-Based Polyplexes as Serum-Tolerant Nanosystems for Enhanced Gene Delivery. *Mol. Pharm.* **16**, 2129–2141 (2019).
97. Taghipour-Sabzevar, V., Sharifi, T. & Moghaddam, M. M. Polymeric nanoparticles as carrier for targeted and controlled delivery of anticancer agents. *Ther. Deliv.* **10**, 527–550 (2019).
98. Raj, S. *et al.* Specific targeting cancer cells with nanoparticles and drug delivery in cancer therapy. *Semin. Cancer Biol.* 0–1 (2019) doi:10.1016/j.semcancer.2019.11.002.
99. Yin, T., Wang, L., Yin, L., Zhou, J. & Huo, M. Co-delivery of hydrophobic paclitaxel and hydrophilic AURKA specific siRNA by redox-sensitive micelles for effective treatment of breast cancer.

*Biomaterials* **61**, 10–25 (2015).

100. Zhu, C. *et al.* Co-delivery of siRNA and paclitaxel into cancer cells by biodegradable cationic micelles based on PDMAEMA-PCL-PDMAEMA triblock copolymers. *Biomaterials* **31**, 2408–2416 (2010).
101. Sun, T. M. *et al.* Simultaneous delivery of siRNA and paclitaxel via a ‘two-in-one’ micelleplex promotes synergistic tumor suppression. *ACS Nano* **5**, 1483–1494 (2011).
102. Xie, X. *et al.* Polymeric Hybrid Nanomicelles for Cancer Theranostics: An Efficient and Precise Anticancer Strategy for the Codelivery of Doxorubicin/miR-34a and Magnetic Resonance Imaging. *ACS Appl. Mater. Interfaces* **11**, 43865–43878 (2019).
103. Huang, H. Y., Kuo, W. T., Chou, M. J. & Huang, Y. Y. Co-delivery of anti-vascular endothelial growth factor siRNA and doxorubicin by multifunctional polymeric micelle for tumor growth suppression. *J. Biomed. Mater. Res. - Part A* **97 A**, 330–338 (2011).
104. Shi, S. *et al.* The use of cationic MPEG-PCL-g-PEI micelles for co-delivery of Msurvivin T34A gene and doxorubicin. *Biomaterials* **35**, 4536–4547 (2014).
105. Peng, Y., Huang, J., Xiao, H., Wu, T. & Shuai, X. Codelivery of temozolomide and siRNA with polymeric nanocarrier for effective glioma treatment. *Int. J. Nanomedicine* **13**, 3467–3480 (2018).
106. Yang, S. *et al.* Nucleolin-Targeting AS1411-Aptamer-Modified Graft Polymeric Micelle with Dual pH/Redox Sensitivity Designed to Enhance Tumor Therapy through the Codelivery of Doxorubicin/TLR4 siRNA and Suppression of Invasion. *Mol. Pharm.* **15**, 314–325 (2018).
107. Chen, Y. *et al.* Targeted Codelivery of Doxorubicin and IL-36 $\gamma$  Expression Plasmid for An Optimal Chemo-Gene Combination Therapy against Cancer Lung Metastasis. *Nanomedicine* **15**, 129–141 (2019).
108. Lee, S. Y. *et al.* A theranostic micelleplex co-delivering SN-38 and VEGF siRNA for colorectal cancer therapy. *Biomaterials* **86**, 92–105 (2016).
109. Jia, F., Li, Y., Lu, J., Deng, X. & Wu, Y. Amphiphilic Block Copolymers-Guided Strategies for Assembling Nanoparticles: From Basic Construction Methods to Bioactive Agent Delivery Applications. *ACS Appl. Bio Mater.* **3**, 6546–6555 (2020).
110. Nelemans, L. C. & Gurevich, L. Drug delivery with polymeric nanocarriers-cellular uptake mechanisms. *Materials (Basel)*. **13**, 1–21 (2020).
111. Zhang, Y., Chan, J. W., Moretti, A. & Uhrich, K. E. Designing polymers with sugar-based advantages for bioactive delivery applications. *J. Control. Release* **219**, 355–368 (2015).
112. Hayat, S. M. G., Farahani, N., Safdarian, E., Roointan, A. & Sahebkar, A. Gene delivery using lipoplexes and polyplexes: Principles, limitations and solutions. *Crit. Rev. Eukaryot. Gene Expr.* **29**, 29–36 (2019).
113. Ita, K. Polyplexes for gene and nucleic acid delivery: Progress and bottlenecks. *Eur. J. Pharm. Sci.* **150**, 105358 (2020).
114. Lai, W. F. & Wong, W. T. Design of Polymeric Gene Carriers for Effective Intracellular Delivery. *Trends Biotechnol.* **36**, 713–728 (2018).
115. Kloeckner, J., Prasmickaite, L., Høgset, A., Berg, K. & Wagner, E. Photochemically enhanced gene delivery of EGF receptor-targeted DNA polyplexes. *J. Drug Target.* **12**, 205–213 (2004).
116. Gao, Y. *et al.* PH/Redox Dual-Responsive Polyplex with Effective Endosomal Escape for Codelivery of siRNA and Doxorubicin against Drug-Resistant Cancer Cells. *ACS Appl. Mater. Interfaces* **11**, 16296–16310 (2019).
117. Mastrobattista, E. *et al.* Lipid-coated polyplexes for targeted gene delivery to ovarian carcinoma cells. *Cancer Gene Ther.* **8**, 405–413 (2001).

118. Chen, G. *et al.* Fluorination Enhances Serum Stability of Bioreducible Poly(amido amine) Polyplexes and Enables Efficient Intravenous siRNA Delivery. *Adv. Healthc. Mater.* **7**, 1–14 (2018).
119. Lou, B. *et al.* Small nanosized poly(vinyl benzyl trimethylammonium chloride) based polyplexes for siRNA delivery. *Int. J. Pharm.* **525**, 388–396 (2017).
120. Hwa Kim, S., Hyeon Lee, S., Tian, H., Chen, X. & Gwan Park, T. Prostate cancer cellspecific VEGF siRNA delivery system using cell targeting peptide conjugated polyplexes. *J. Drug Target.* **17**, 311–317 (2009).
121. Lou, B. *et al.* RGD-decorated cholesterol stabilized polyplexes for targeted siRNA delivery to glioblastoma cells. *Drug Deliv. Transl. Res.* **9**, 679–693 (2019).
122. Lu, S., Morris, V. B. & Labhasetwar, V. Codelivery of DNA and siRNA via arginine-rich PEI-based polyplexes. *Mol. Pharm.* **12**, 621–629 (2015).
123. Jafari, F., Yilmaz, G. & Becer, C. R. Stimuli-responsive glycopolymers and their biological applications. *Eur. Polym. J.* **142**, 110147 (2021).
124. D'Souza, A. A. & Devarajan, P. V. Asialoglycoprotein receptor mediated hepatocyte targeting - Strategies and applications. *J. Control. Release* **203**, 126–139 (2015).
125. Lu, J., Wang, J. & Ling, D. Surface Engineering of Nanoparticles for Targeted Delivery to Hepatocellular Carcinoma. *Small* **14**, 1–25 (2018).
126. Alonso, S. Exploiting the bioengineering versatility of lactobionic acid in targeted nanosystems and biomaterials. *J. Control. Release* **287**, 216–234 (2018).
127. Li, J. *et al.* Collaborative assembly of doxorubicin and galactosyl diblock glycopolymers for targeted drug delivery of hepatocellular carcinoma. *Biomater. Sci.* **8**, 189–200 (2020).
128. Han, S. O., Mahato, R. I., Sung, Y. K. & Kim, S. W. Development of biomaterials for gene therapy. *Mol. Ther.* **2**, 302–317 (2000).
129. Van Bruggen, C., Hexum, J. K., Tan, Z., Dalal, R. J. & Reineke, T. M. Nonviral Gene Delivery with Cationic Glycopolymers. *Acc. Chem. Res.* (2019) doi:10.1021/acs.accounts.8b00665.
130. Tang, R., Palumbo, R. N., Nagarajan, L., Krogstad, E. & Wang, C. Well-defined block copolymers for gene delivery to dendritic cells: Probing the effect of polycation chain-length. *J. Control. Release* **142**, 229–237 (2010).
131. Nel, A. E. *et al.* Understanding biophysicochemical interactions at the nano-bio interface. *Nat. Mater.* **8**, 543–557 (2009).
132. Shahed Behzadia, Vahid Serpooshanb, Wei Taoa, Majd A. Hamalyc, Mahmoud Y. Alkawareekd, Erik C. Dreadene, Dennis Brownf, Alaaldin M. Alkilanyd, Omid C. Farokhzada, and M. M. Cellular Uptake of Nanoparticles: Journey Inside the Cell. *Chem Soc Rev.* **176**, 139–148 (2017).
133. Foroozandeh, P. & Aziz, A. A. Insight into Cellular Uptake and Intracellular Trafficking of Nanoparticles. *Nanoscale Res. Lett.* **13**, (2018).
134. Tros de Ilarduya, C., Sun, Y. & Düzgüneş, N. Gene delivery by lipoplexes and polyplexes. *Eur. J. Pharm. Sci.* **40**, 159–170 (2010).
135. Yang, S. & May, S. Release of cationic polymer-DNA complexes from the endosome: A theoretical investigation of the proton sponge hypothesis. *J. Chem. Phys.* **129**, (2008).
136. Torres-Vanegas, J. D., Cruz, J. C. & Reyes, L. H. Delivery systems for nucleic acids and proteins: Barriers, cell capture pathways and nanocarriers. *Pharmaceutics* **13**, 1–38 (2021).
137. Li, Y., Huang, G., Diakur, J. & Wiebe, L. Targeted Delivery of Macromolecular Drugs: Asialoglycoprotein Receptor (ASGPR) Expression by Selected Hepatoma Cell Lines used in Antiviral Drug Development. *Curr. Drug Deliv.* **5**, 299–302 (2008).

138. Guo, X. D. *et al.* Cationic micelles self-assembled from cholesterol-conjugated oligopeptides as an efficient gene delivery vector. *Biomaterials* **29**, 4838–4846 (2008).
139. Jeong, J. H. & Park, T. G. Poly(L-lysine)-g-poly(D,L-lactic-co-glycolic acid) micelles for low cytotoxic biodegradable gene delivery carriers. *J. Control. Release* **82**, 159–166 (2002).
140. Yue, Y. & Wu, C. Progress and perspectives in developing polymeric vectors for in vitro gene delivery. *Biomater. Sci.* **1**, 152–170 (2013).
141. Yang, C. *et al.* PH-sensitive mixed micelles assembled from PDEAEMA-PPEGMA and PCL-PPEGMA for doxorubicin delivery: Experimental and DPD simulations study. *Pharmaceutics* **12**, (2020).
142. Almulathanon, A. A. Y., Ranucci, E., Ferruti, P., Garnett, M. C. & Bosquillon, C. Comparison of Gene Transfection and Cytotoxicity Mechanisms of Linear Poly(amidoamine) and Branched Poly(ethyleneimine) Polyplexes. *Pharm. Res.* **35**, (2018).
143. Ahmed, M. & Narain, R. The effect of polymer architecture, composition, and molecular weight on the properties of glycopolymer-based non-viral gene delivery systems. *Biomaterials* **32**, 5279–5290 (2011).
144. GonçalvesGon, C. *et al.* Macropinocytosis of polyplexes and recycling of plasmid via the clathrin-dependent pathway impair the transfection efficiency of human hepatocarcinoma cells. *Mol. Ther.* **10**, 373–385 (2004).
145. Barua, S. & Rege, K. The influence of mediators of intracellular trafficking on transgene expression efficacy of polymer-plasmid DNA complexes. *Biomaterials* **31**, 5894–5902 (2010).
146. Gu, J., Hao, J., Fang, X. & Sha, X. Factors influencing the transfection efficiency and cellular uptake mechanisms of Pluronic P123-modified polypropyleneimine/pDNA polyplexes in multidrug resistant breast cancer cells. *Colloids Surfaces B Biointerfaces* **140**, 83–93 (2016).